

## Relevant Changes

In accordance with our replies to the referee comments, the following changes have been applied to manuscript and supplement. The changes to the manuscript are highlighted further below.

### **33497 | 4 Added:**

“The mixed solution parameterization framework has been determined by a multi-functional fitting, limited to one parameter per compound, to match the results of ISORROPIA II. Subsequently, the multi-phase and multi-component thermodynamic system has an analytical solution by using our consistent set of analytical equations together with the  $\nu_i$ -coefficient of M2012. Therefore, our mixed solution parameterization framework has similar applicability as ISORROPIA II.”

### **33500 | 5-6 Changed:**

“subsequent reactions” to “the reactions“

### **33504 | 21 Changed:**

“... concentrations constant, which we directly obtain from the NRO (see Sect. 2.5)”  
to “... concentrations constant. Since we do not use at this computation step any dissociation constant, we obtain the maximum concentrations (NRO, max) directly obtain from the NRO.”

### **33507 | 9 Changed:**

“Despite the large differences” to “Despite fundamental differences”

### **33510 | 19 Changed:**

“we compute the RHD<sub>MIN</sub> from Eq. (5b) of M2012”  
to “we compute the RHD<sub>MIN</sub> from Eq. (5b) of M2012 (or Eq. A6 of the Appendix).”

### **33512 | 8 Added:**

“See Fig. S2.2 for a flowchart of the Mixed solution RHD calculation.”

New Figure S2.2 added to the supplement:

“S2.2: Mixed solution RHD calculation (B9 of the EQSAM4clim flowchart, Fig. S2.1).”

### **33512 | 14 Changed:**

“(partial) aerosol water” to: “partial aerosol water”

### **33513 | 20 Added:**

“Note that Eq.(22) can be equally used for so-called metastable aerosols, for which the formation of solid salts is generally not considered.”

### **33513 | 21 Added:**

“We evaluate our parameterization” to “We apply our parameterization”

**33516 | 23 Changed:**

“gas-liquid-solid-partitioning” to “gas-liquid-solid partitioning”

**33517 | 7 Changed:**

“we refer to this article” to “we refer to Metzger et al. (2006)”

**33517 | 14-16 Changed:**

“(see also the comparison in the Supplement, Sect. S3.4).”

to “(see Table 5 for the statistics and the Appendix for the evaluation metrics).”

**33517 | 18 Changed:** “extent” to “extend”

**33526 | 23-24 Changed:**

“Besides significant computational speed-up, another advantage is that our framework minimizes the number of thermodynamic data that are normally required, and reduces the associated uncertainty, while it enables a larger flexibility with respect to the extension to other compounds, not considered in this evaluation. ”

to “Besides significant computational speed-up, another advantage is that our framework minimizes the number of thermodynamic data that are typically required, while it enables greater flexibility with respect to the extension to other compounds, not considered in this evaluation.”

**33526 | 23-24 Changed:** “sneak preview. Figure S2” to “sample. Figure S2.1”

**33527 | 2 Added:** “Appendix C: Evaluation metrics”

***B. Tables and Figures***

Table 1. **Added** the definition of terms in the left-most column to the Table caption.

**New:** “Table 5. MINOS aerosol statistics (Fig.8-9): (top) fine mode, (bottom) coarse mode. EQSAM4clim (EQ4c) and ISORROPIA II (ISO2) versus MINOS observations (Aug 2001).”

**Figure 5. Changed:**

“This figure is extended by Fig. S4” to “Note that at zero ammonia, H<sub>2</sub>SO<sub>4</sub> is at a maximum; shown in Fig. S4.”

**Figure 6. Changed:**

“20 Cases Comparison – case 16. Bulk aerosol water mass as a function of RH for various sulfate molar ratios, fixed for the entire RH range (at constant T = 298.15 K).”

to “EQUISOLV II Comparison – case 16. Bulk aerosol water mass as a function of RH for different sulfate molar ratios, fixed for the entire RH range (at constant T = 298.15 K).”

**Figure 7. Changed:**

“20 Cases Comparison” to “EQUISOLV II Comparison”

Manuscript prepared for Atmos. Chem. Phys. Discuss.  
with version 2014/07/29 7.12 Copernicus papers of the L<sup>A</sup>T<sub>E</sub>X class copernicus.cls.  
Date: 16 April 2016

# Aerosol water parameterization: a single parameter framework

**S. Metzger<sup>1,2</sup>, B. Steil<sup>2</sup>, M. Abdelkader<sup>1</sup>, K. Klingmüller<sup>2</sup>, L. Xu<sup>3</sup>, J. E. Penner<sup>4</sup>,  
C. Fountoukis<sup>5,1</sup>, A. Nenes<sup>6,5,7</sup>, and J. Lelieveld<sup>1,2</sup>**

<sup>1</sup>The Cyprus Institute, Nicosia, Cyprus

<sup>2</sup>Max Planck Institute For Chemistry, Mainz, Germany

<sup>3</sup>Scripps Institution of Oceanography, San Diego, USA

<sup>4</sup>University of Michigan, Ann Arbor, Michigan, USA

<sup>5</sup>Institute of Chemical Engineering Sciences, Foundation for Research and Technology Hellas, Patras, Greece

<sup>6</sup>Schools of Earth and Atmospheric Sciences and Chemical and Biomolecular Engineering, Georgia Institute of Technology, Atlanta, GA, USA

<sup>7</sup>Institute of Environmental Research and Sustainable Development, National Observatory of Athens, Palea Penteli, Greece

Correspondence to: S. Metzger (s.metzger@cyi.ac.cy, swen.metzger@mpic.de)

## Abstract

We introduce a framework to efficiently parameterize the aerosol water uptake for mixtures of semi-volatile and non-volatile compounds, based on the coefficient,  $\nu_i$ . This solute specific coefficient was introduced in Metzger et al. (2012) to accurately parameterize the single solution hygroscopic growth, considering the Kelvin effect – accounting for the water uptake of concentrated nanometer sized particles up to dilute solutions, i.e., from the compounds relative humidity of deliquescence (RHD) up to supersaturation (Köhler-theory). Here we extend the  $\nu_i$ -parameterization from single to mixed solutions. We evaluate our framework at various levels of complexity, by considering the full gas-liquid-solid partitioning for a comprehensive comparison with reference calculations using the E-AIM, EQUISOLV II, ISORROPIA II models as well as textbook examples. We apply our parameterization in EQSAM4clim, the Equilibrium Simplified Aerosol Model V4 for climate simulations, implemented in a box model and in the global chemistry-climate model EMAC. Our results show: (i) that the  $\nu_i$ -approach enables to analytically solve the entire gas-liquid-solid partitioning and the mixed solution water uptake with sufficient accuracy, (ii) that, e.g., pure ammonium nitrate and mixed ammonium nitrate – ammonium sulfate mixtures can be solved with a simple method, and (iii) that the aerosol optical depth (AOD) simulations are in close agreement with remote sensing observations for the year 2005. Long-term evaluation of the EMAC results based on EQSAM4clim and ISORROPIA II will be presented separately.

## 1 Introduction

The most comprehensive description of aerosol composition and hygroscopic growth is provided by models that calculate the full gas-liquid-solid partitioning, i.e., the composition and state of the ion-pairs over the wide range of temperatures and relative humidities from the surface in the tropics to the winter polar stratosphere. Since thermodynamic equilibrium is the final state of kinetic processes, many modeling approaches assume equilibrium, which

is reasonable if the atmospheric processes that lead toward it are fast compared to those that lead away from it (Wexler and Potukuchi, 1998).

To calculate the multiphase partitioning, composition and associated water uptake of multicomponent atmospheric aerosols, various equilibrium models (EQMs) have been developed over the past decades including: EQUIL (Bassett and Seinfeld, 1983), KEQUIL (Bassett and Seinfeld, 1984), MARS (Saxena et al., 1986), MARS-A (Binkowski and Shankar, 1995), SEQUILIB (Pilinis and Seinfeld, 1987), AIM (Wexler and Seinfeld, 1991), SCAPE (Kim et al., 1993a, b; Kim and Seinfeld, 1995), SCAPE2 (Meng et al., 1995), EQUISOLV (Jacobson et al., 1996), ISORROPIA (Nenes et al., 1998, 1999), EQUISOLV II (Jacobson, 1999), GFEMN (Ansari and Pandis, 1999, 2000), EQSAM (Metzger et al., 2002a, b), AIM2 and E-AIM (Wexler and Clegg, 2002), HETV (Makar et al., 2003), ADDEM (Topping et al., 2005a, b), MESA (Zaveri, 2005), EQSAM2 (Metzger et al., 2006), UHAERO (Amundson et al., 2006), ISORROPIA II (Fountoukis and Nenes, 2007), EQSAM3 (Metzger and Lelieveld, 2007), UCD (Zhang and Wexler, 2008), AIOMFAC (Zuend et al., 2011) and EQSAM4clim (this work).

These EQMs are often embedded in aerosol dynamical models (e.g., Pilinis et al., 2000), but the gas-aerosol partitioning and especially the associated water uptake controls the aerosol size distribution, if treated explicitly, which makes the development of EQMs most critical. As a consequence, EQMs vary in the degree of complexity and computational approaches, while almost all EQMs are computationally expensive, due to the complexity of the underlying multicomponent and multiphase thermodynamics. Either numerical accuracy has higher priority than computational efficiency (i.e., iterations to reach equilibrium are extensive), or the computational approaches are comprehensive. Often both applies. Despite the large efforts, computational efficiency, especially if combined with accuracy and flexibility regarding the number of chemical compounds that can be considered, remains to be a challenge, which is especially relevant for global atmospheric aerosol-chemistry and climate modeling.

To meet this challenge we introduce in Sect. 2 an unique single parameter framework, which is subsequently applied in Sect. 3. Our framework allows to efficiently parameterize

the aerosol water uptake for mixtures of semi-volatile and non-volatile compounds, being entirely based on the single solute specific coefficient introduced in Metzger et al. (2012). Additional results and textbook examples of Seinfeld and Pandis (2006) are presented in the Supplement. We conclude with Sect. 4.

## 2 Mixed solution parameterization framework

We introduce a mixed solution parameterization framework to efficiently calculate the aerosol water uptake for mixtures of semi-volatile and non-volatile compounds with the constraint of using only one parameter, i.e.  $\nu_i$ . The solute specific coefficient  $\nu_i$  was introduced in Metzger et al. (2012) – referred to in the following as M2012 – to accurately parameterize the single solution hygroscopic growth, also considering the Kelvin effect. M2012 have shown that the  $\nu_i$ -approach is valid for a wide range of atmospheric conditions. To investigate the potential of the  $\nu_i$ -approach with respect to mixtures of salt compounds, we extend in this work the  $\nu_i$ -parameterizations from single to mixed solutions. Since computational efficiency is a requirement for our parameterization framework, we minimize the overall computational burden by a set of key-constraints:

1. Solving the multicomponent and multiphase partitioning analytically, by using a consistent set of equations, based on one compound specific single solute coefficient,  $\nu_i$  [–]. This set of equations includes the solute molality,  $\mu_s$  [mol(solute) kg<sup>-1</sup>(H<sub>2</sub>O)], and its equivalent expression in terms of the mass fraction solubility,  $\chi_s$  [–]. Both are the essential thermodynamic properties in our framework and only depend on  $\nu_i$ ; the temperature ( $T$ ), relative humidity (RH) and the particle dry diameter ( $D_s$ ) are given;
2. Breaking down the complexity of aerosol thermodynamics as much as possible, without the loss of crucial information and critical numerical accuracy, by using chemical domains with a neutralization order for all salt compounds listed in Table 1;
3. Minimizing the dependencies on the required thermodynamic data by using a pre-determined  $\nu_i$ -coefficient for each electrolyte listed in Table 1;

4. Assuming  $\nu_i$ , constant for the entire range of water activity,  $a_w$ .

The relevant single solute equations (of M2012) are summarized in Appendix A. The mixed solution parameterization framework has been determined by a multi-functional fitting, limited to one parameter per compound, to match the results of ISORROPIA II. The multi-phase and multi-component thermodynamic system has an analytical solution when our consistent set of analytical equations and the  $\nu_i$ -coefficient of M2012 are used. Consequently, our parameterization framework has a similar applicability as ISORROPIA II.

## 2.1 Pre-determined $\nu_i$

M2012 have detailed that a (unitless) single solute coefficient, i.e.,  $\nu_i [-]$ , can be accurately deduced from one reference data-pair of solute molality,  $\mu_s$ , and the corresponding water activity,  $a_w [-]$ . We use a data-pair at solute saturation to pre-determine  $\nu_i$ , since measurements are available for all major salt compounds that are of interest in atmospheric aerosol modeling. For the salt compounds listed in Table 1 we use the mass fraction solubility,  $w_s [-]$ , which is an equivalent expression to the saturation molality,  $\mu_{s,\text{sat}}$ . For the corresponding  $a_w$ , we use the available Relative Humidity of Deliquescence (RHD) values and obtain  $\nu_i$  by solving Eq. (5b) of M2012 with a root finding method (bisection). To be consistent with ISORROPIA II we determine here  $\nu_i$  from  $w_s$  and RHD data at temperature  $T_o = 298$  [K]. The water activity data used by ISORROPIA II (and other EQMs), are tabulated only for room temperature. We therefore do not consider the  $T$ -dependency of  $\nu_i$  in this work.

Table 1 lists the pre-calculated  $\nu_i$  values for each salt compound considered, together with the required thermodynamic data: Stoichiometric coefficient  $\nu_s [-]$ , the ion-pair charge  $Z_s [-]$ , the single solute parameter  $\nu_i [-]$ , the mass fraction solubility in percent  $W_s$  [%] ( $w_s = W_s/100$ ), the molar masses  $M_s$  [ $\text{kg mol}^{-1}$ ], the densities  $D_s$  [ $\text{kg m}^{-3}$ ],  $\text{RHD}(T_o) [-]$  at reference temperature  $T_o = 298.15$  [K], and the corresponding temperature coefficients,

$T_{\text{coef(RHD)}} [-]$ . The RHD values are taken from Fountoukis and Nenes (2007); the other values of Table 1 are taken from the Handbook of Chemistry and Physics (Lide, 2005).

## 2.2 Chemical domains

To break down the complexity of aerosol thermodynamics as much as possible, we minimize the number of chemical compounds and equilibrium reactions that have to be considered. Following the original EQSAM approach (Metzger et al., 2002a), we define chemical domains with a sub-set of neutralization reactions that are considered for a given  $T$ , RH and input concentrations (total of aerosol cations/anions and precursor gases); with all concentration units in  $[\text{mol m}^{-3}(\text{air})]$ . Our domain definition is listed in Table 2 and applied in our mixed solution framework with if-else logic and top-down approach. The potential aerosol neutralization levels depend on the input concentration ratio of total cations, tCAT. The cations are balanced against the total sulfate anions, for which we consider for sulfate rich cases the total sulfates as bi-sulfate, tHSO<sub>4</sub>, or, for sulfate poor cases as total sulfate, tSO<sub>4</sub>. In any case, these totals “t” need to exceed a threshold, MIN =  $1 \times 10^{-15} [\text{mol m}^{-3}(\text{air})]$ ; below the computations are neglected for a given domain. Our definition of totals is given by our domain classification (Table 2), implicitly taking into account the maximum neutralization level that is theoretically possible for each domain:

$$- \text{tSO}_4 = \sum (1 \cdot \text{HSO}_4^- + 2 \cdot \text{SO}_4^{2-})$$

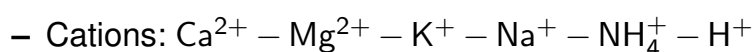
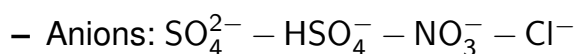
$$- \text{tHSO}_4 = \sum (1 \cdot \text{HSO}_4^- + 1 \cdot \text{SO}_4^{2-})$$

$$- \text{tCAT} = \sum (2 \cdot \text{Ca}^{2+} + 2 \cdot \text{Mg}^{2+} + 1 \cdot \text{Na}^+ + 1 \cdot \text{K}^+ + 1 \cdot \text{NH}_4^+)$$

The domain definition (Table 2) is subsequently used to define the neutralization reaction order (see Sect. 2.3). The two semi-volatile compounds listed in Table 1, NH<sub>4</sub>NO<sub>3</sub> and NH<sub>4</sub>Cl, are considered in our approach only in the sulfate neutral (D1) domain. On the other hand, bi-sulfate is taken into account only for the sulfate rich (D2) and very rich (D3) cases, while free sulfuric acid is considered only for the unneutralized sulfate case (D4).

### 2.3 Domain dependent neutralization reaction order

To avoid the numerical minimization of the Gibbs free energy, which is required to obtain the equilibrium composition of mixed solutions (Seinfeld and Pandis, 2006), we define for each domain (Table 2) a neutralization reaction order (NRO), which can practically be considered  
5 as the salting-out effect of salt solutes (Metzger and Lelieveld, 2007). For this work, we rank the cations and anions according to their preferred neutralization reaction by:



10 which yields the NRO listed in Table 3. The ordering is based on numerous modeling studies, both extensive box-modeling comparisons (Metzger et al., 2002a, 2006, 2012) and global applications (Metzger et al., 1999, 2002b; Metzger and Lelieveld, 2007). Note that we have constrained the ordering for this work to achieve the closest agreement with ISORROPIA II for two reasons: (1) ISORROPIA II is currently the only EQM that is widely applied in global modeling; (2) and it also considers the mineral cations  $\text{Ca}^{2+}$ ,  $\text{Mg}^{2+}$ ,  $\text{K}^+$ .

15 To solve the mixed solution framework we apply the NRO to balance cation-anion pairs that have a non-zero ion-ion product. Within a chemical domain (Table 2), the electrolyte compounds listed in Table 3 are subsequently formed for non-zero ion-ion product, until all cation-anion pairs are paired, or either all cations or anions are fully neutralized. To analytically solve the entire gas-liquid-solid partitioning, we consider at this stage all electrolytes  
20 in solution (computing totals of gas and ions). The gas-solid and gas-liquid partitioning of semi-volatile compounds, the liquid-solid partitioning and the water uptake are determined in that order in subsequent and independent computational steps (Sect. S2 in the Supplement).

### 2.4 Treatment of semi-volatile compounds

25 Table 1 includes two semi-volatile compounds that exhibit the gas-liquid-solid partitioning, i.e., ammonium nitrate,  $\text{NH}_4\text{NO}_3$ , and ammonium chloride,  $\text{NH}_4\text{Cl}$ . Both are allowed in our

framework only in D1, provided that a surplus ammonium,  $\text{NH}_4^+$ , is available. Our implicit assumption is that all sulfates are neutralized first through **subsequent** the reactions with cations (Sect. 2.3). Only excess ammonium may further neutralize anions, nitrate,  $\text{NO}_3^-$ , and/or chloride,  $\text{Cl}^-$ . Thus, semi-volatile compounds can only partition into the particles, if the concentration product exceeds a threshold that is given by the temperature and humidity dependent equilibrium dissociation constant,  $K_p(T, \text{RH})$ . The equilibrium partitioning is detailed in Seinfeld and Pandis (2006) – in the following SP2006 (Sect. 10.4.3 ff).

### 2.4.1 $\text{RH} < \text{RHD}$ – pure and mixed compounds

When the RH is below the RHD and the partial pressure product of gaseous (g) ammonia,  $\text{NH}_3(\text{g})$ , and nitric acid,  $\text{HNO}_3(\text{g})$ , with units either in [ppbv] or  $[\text{mol m}^{-3}(\text{air})]$ , equals or exceeds temperature dependent equilibrium dissociation constant,  $K_p(T)$ , solid (s) ammonium nitrate (AN),  $\text{NH}_4\text{NO}_3(\text{s})$ , is assumed to be formed instantaneously:



$$\text{EQ: } [\text{NH}_3(\text{g})] \cdot [\text{HNO}_3(\text{g})] = K_{p,\text{AN}}(T)$$

For Reaction (R1) the equilibrium concentration of solid ammonium nitrate can be analytically computed from the gaseous concentrations by solving a quadratic equation – for our examples in the Supplement we use [ppbv]. We compute the temperature dependency of the equilibrium dissociation constants,  $K_p(T)$ , following (Fountoukis and Nenes, 2007):

$$K_p(T) = K_p^\circ \times \exp[a \times (T_o/T - 1) + b \times (1 + \ln(T_o/T) - T_o/T)] \quad (1)$$

with  $T$  and  $T_o = 298.15 \text{ K}$ , the ambient temperature and reference temperature, respectively. The  $K_p^\circ(T_o)$  values are given in Table 4 in  $[\text{ppbv}^2]$  for  $T_o$  and reference pressure,  $P_o = 1 [\text{atm}] = 101325 [\text{Pa}]$ , together with the dimensionless temperature coefficients,  $a$  and  $b$  [–]. For applications on a mole basis (e.g., for EQSAM4clim),  $K_p(T)$   $[\text{ppbv}^2]$  can be converted to  $[(\text{mol m}^{-3}(\text{air}))^2]$ , using  $K_{p,\text{mol}}(T) = K_p(T)/(R/P \times T)^2$ ,

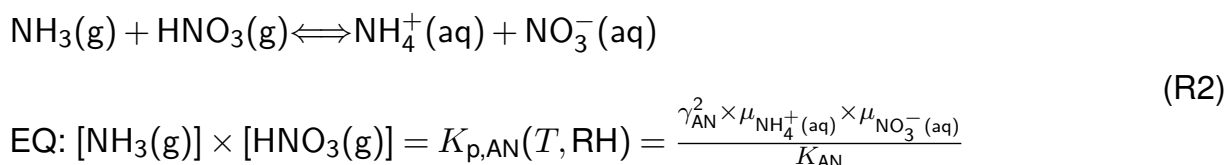
with  $R = 8.314409 \text{ [Pa m}^3 \text{ mol}^{-1} \text{ K}^{-1}]$  the gas constant and  $P = 101325 \text{ [Pa]}$  ( $R/P_o \times T_o = 24.465 \text{ [L mol}^{-1}]$ ).

The equilibrium dissociation constant of  $\text{NH}_4\text{NO}_3$  is sensitive to temperature changes and varies over more than two orders of magnitude for typical ambient conditions. This is illustrated in Fig. 10.19 of SP2006 to which we refer for a detailed discussion. For comparison, Fig. 1 shows the same  $K_{p,AN}$  values as a function of  $T$  at  $\text{RH} < \text{RHD}$  for the EQSAM4clim and ISORROPIA II applications. Although the results are similar, those of SP2006 are slightly lower since their values are obtained from a slightly different equation, i.e.,  $K_{p,AN}(T) = \exp(84.6 - 24220/T - 6.1 \times \ln(T/T_o))$  – see Eq. (10.91) of SP2006 (respectively Eq. (9.91) and Fig. 9.19 of Seinfeld and Pandis, 1998). Note that Reaction (R1) applies for the gas-aerosol partitioning over dry aerosols – pure  $\text{NH}_4\text{NO}_3(\text{s})$ , or any mixture of  $\text{NH}_4\text{NO}_3(\text{s})$  with other dry salt-compounds. An example is given in Sect. S1.1 in the Supplement.

## 2.4.2 $\text{RH} \geq \text{RHD}$ – pure compound

For the wet case, with  $\text{RH}$  above the compound  $\text{RHD}$  or mixed solution  $\text{RHD}$  (see below), the situation is more complicated. In contrast to the gas-solid partitioning described above, the gas-liquid equilibrium partitioning of, e.g., gaseous ammonia,  $\text{NH}_3(\text{g})$ , and nitric acid,  $\text{HNO}_3(\text{g})$ , is in equilibrium with aqueous ammonium nitrate,  $\text{NH}_4\text{NO}_3(\text{aq})$ , when the vapor pressure product of the gases exceeds its temperature and humidity dependent equilibrium dissociation constant,  $K_{p,AN}(T, \text{RH})$ . The salt compound formed is – when equilibrium is reached – additionally dissociated into a cation  $\text{NH}_4^+(\text{aq})$  and anion  $\text{NO}_3^-(\text{aq})$  pair.

1. Following SP2006 (their Sect. 10.4.3) Reaction (R1) expands to:



$$\text{EQ: } [\text{NH}_3(\text{g})] \times [\text{HNO}_3(\text{g})] = K_{p,AN}(T, \text{RH}) = \frac{\gamma_{AN}^2 \times \mu_{\text{NH}_4^+(\text{aq})} \times \mu_{\text{NO}_3^-(\text{aq})}}{K_{AN}}$$

For Reaction (R2) the equilibrium partitioning dissociation constant is now a function of  $T$  and RH. In the notation of SP2006 (see their Eq. 10.99),  $K_{p,AN}(T, RH)$  is related to the temperature dependent equilibrium constant  $K_{AN}$ .  $K_{AN}$  [ $\text{mol}^2 \text{kg}^{-2} \text{atm}^{-2}$ ], depends on the ion molalities [ $\text{mol kg}^{-1}(\text{H}_2\text{O})$ ] of ammonium and nitrate, i.e.,  $\mu_{\text{NH}_4^+(\text{aq})}$  and  $\mu_{\text{NO}_3^-(\text{aq})}$ , and on the corresponding mean molal binary activity coefficient of aqueous ammonium nitrate, i.e.,  $\gamma_{AN}^2$ ; squared because of the cation–anion product. Solving Reaction (R2) requires iterations. To determine the aqueous phase concentration of all compounds that can exist in solution at given  $T$  and RH requires knowledge of the total aerosol water mass (see below), which in turn depends on the solute concentrations and according to Reaction (R2) on activity coefficients. Thus, since  $\gamma_{AN}$  is a function of the aqueous phase concentration,  $K_{p,AN}(T, RH)$  has no analytical solution. According to the thermodynamic literature, the standard treatment is therefore quite comprehensive and requires complex thermodynamic codes.

- Here we express the product ( $\gamma_{AN}^2 \times \mu_{\text{NH}_4^+(\text{aq})} \times \mu_{\text{NO}_3^-(\text{aq})}$ ) of Reaction (R2) to be only a function of  $\nu_i$  and RH, which is motivated by M2012, since their  $\mu_s$  is only a function of  $\nu_i$  and RH. To be able to solve Reaction (R2) analytically, we parameterize  $K_{p,AN}(T, RH)$  by introducing a solute specific correction term for Reaction (R1) which only depends on RH:

$$K_p(T, RH) = K_p(T) \times \text{COEF}(RH) \quad (2)$$

At given  $T$  and RH,  $K_p(T, RH)$  is then a priori known, if  $\text{COEF}(RH)$  is independent of the solute concentration and associated water mass. This can be achieved either by fitting data (Metzger et al., 1999, 2002a; Hauglustaine et al., 2014), or expressing  $\text{COEF}(RH)$  in terms of the  $\nu_i$  and the RH-dependent solute molality parametrization of M2012; using their Eq. (5a). Utilizing further the relation Eq. (A11) of M2012, we can express the solute molality in terms of the solute mass fraction,  $\chi_s$ , and define  $\text{COEF}(RH)$  for pure  $\text{NH}_4\text{NO}_3(\text{aq})$  solutions in terms of  $\chi_s(\text{RH})$ , i.e., for  $\text{RH} \geq \text{RHD}$ :

$$\text{COEF}(RH) := 2 \times \chi_s^2(\text{RH}) \quad (3)$$

with  $\text{COEF}(\text{RH}) := 1$  for  $\text{RH} < \text{RHD}$ . Equation (3) has been empirically derived to approximate the results obtained by ISORROPIA II (see Sect. 3).  $\chi_s(\text{RH})$  denotes the solute mass fraction, which requires in our mixed solution parameterization framework only knowledge of RH and the solute specific coefficient,  $\nu_i$ . In accord with the dry case (Reaction R1), aqueous solutions (Reaction R2) can now be analogously solved. Using Eqs. (2) and (3) to obtain  $K_{\text{p,AN}}(T, \text{RH})$  at a given  $T$  and RH, the quadratic equation, which has an analytical solution for the dry case, can now also be applied to pure  $\text{NH}_4\text{NO}_3(\text{aq})$  solutions. The direct solution of Reaction (R2) by using Eqs. (2) and (3) is exemplified in the Supplement.

The  $T$ -dependent equilibrium dissociation constant of  $\text{NH}_4\text{NO}_3$ , shown in Fig. 1, is also sensitive to changes in relative humidity and varies over orders of magnitude for typical ambient conditions. This is illustrated in Fig. 10.21 of SP2006 to which we refer for a detailed discussion. For comparison, Fig. 2 extends Fig. 1 showing the  $K_{\text{p,AN}}(T, \text{RH})$  values as a function of RH at  $T = 298.15$  [K] for the EQSAM4clim and ISORROPIA II applications. The line-points, which refer to pure  $\text{NH}_4\text{NO}_3(\text{aq})$  solutions, are relatively close for the EQSAM4clim and ISORROPIA II results, but both are (for  $\text{RH} \leq \text{RHD}$ ) roughly a factor two higher than the corresponding values of SP2006 (see Fig. 1); the constant  $K_{\text{p,AN}}(T)$  of SP2006 is included for reference (at  $T = 298.15$  [K]). Note that with Eq. (2) and the quadratic form of Eq. (3) we can analytically approximate the solution of  $K_{\text{p,AN}}(T, \text{RH})$  for  $Y = 1.0$  (Fig. 2).

### 2.4.3 $\text{RH} \geq \text{RHD}$ – mixed compound

According to SP2006 (and references therein), Reaction (R2) needs to be extended for mixed aqueous solutions to include an ionic strength factor.

1. Following the notation of SP2006 (see their Eq. 10.100), the equilibrium concentration (either in [ppbv] or [ $\text{mol m}^{-3}(\text{air})$ ]) of  $[\text{NH}_4\text{NO}_3]$  in mixed aqueous solutions is

controlled by the presence of ammonium sulfate,  $[(\text{NH}_4)_2\text{SO}_4]$ , and depends on a dimensionless ionic strength factor  $Y$ , which is defined by the ratio:

$$Y := \frac{[\text{NH}_4\text{NO}_3]}{[\text{NH}_4\text{NO}_3] + 3 \times [(\text{NH}_4)_2\text{SO}_4]} \quad (4)$$

To extend the calculation of the  $T$  and RH-dependent equilibrium dissociation constant to the case of multicomponent aqueous solutions of  $\text{NH}_4\text{NO}_3$ , shown in Fig. 2, Eq. (4) needs to be considered such that  $K_{p,\text{AN}}(T, \text{RH})$  becomes  $K_{p,\text{AN}}(T, \text{RH}, Y)$ .

- To satisfy our key-constraint (see Sect. 2) we avoid iterations in our mixed solution parameterization. We therefore parameterize  $K_{p,\text{AN}}(T, \text{RH}, Y)$  by expanding Eq. (2) to be additionally a function of  $Y$  (Eq. 4):

$$K_p(T, \text{RH}, Y) = K_p(T) \times \text{COEF}(\text{RH}, Y) \quad (5)$$

For Eq. (5),  $\text{COEF}(\text{RH}, Y) := \text{COEF}(\text{RH}) \times Y^{0.8}$ , where  $\text{COEF}(\text{RH})$  is given by Eq. (3) and  $Y$  by Eq. (4), for which we use the concentration given by the NRO (Sect. 2.3), i.e.,  $Y := \frac{[\text{NH}_4\text{NO}_3]_{(\text{nro}, \text{max})}}{[\text{NH}_4\text{NO}_3]_{(\text{nro}, \text{max})} + 3 \times [(\text{NH}_4)_2\text{SO}_4]_{(\text{nro})}}$ . The  $Y^{0.8}$ -term has been empirically determined to approximate the results of ISORROPIA II by keeping the initial  $\text{NH}_4\text{NO}_3$  and  $(\text{NH}_4)_2\text{SO}_4$  concentrations constant, ~~which we directly obtain~~. Since we do not use at this computation step any dissociation constant, we obtain the maximum concentrations (NRO, max) directly from the NRO (see Sect. 2.5.2.3). Equation (5) and the quadratic equation can be solved non-iteratively. The solution is detailed below (Sect. 2.5); examples are given in Sect. S1 in the Supplement.

Figure 2 shows that the results of EQSAM4clim and ISORROPIA II exhibit a similar dependency on  $Y$  for  $K_{p,\text{AN}}(T, \text{RH}, Y)$ , where the values decrease with decreasing  $Y$  according to the results and the discussion of SP2006 (see their Fig. 10.21).  $K_{p,\text{AN}}(T, \text{RH}, Y)$  is given here by the product of the gaseous concentrations of ammonia,  $[\text{NH}_3]_{(\text{g}, \text{AN})}$ , and

nitric acid,  $[\text{HNO}_3]_{(\text{g},\text{AN})}$ , which are in equilibrium with either the solid  $[\text{NH}_4\text{NO}_3]_{(\text{s})}$  concentration, if  $\text{RH} < \text{RHD}$ , or in equilibrium with the aqueous  $[\text{NH}_4\text{NO}_3]_{(\text{aq})}$  concentration when  $\text{RH} \geq \text{RHD}$  in case of pure  $[\text{NH}_4\text{NO}_3]$  (zero  $[(\text{NH}_4)_2\text{SO}_4]$ , where  $Y = 1$ ). Below the RHD,  $K_p(T, \text{RH}, Y)$  reduces to  $K_p(T)$  as given by Eq. (1) in Reaction (R1). Differences, which occur mainly in the mixed deliquescence humidity range, are discussed below (Sect. 2.6).

## 2.5 Solving $\text{NH}_4\text{NO}_3/\text{NH}_4\text{Cl}$ -thermodynamic equilibrium – this work

To analytically compute the equilibrium concentrations of the two semi-volatile compounds,  $\text{NH}_4\text{NO}_3$  and  $\text{NH}_4\text{Cl}$ , for a given  $\text{RH}$  and  $T$  with our mixed solution parameterization, we first solve all neutralization reactions at once for the domain by using the NRO (Table 3, Sect. 2.3) and the totals (gas + aerosol) of the cation and anion input concentrations. Thus we obtain the free ammonium  $\text{TA} = [\text{NH}_4^+]_{(\text{nro},\text{free})}$  and nitrate  $\text{TN} = [\text{NO}_3^-]_{(\text{nro},\text{free})}$ , after all higher ranked cation-anion pairs are paired. To enable a non-iterative solution, we do not use at this computation step any dissociation constant, so that we directly obtain from  $[\text{TA}]$  and  $[\text{TN}]$  the corresponding maximum ammonium nitrate concentration  $[\text{NH}_4\text{NO}_3]_{(\text{nro},\text{max})} = \text{MIN}([\text{TA}], [\text{TN}])$ , which is possible for  $K_p(T, \text{RH}, Y) = 1$  and the given input concentration,  $T$  and  $\text{RH}$ . Analogously, we compute the maximum ammonium chloride concentration from the final free ammonium and free chloride,  $[\text{TC}] = [\text{Cl}^-]_{(\text{nro},\text{free})}$ , with  $[\text{NH}_4\text{Cl}]_{(\text{nro},\text{max})} = \text{MIN}(\text{TA}, \text{TC})$ .

With the initial (maximum) values of  $[\text{NH}_4\text{NO}_3]_{(\text{nro},\text{max})}$  and  $[(\text{NH}_4)_2\text{SO}_4]_{(\text{nro},\text{max})}$  we can further solve Eq. (4). To obtain the final equilibrium concentrations, we compute the evaporative loss. For  $[\text{NH}_4\text{NO}_3]_{(\text{nro})}$ , we compute the gaseous ammonia,  $[\text{NH}_3]_{(\text{g},\text{AN})}$ , and nitric acid,  $[\text{HNO}_3]_{(\text{g},\text{AN})}$  from  $[\text{NH}_4\text{NO}_3]_{(\text{nro},\text{max})}$ :

$$[\text{TN}] = [\text{NO}_3^-]_{(\text{nro},\text{free})} \quad (6)$$

$$[\text{TA}] = [\text{NH}_4^+]_{(\text{nro},\text{free})} \quad (7)$$

$$[X] = \frac{1}{2} \times \left( -([\text{TA}] + [\text{TN}]) + \sqrt{([\text{TA}] + [\text{TN}])^2 + 4 \times K_p(T, \text{RH}, Y) / (\text{RT})^2} \right) \quad (8)$$

where the variable  $[X]$  is used to obtain:

$$[\text{NH}_3]_{(\text{g},\text{AN})} = [\text{HNO}_3]_{(\text{g},\text{AN})} = \text{MIN}([\text{NH}_4\text{NO}_3]_{(\text{nro},\text{max})}, [X]) \quad (9)$$

With Eq. (9) we compute the final gaseous concentrations of  $\text{HNO}_3_{(\text{g})}$  and  $\text{NH}_3_{(\text{g})}$  from:

$$[\text{NH}_3]_{(\text{g})} = [\text{TA}] + [\text{NH}_3]_{(\text{g},\text{AN})} \quad (10)$$

$$[\text{HNO}_3]_{(\text{g})} = [\text{TN}] + [\text{HNO}_3]_{(\text{g},\text{AN})} \quad (11)$$

and the final ammonium nitrate equilibrium concentration from:

$$[\text{NH}_4\text{NO}_3]_{(\text{nro})} = [\text{NH}_4\text{NO}_3]_{(\text{nro},\text{max})} - [\text{HNO}_3]_{(\text{g},\text{AN})} \quad (12)$$

One can now solve with Eqs. (6)–(12) the quadratic equation for the dry, pure or mixed solution cases. But, in contrast to Seinfeld and Pandis (1998) (see their Eq. 9.103), we compute with Eq. (8) the evaporative losses of gaseous concentrations at equilibrium.

Figure 3 shows a comparison of idealized box model calculations of EQSAM4clim (see Appendix B) and ISORROPIA II (more comprehensive calculations are shown in Sect. 3). The upper panels show the gas-liquid-solid partitioning concentration of  $\text{NH}_4\text{NO}_3$  for a binary solution with a fixed concentration of  $1 \text{ } [\mu\text{mol m}^{-3}(\text{air})]$  of pure  $\text{NH}_4\text{NO}_3$ , while the lower panels show the same for a mixed solution with each  $1 \text{ } [\mu\text{mol m}^{-3}(\text{air})]$  of  $\text{NH}_4\text{NO}_3$  and  $(\text{NH}_4)_2\text{SO}_4$  (both at  $T = 298.15 \text{ K}$ ). The left panels show  $\text{NH}_4\text{NO}_3$ , the right the corresponding total mass loading. To solve the gas-solid and gas-liquid partitioning we have used the  $\nu_i$  based framework (Sect. 2) for EQSAM4clim, and for ISORROPIA II the option to iteratively calculate activity coefficients. A detailed calculation for this example is given in the Supplement (Sect. S1). Despite **the large fundamental** differences in both approaches, the comparison of these results is satisfactory for mixed solute concentration from which the aerosol water mass is derived in a subsequent calculation step – for EQSAM4clim without iterations.

## 2.6 Mixed solution RHD

To calculate the liquid-solid partitioning, we follow (Fountoukis and Nenes, 2007) and consider a mutual deliquescence RH range. In our framework, it depends on a minimum and maximum threshold: RHDMIN and RHDMAX, which are defined below. When the RH is below RHDMIN the aerosol is considered to be dry, while for RH above RHDMAX the aerosol is considered wet with all ionic compounds dissolved. In between a mixture can exist, with some compounds dissolved while other compounds are precipitated from the solution.

For mixed solutions (two or more compounds and water), only the amount that exists for  $RH > RHDMIN$  is considered in solution and allowed to contribute to the mixed solution water uptake. Otherwise, the compounds are considered to be instantaneously solid and precipitated from the solution. For all non-precipitated compounds, a weighted solute concentration is computed from which subsequently all partial water masses are obtained. The sum of all partial water masses yields the total water for the given aerosol composition, size,  $T$  and RH (see Sect. 2.7).

However, comparing the water uptake calculation of EQSAM4clim with reference calculations of, e.g., ISORROPIA II and E-AIM, is somewhat precarious. The reason is that for mixed solutions the calculated water mass mainly depends on the threshold at which the mixture is considered to take up water. The assumptions made to define the mixed solution RHD, or the mutual deliquescence RH range, are generally a major source of uncertainty in modeling the aerosol associated water uptake. First we discuss the procedure of Fountoukis and Nenes (2007), and then we describe our single parameter approach.

1. For ISORROPIA II, if the RH is within a mutual deliquescence RH range, the so-called MDRH region, the solution is assumed to be the sum of two weighted solutions; a “dry solution” (considering a pure dry case) and a “saturated liquid” solution (considering a pure liquid case). Then a numerical solution needs to be found based on a weighting factor (WF) for the dry and liquid solution that could be present in the given sub-domain (solute composition). The weighting factors are obtained from  $(RHD - RH)/(RHD - MDRH)$  using prescribed MDRH values, which have been mea-

sured and tabulated for certain mixtures of salt solutes (see Fountoukis and Nenes, 2007). When the RH is below the MDRH, only a solid phase is possible. Otherwise a liquid and solid phase may coexist (with  $\text{MDRH} < \text{RH} < \text{RHD}$ ). For the latter case the aqueous phase concentrations are determined by WF. The summation over all partial water masses then yields the total aerosol water mass. But the gas-liquid-solid partitioning is re-iterated until the solution converges and the concentrations do not change further (equilibrate). For details see Fountoukis and Nenes (2007).

2. Here we follow the idea of a weighted mixed solution approach of ISORROPIA II, but we approximately solve the liquid-solid partitioning by computing the weighting factor non-iteratively. We compute the liquid-solid partitioning after solving the NRO (Sect. 2.3) and the gas-liquid partitioning (Sect. 2.4). For each salt compound ( $j$ ) we analytically obtain the solid concentration  $n_{j(\text{s})}$  from its aqueous  $n_{j(\text{nro})}$  concentration (determined in the previous computation steps), using analogously to Fountoukis and Nenes (2007) a mixed solution weighting factor,  $\text{WF}_{j,\text{mix}}$ :

$$n_{j(\text{s})} = n_{j(\text{nro})} \times \text{WF}_{j,\text{mix}} \quad (13)$$

with

$$n_{j(\text{aq})} = n_{j(\text{nro})} - n_{j(\text{s})} \quad (14)$$

where  $n_{j(\text{nro})}$  denotes an aqueous concentration of, e.g.,  $[\text{NH}_4\text{NO}_3]_{(\text{nro})}$  from Eq. (12).  $\text{WF}_{j,\text{mix}}$  is defined for each compound (the  $j$ th salt solute in Table 3) by:

$$\text{WF}_{j,\text{mix}} := (\text{RHDMAX}_j - \text{RH}) / (\text{RHDMAX}_j - \text{RHDMIN}) \quad (15)$$

with always a positive sign:  $\text{RHDMIN} < \text{RHDMAX}_j$  and  $\text{RH} < \text{RHDMAX}_j$ .  $\text{RHDMIN}$ ,  $\text{RHDMAX}_j$  are defined below. For  $\text{RH} \geq \text{RHDMAX}_j$ ,  $\text{WF}_{j,\text{mix}} = 0$ ;  $\text{RH} \leq \text{RHDMIN}$ ,  $\text{WF}_{j,\text{mix}} = 1$ . Note that we use a different notation of  $\text{RHDMIN}$  and  $\text{RHDMAX}_j$  (instead of the  $\text{MDRH}$  and  $\text{RHD}$  used by Fountoukis and Nenes, 2007) to indicate that

we are using different values and underlying mixed solution calculations, which do not necessarily have to yield the same results despite our constraint that the overall liquid-solid partitioning aims to be comparable.

To solve the liquid-solid partitioning analytically, i.e., without iteration, we modify the approach of Fountoukis and Nenes (2007). Each binary concentration  $n_{j(\text{nro})}$  is weighted by the total solute concentration,  $n_{\text{s,sum}(\text{nro})} = \sum_{j=1, N_{\text{max}}} n_{j(\text{nro})}$  with all concen-

tration units in  $[\text{mol m}^{-3}(\text{air})]$ . But in our framework,  $n_{\text{s,sum}(\text{nro})}$  is directly obtained from the sum of all single solute concentrations that are formed by solving the neutralization reaction order (Sect. 2.3). In case a semi-volatile compound has been initially neutralized, e.g.  $[\text{NH}_4\text{NO}_3]_{(\text{nro,max})}$ , we additionally solve Eqs. (6)–(12) to obtain  $n_{j(\text{nro})} = [\text{NH}_4\text{NO}_3]_{(\text{nro})}$  (Sect. 2.4), before we obtain a solute specific weighting factor,  $\text{WF}_j$ , from:

$$\text{WF}_j := \frac{n_{j(\text{nro})}}{n_{\text{s,sum}(\text{nro})}} = \frac{n_{j(\text{nro})}}{\sum_{j=1, N_{\text{max}}} n_{j(\text{nro})}} \quad (16)$$

The maximum value of  $N_{\text{max}}$  is limited by the domain dependent NRO (see Table 3). It refers to aqueous solutes at this stage. The liquid-solid partitioning is computed below.

The concentration weighted maximum  $\text{RHD}_j$  (upper threshold), which normally needs to be computed iteratively for each compound, is here directly obtained using  $\text{WF}_j$ :

$$\text{RHDMAX}_j := \text{RHDMIN} \times \text{WF}_j^{0.25} + \text{RHD}_j \times (1 - \text{WF}_j^{0.25}) \quad (17)$$

In case of mixed solutions, Eq. (17) is used to obtain the upper RH-threshold, otherwise the compound's  $\text{RHD}_j$  given in Table 1 are used, while  $\text{RHDMIN}$  is computed here directly for  $n_{\text{s,sum}(\text{nro})}$  only from  $\nu_i$  (see below).  $\text{WF}_j$  is introduced here with an exponent (empirically derived) to parameterize the results of ISORROPIA II, which uses iterations to solve the liquid-solid partitioning using MDRH measurements as the lower RH-threshold in Eq. (17).

To adhere to our key-constraints (Sect. 2, i.e., to minimize the dependency on the required thermodynamic data) we compute the RHDMIN from Eq. (5b) of M2012 (or Eq. (A6) of the Appendix), by using the mixed solution values for  $\mu_s$  and  $\nu_i$  that correspond to  $n_{s,\text{sum(nro)}}$  (Eq. 16). Assuming  $K_e = 1$ ,  $A = 1$  and  $B = 0$ , the single RHDMIN value can be obtained from:

$$\text{RHDMIN} := \left( 1 + \mu_s^{\circ} \times M_w \times \nu_{i,\text{mix}} \times \left( \frac{1}{\mu_s^{\circ}} \times \mu_{s,\text{sat,mix}} \right)^{\nu_{i,\text{mix}}} \right)^{-1} \quad (18)$$

$\mu_{s,\text{sat,mix}}$  is the saturation solute molality and  $\nu_{i,\text{mix}}$  the solute specific constant of the mixed solution.  $\mu_{s,\text{sat,mix}}$  and  $\nu_{i,\text{mix}}$  are introduced here.  $\mu_s^{\circ} = 1 \text{ [mol kg}^{-1}\text{]}$  is the reference molality to match units.  $M_w \text{ [kg mol}^{-1}\text{]}$  is the molar mass of water.

Due to a lack of experimental data, we approximate  $\mu_{s,\text{sat,mix}}$  from the summation over all single solute molalities,  $\mu_{s,\text{sat,single}} \text{ [mol kg}^{-1}\text{]}$ , using the relation to the mass fraction solubility (see, e.g., Eq. A11 of M2012). We therefore obtain  $\mu_{s,\text{sat,mix}}$  from:

$$\mu_{s,\text{sat,mix}} := \sum_{j=1, N_{\text{max}}} \left[ \frac{1}{M_{j(\text{single})} \times (100/W_{j(\text{single})} - 1)} \right] \quad (19)$$

$M_{j(\text{single})} \text{ [kg mol}^{-1}\text{]}$  is the single solute molar mass,  $W_{j(\text{single})} \text{ [%]}$  its mass fraction solubility. The data are given in Table 1 for all compounds considered in this work.

With the mixed solution molality,  $\mu_{s,\text{sat,mix}}$ , we can directly compute the mixed solution solubility,  $w_{s,\text{mix}}$ , if we use as the corresponding total molar mass the sum of the molar masses over all ( $N_{\text{max}}$ ) compounds that can dissolve in the mixed solution, i.e.,

$$M_{s,\text{mix}} = \sum_{j=1, N_{\text{max}}} M_{j(\text{single})} \text{ (same compounds and } N_{\text{max}} \text{ as in Eq. 16):}$$

$$w_{s,\text{mix}} := \frac{1}{(\mu_{s,\text{sat,mix}} \times M_{s,\text{mix}})^{-1} + 1} \quad (20)$$

with  $0.1 < w_{s,\text{mix}} < 1$ . Finally, we can obtain with Eq. (20) the solute specific constant that corresponds to the mixed solution,  $\nu_{i,\text{mix}}$ , using an empirical equation that approximates  $\nu_{i,\text{mix}}$  from the corresponding mixed solution solubility  $w_{s,\text{mix}}$ :

$$\nu_{i,\text{mix}} := (0.25 \times \ln(w_{s,\text{mix}}) + 1)^{-1} \quad (21)$$

Thus, with Eq. (19) we solve Eq. (20) and with Eq. (20) we solve Eq. (21). With Eqs. (21) and (19) we solve Eq. (18) to obtain RHDMIN. And with Eq. (16) we solve Eq. (17) to obtain RHDMAX<sub>*j*</sub>. Together with RHDMIN we solve Eq. (15) to obtain  $WF_{j,\text{mix}}$ .  $WF_{j,\text{mix}}$  is then used to compute the liquid-solid partitioning from Eqs. (13)–(14) after solving the NRO (Sect. 2.3) and the gas-liquid partitioning (Sect. 2.4), in case of semi-volatile compounds. Finally, the aerosol water uptake is computed for each salt compound that exists in the aqueous phase at the given  $T$  and RH from  $n_{j(\text{aq})}$  (Eq. 14). [See Figure S2.2 in the Supplement for a flowchart of the calculation.](#)

## 2.7 Aerosol water uptake

To calculate the mixed solution aerosol water uptake, the standard procedure employs the widely used ZSR-mixing rule (see, e.g., SP2006, Eq. 10.98). Assuming that solute concentrations are in equilibrium with the ambient air, the total aerosol water mass,  $m_{w(\text{mix})}$  [ $\text{kg m}^{-3}(\text{air})$ ], can be directly obtained from the sum of all pure compound ~~(partial)-~~[partial](#) aerosol water masses in case of a mixed solution ( $N$ -compounds dissolved):

$$m_{w,\text{mix}} = \sum_{j=1,N} m_{w,j} = \sum_{j=1,N} \frac{n_{j(\text{aq})}}{\mu_{j(\text{aq})}} \quad (22)$$

Here we follow the standard procedure, while the liquid-solid partitioning and the  $N$ -compounds in the aqueous phase are solved non-iteratively with Sect. 2.6.  $N$  can differ from  $N_{\text{max}}$  considered in Eq. (16), because certain salt solutes may precipitate from the mixed solution during the liquid-solid partitioning so that  $N \leq N_{\text{max}}$ . With increasing RH (from RHDMIN up to RHDMAX<sub>*j*</sub>) an increasing number of compounds is considered for the

water uptake calculations by Eq. (22). The partial aerosol water masses,  $m_{w,j}$ , which are associated with each binary solution (one compound and water),  $n_{j(\text{aq})}$  [ $\text{mol m}^{-3}(\text{air})$ ], can be directly obtained from tabulated single solute molalities,  $\mu_{j(\text{aq})}$  [ $\text{mol}(\text{solute}) \text{kg}^{-1}(\text{H}_2\text{O})$ ] (see Appendix A1), or parameterized based on Eq. (5a) of M2012 (Appendix A2, Eq. A3).

5 In case the RH is below the  $T$ -dependent RHD, or the RHDMIN, we assume the compound to be dry and the partial aerosol water mass to be zero. Using the RH-dependent  $\mu_{j(\text{aq})}$  parameterization of M2012 (their Eq. 5a), we can solve Eq. (22) without iterations.

Our mixed solution framework is independent of the total aerosol water mass, because:

1.  $n_{j(\text{aq})}$  is independent of  $m_{w,\text{mix}}$ , since it is directly given by our NRO (Sect. 2.3);

10 2.  $K_{p,\text{AN}}(T, \text{RH}, Y)$  is independent of  $m_{w,\text{mix}}$ , because of our  $\chi_s(\text{RH})$ -based parameterizations of semi-volatile compounds, i.e., the Eqs. (2)–(5) (Sect. 2.4)

3.  $\chi_s(\text{RH})$  is independent of  $m_{w,\text{mix}}$ , since it is directly given by  $\mu_{j(\text{aq})}(\text{RH})$  (depending also only on  $\nu_i$ , and RH due to the relation Eq. A11 of M2012);

15 4.  $\mu_{j(\text{aq})}$  is independent of  $m_{w,\text{mix}}$ , since it only depends on  $\nu_i$ , and RH ( $\mu_{j(\text{aq})}$  is based on Eq. 5a of M2012 and included with  $\chi_s$  in Appendix A);

5. Mixed solution RHDMIN is independent of  $m_{w,\text{mix}}$ , because of our mixed solution weighting factor,  $\text{WF}_{\text{mix}}$ , parameterizations, which also only depend on  $\nu_i$ , and RH.

6.  $m_{w,j}$  is independent of  $m_{w,\text{mix}}$ , because of the independence of 1.–5.

20 Finally, Eq. (22) is solved for diagnostic output only, since  $m_{w,\text{mix}}$  does not need to be recalculated. Different from ISORROPIA II  $m_{w,j}$  and  $m_{w,\text{mix}}$  are not central in our gas-liquid-solid partitioning computations because of the  $\nu_i$ -concept, which requires that the thermodynamic key-properties,  $\mu_{j(\text{aq})}$  and  $\chi_s$ , only depend on RH and  $\nu_i$ . Note that Eq. (22) can be equally used for so-called metastable aerosols, for which the formation of solid salts is generally not considered.

### 3 Application

We ~~evaluate~~ ~~apply~~ our parameterization using EQSAM4clim. EQSAM4clim is entirely based on the mixed solution framework described in Sect. 2, which builds on the  $\nu_i$ -approach of M2012. The underlying single solute parameterization of solute molality,  $\mu_s$ , and the  
5 relation to the solute mass fraction,  $\chi_s$ , are summarized in Appendix A. The Appendix also includes a short description of EQSAM4clim (Sect. B), while the computational algorithm of EQSAM4clim is detailed in the Supplement (Sect. S2).

To evaluate EQSAM4clim we compare the single solute and mixed solution aerosol water uptake, as well as various other aerosol properties, against different reference models using  
10 box and global modeling calculations at various levels of complexity:

1. Fixed solute concentrations (9 cases): ISORROPIA II and E-AIM  
(see also Sect. S3.1 in the Supplement)
2. Variable ammonia concentration: ISORROPIA II and SP2006  
(see also Sect. S3.2 in the Supplement)
- 15 3. Variable solute concentrations (20 cases): ISORROPIA II and EQUISOLV II  
(see also Sect. S3.3 in the Supplement)
4. Field observations (MINOS campaign, 184 cases): ISORROPIA II  
(see also Sect. S3.4 in the Supplement)
5. EMAC chemistry-climate model (year 2005): ISORROPIA II

20 Selected results of each application case (1–5) are shown below, while the complete set of results are shown in the Supplement (Sect. S3). Throughout this work, all EQSAM4clim results will be primarily evaluated with respect to its ability to accurately simulate the water uptake of atmospheric aerosols, as this is a key process in climate modeling with our EMAC  
25 chemistry-climate model.

### 3.1 Fixed solute concentrations (9 cases): ISORROPIA II and E-AIM

Figure 4 shows the total aerosol water mass,  $m_{w,mix}$  [ $\text{kg m}^{-3}(\text{air})$ ] obtained by Eq. (22) for EQSAM4clim in comparison to the results of ISORROPIA II and E-AIM for the mixed solution case of  $\text{NH}_4\text{NO}_3$  and  $(\text{NH}_4)_2\text{SO}_4$  shown in Fig. 3 (lower panels). The results are based on the full gas-liquid-solid partitioning; for EQSAM4clim on Sect. 2. This first example considers the simplest calculation case: dry compound concentration fixed to 1 [ $\mu\text{mol m}^{-3}(\text{air})$ ]. Figures 4 and S3 in the Supplement (see Supplement, Sect. 3.1) show that the relatively largest differences occur for all cases in the (mutual) deliquescence range, while the general water uptake above this range is very similar for all three equilibrium models, despite the fundamental differences in the underlying approaches of the thermodynamic models.

### 3.2 Variable $\text{NH}_3$ concentration: ISORROPIA II and SP2006

To further evaluate the aerosol water uptake calculations of EQSAM4clim for variable concentrations, we first compare the mixed solution composition of  $\text{NH}_4\text{NO}_3$  and  $(\text{NH}_4)_2\text{SO}_4$  (at  $T = 298.15 \text{ K}$ ) as a function of total ammonia ( $\text{NH}_3 + \text{NH}_4^+$ ), following SP2006; see their Fig. 10.23. Figure 5 shows the corresponding results in [ $\mu\text{g m}^{-3}(\text{air})$ ] of EQSAM4clim and ISORROPIA II – (from top to bottom) for: ammonium, nitrate, sulfate and aerosol water, with bi-sulfate, sulfuric acid shown in the Supplement (Fig. S4). Overall, the results of EQSAM4clim and ISORROPIA II are close to those of Fig. 10.23 of SP2006. Minor differences in ammonium, nitrate and water occur at ammonia concentrations above 6 [ $\mu\text{g m}^{-3}(\text{air})$ ], since the gaseous uptake of  $\text{NH}_3$  and  $\text{HNO}_3$  on saturated solutions is not considered for EQSAM4clim, see Supplement (Sect. S2). The EQSAM4clim results are for ammonia concentrations below 6 [ $\mu\text{g m}^{-3}(\text{air})$ ] somewhat closer to those of SP2006 (see their Fig. 10.23), while the opposite is true for higher ammonia concentrations.

### 3.3 Variable solute concentrations (20 cases): ISORROPIA II and EQUISOLV II

To scrutinize the differences between EQSAM4clim and ISORROPIA II, we further evaluate 20 variable mixed solution cases, following the comparison presented in Xu et al. (2009),

using the corresponding sulfate molar ratios of their Table 3. Figures 6 and 7 show the modelling results for the following RHs: 10, 20, 30, 40, 50, 60, 70, 80, 90, 95 [%] in comparison to EQUISOLV II for case 16, which corresponds to domain D1 of Tables 2 and 3. The remaining cases are shown in Figs. S5–S7 in the Supplement. The aerosol composition is calculated from the full gas-liquid-solid equilibrium partitioning with the assumption that the aerosol lies on the deliquescence branch. Again, this comparison indicates that the relatively largest differences in the aerosol water mass calculations occur in the mutual deliquescence humidity range, while the general water uptake above this range is rather similar for all three equilibrium models (Fig. 6). This finding is also supported by the solid and total PM and confirmed by the total aerosol ammonium and nitrate comparison (Fig. 7). For all cases, the results of EQSAM4clim are close to the results of ISORROPIA II and EQUISOLV II (see also Supplement, Sect. S3.3).

The comparison of total nitrate and aerosol ammonium (Fig. 7) further reveals that also the semi-volatile compounds are rather well represented by EQSAM4clim, despite the underlying simplified analytical approach. Note that the lumped concentrations of the semi-volatile ions are shown only for the most complex cases, i.e., for the 10 sulfate neutral/poor cases (11–20). The common treatment among these EQMs is that both ammonium nitrate and ammonium chloride can be formed only when sulfate has been fully neutralized. A surplus of ammonia must exist to neutralize nitric acid and/or hydrochloric acid. Thus, their neutralization also critically depends on the presence of the non-volatile, mineral cations, i.e.,  $\text{Ca}^{2+}$ ,  $\text{Mg}^{2+}$ ,  $\text{K}^+$ ,  $\text{Na}^+$ , which have been considered for certain cases (e.g., case 16). Depending on the sulfate loadings, these cations can practically determine the whole ~~gas-liquid-solid-partitioning~~ gas-liquid-solid partitioning and the water uptake (Metzger et al., 2006).

### 3.4 Field observations (MINOS campaign, 184 cases): ISORROPIA II

To scrutinize further mineral rich cases and to extend our model inter-comparison to size-resolved aerosol observations, we further apply both gas/aerosol partitioning schemes to (184) field measurements of the Mediterranean INTensive Oxidant Study (MINOS) that

were obtained during a campaign in Crete in the period of 27 July to 25 August 2001 (Lelieveld et al., 2002; Salisbury et al., 2003). Figures 8 and 9 compare the fine and coarse mode total particulate matter [ $\mu\text{mol m}^{-3}(\text{air})$ ], the predicted associated water mass [ $\mu\text{g m}^{-3}(\text{air})$ ] and the residual gases [ $\mu\text{mol m}^{-3}(\text{air})$ ], i.e.,  $[\text{NH}_3]_{(\text{g})}$ ,  $[\text{HNO}_3]_{(\text{g})}$ ,  $[\text{HCl}]_{(\text{g})}$  obtained for EQSAM4clim from Eqs. (6)–(12) with the results of ISORROPIA II and the MINOS observations, following Metzger et al. (2006). For a general description of the measurements and the modeling set-up we refer to [this article Metzger et al. \(2006\)](#). Here we apply both gas-aerosol partitioning models at the same level of complexity by considering the ammonium-sulfate-nitrate-chloride-sodium-calcium-magnesium-potassium-water system, i.e., F4 and C4 in Table 1 of Metzger et al. (2006). Note that we omit here organic compounds for a consistent model inter-comparison, despite their relevance for the absolute comparison with observations. We refer to Metzger et al. (2006) for the influence of organic compounds on the ammonium partitioning during the MINOS campaign. Overall, also the size-resolved aerosol results of EQSAM4clim and ISORROPIA II are in close agreement with each other and reproduce field observations (see [also the Table 5 for the statistics and Appendix C for the evaluation metrics and the additional comparison in the Supplement, Sect. S3.4](#)).

### 3.5 EMAC vs. satellite and AERONET observations

To [extent extend](#) the model inter-comparison of EQSAM4clim and ISORROPIA II to global modelling applications, we use the atmospheric chemistry-climate model EMAC in a setup following Abdelkader et al. (2015). Both gas-aerosol partitioning schemes are implemented in the GMXe aerosol microphysics submodule, as described in Pringle et al. (2010) – fully coupled with the EMAC chemistry, transport and radiation schemes. EQSAM4clim and ISORROPIA II are embedded in EMAC in exactly the same way, so that a direct comparison of the global modeling results can be made. Deviations can be fully explained by differences in the gas/aerosol partitioning and water uptake calculation approach.

To evaluate the EMAC results, we compare the aerosol optical depth (AOD) to three independent observational data sets, i.e., two satellites products, i.e., MODIS and MISR,

and one ground based product, i.e., from the AERosol RObotic NETwork (AERONET), <http://aeronet.gsfc.nasa.gov>. The AOD, or extinction coefficient, is a measure of radiation scattering and absorption at different wavelengths and sensitive to the gas-liquid-solid partitioning and aerosol hygroscopic growth. MODIS monitors the ambient AOD over the oceans and over a portion of the continents (see <http://modis-atmos.gsfc.nasa.gov/>). The MISR aerosol product is available globally. Both data products (and further information) are available from <http://disc.sci.gsfc.nasa.gov/giovanni>.

Figure 10 compares the model simulations and observations for the year 2005 (annual mean based on 5 hourly values). The upper left panel shows the EMAC results based on ISORROPIA II, the upper right panel shows the results based on EQSAM4clim; the results represent two independent simulations with an identical model set-up and spin-up. The AOD observations of MODIS and MISR are shown in the lower left and right panels, respectively. The qualitative comparison already shows that the differences between the two EMAC simulations and the satellite observations is larger than the differences between the two different EMAC simulations (despite the two distinct different gas-aerosol partitioning schemes). This result is supported by the AERONET observations, which are included in Fig. 10 as squares (with the same AOD color scale). With respect to the observations, EMAC slightly underestimates the AOD, mainly over the open oceans, intense biomass burning and dust outbreaks, including the trans-Atlantic dust transport. Although the global dust belt seems to be captured rather well by the EMAC simulations, the current model set-up somewhat underestimates the AOD for the year 2005. The main reason is that we have limited the water uptake only to major inorganic salt compounds (those considered above in Sect. 3.4) for the sake of a consistent model inter-comparison of the two gas/aerosol partitioning schemes. A more complete set-up that includes the water uptake of, e.g., biomass burning and organic compounds, will be presented separately. Nonetheless, considering the differences between the observations and the uncertainty of the AOD products, also these EMAC model predictions of EQSAM4clim and ISORROPIA II seem reasonable.

## 4 Conclusions

We have successfully extended the  $\nu_i$ -parameterizations from single to mixed solutions. The novelty of our single parameter framework is given by the fact that only one coefficient per compound is required to solve the multicomponent gas-liquid-solid partitioning. Our results show that this approach is possible, since we use (i) a consistent set of equations that are all based on the mass fraction solubility  $\chi_s$  (Eq. A1) and  $\nu_i$  (Sect. 2), and (ii) since we can assume  $\nu_i$  to be constant (Sect. 2.1 and A4) for the entire range of water activity,  $a_w$  (for the  $a_w$  parameterization see Eq. 5a of M2012 and Eq. A3). For semi-volatile compounds, we (iii) parameterize the temperature and humidity dependent equilibrium dissociation constant,  $K_{p,AN}(T, RH)$ , by substituting required activity coefficients with a new equation that is also only based on  $\chi_s$  and  $\nu_i$  (Eqs. 1–5). The advantage is that  $\nu_i$  can be accurately determined from one single data pair, i.e., the widely used solute's mass fraction solubility and the corresponding  $a_w$  – for the latter we use in this work RHD measurements (Sects. 2.1 and A4). With M2012 we have demonstrated that the  $\nu_i$ -concept allows to accurately determine the aerosol water mass of binary solutions,  $m_{w,j}$ , for a given solute concentration  $n_{j(aq)}$ . With this work we have shown that this is also true for the total aerosol water mass of mixed solutions,  $m_{w,mix}$  (Eq. 22), by using  $\mu_s$  (Eq. A3). Differences to reference calculations are basically caused by the assumptions made on the mixed solution RHD (Sect. 2.6), i.e., the different assumptions on the mutual deliquescence humidity range. Examples that can be verified with a pocket calculator are presented in the Supplement (Sect. S1) – they support the various box and global modeling results of Sects. 3 and S3.

## Appendix A: Single solute solutions

### A1 Solute mass fraction, $\chi_s$ , and solute molality, $\mu_s$

The relation between solute mass fraction  $\chi_s$  and solute molality  $\mu_s$  is central in our mixed solution parametrization framework (Sect. 2). Both can be expressed through each other

(see, e.g., Eq. A11 of M2012). The solute mass fraction,  $\chi_s$  [-], is defined as the mass [kg] of solute,  $m_s = n_s \times M_s$ , relative to the total mass [kg] of the solution composed out of the mass of solute  $m_s$  and water,  $m_w = n_w \times M_w$ :

$$\chi_s := \frac{m_s}{(m_s + m_w)} = \left(\frac{m_w}{m_s} + 1\right)^{-1} = \left(\frac{n_w \times M_w}{n_s \times M_s} + 1\right)^{-1} = \left(\frac{1}{M_s \times \mu_s} + 1\right)^{-1} \quad (\text{A1})$$

$n_s$  and  $n_w$  [mol] are the number of moles of solute and solvent (water),  $M_s$  and  $M_w$  [kg mol<sup>-1</sup>] are the corresponding molar masses of the solute and water, respectively.

The solute molality is defined as the number of moles of solute per kilogram of water, i.e.,  $\mu_s$  [mol(solute) kg<sup>-1</sup>(H<sub>2</sub>O)]. It can be expressed in terms of the solute mass fraction by:

$$\mu_s := \frac{n_s}{1 \text{ kg H}_2\text{O}} = \frac{n_s}{m_w} = \frac{n_s}{n_w \times M_w} = \frac{1}{M_s \times (1/\chi_s - 1)} \quad (\text{A2})$$

$\mu_s$  measurements, tabulated as a function of water activity ( $a_w$ ), are used in atmospheric modeling under the assumption that  $a_w$  equals RH to obtain the single solute (partial) aerosol water mass that is in equilibrium with a given amount of the single solute,  $n_s$ , at the given RH from Eq. (22); Sect. 2.7. Under this assumption,  $\mu_s$  is a function of RH, actually  $a_w$ , but in any case a function of the available water vapor mass,  $m_w$ , which is in equilibrium associated with the solute mass,  $m_s$ . This illustrated in Figs. A1 and A2 for several electrolytes used in this work; the solid lines refer to  $\mu_s$  measurements, the dotted lines to a parameterization; see Sect. A2. Since for atmospheric applications, the aerosol associated water mass depends on the available water vapor mass, M2012 have expressed the single solute molality as a function of RH and a solute specific coefficient,  $\nu_i$ . The M2012 concept is summarized in the following and has been extended to mixed solutions in Sect. 2.

## A2 Parameterization of $\mu_s$ and $\chi_s$

The representation of water activity (M2012) relates  $a_w$  to the solute molality  $\mu_s$  through a single solute specific constant,  $\nu_i$ . This is a major advantage compared to other parameterizations, because the number of unknowns is reduced to one. To extend

the  $\nu_i$ -approach to mixed solutions we use the parameterization of solute molality  $\mu_s$  [mol(solute) kg<sup>-1</sup>(H<sub>2</sub>O)]. Inverting Eq. (5a) of M2012 allows to express  $\mu_s$  as a function of RH and  $\nu_i$ , with  $a_w := \frac{RH}{K_e}$ :

$$\mu_s = \mu_s^o \times \left( \left[ \frac{1}{\mu_s^o \times M_w \times \nu_i} \times \left( \frac{K_e}{RH} - A \right) \right]^{\frac{1}{\nu_i}} - B \right) \quad (\text{A3})$$

The equivalent expression for  $\chi_s$  [-] is given by inserting Eq. (A3) in Eq. (A1).

$\mu_s^o = 1$  [mol kg<sup>-1</sup>] denotes a reference to match units.  $M_w$  [kg mol<sup>-1</sup>] is the molar mass of water and  $\nu_i$  a single solute specific constant.  $K_e$  denotes the Kelvin-term (see Sect. A5) and depends on the mass equivalent hygroscopic growth factor, GF (see Sect. A6). The terms  $A$  and  $B$  are defined by M2012; see their Eqs. (2) and (3) and are slightly revised (further simplified) in the following.

### A3 Parameterization of $A$ and $B$ -terms

To break down the thermodynamics as much as possible, we use a simplified representation of the  $A$  and  $B$ -terms compared to M2012. Throughout this work, we use a  $B$ -term that has been empirically determined to be a function of  $\nu_i$  with the constraint that  $A := 1$ . Here,  $B$  is expressed in terms of the solute mass fraction  $\chi_s$  and defined as:

$$B := \chi_s^{\left[ \frac{1}{1 + \nu_i + \chi_s} \right]} \quad (\text{A4})$$

To express  $\chi_s$  in Eq. (A4), we use Eq. (A3) for  $\mu_s$  (right term of Eq. A1).

### A4 Relative Humidity of Deliquescence (RHD)

To pre-determine  $\nu_i$  for our mixed solutions framework we use RHD measurements at  $T_o = 298$  [K]; see Sects. 2.1 and 2.3 in M2012. To solve our mixed solution framework we calculate the temperature dependency from (Wexler and Potukuchi, 1998):

$$\text{RHD}(T) = \text{RHD}(T_o) \times \exp \left[ T_{\text{coef}} \times \left( \frac{1}{T} - \frac{1}{T_o} \right) \right] \quad (\text{A5})$$

The RHD measurements at  $T_o = 298$  and the corresponding temperature coefficients are taken from (Fountoukis and Nenes, 2007) and listed in Table 1.

To determine  $\nu_i$ , we solve Eq. (5b) of M2012, which we include here for completeness:

$$\text{RHD} = \frac{K_e}{\left( A + \mu_s^o \times M_w \times \nu_i \times \left[ \frac{1}{\mu_s^o} \times \frac{1}{M_s \times (1/w_s - 1)} + B \right]^{\nu_i} \right)} \quad (\text{A6})$$

The RHD [–] describes the point of water activity,  $a_w$  [–], where a solution is saturated. Any excess of solute leads to solute precipitation and co-existence of a solid and liquid phase (see Sects. 2.6 and 2.7). At solute saturation, the solute mass fraction (Eq. A1) is measured by the widely used mass fraction solubility  $w_s$  [–]. Since the saturation molality  $\mu_{s,\text{sat}}$  and the mass fraction solubility  $w_s$  are related by Eq. (A2), i.e.,  $\mu_{s,\text{sat}} = \frac{1}{M_s \times [1/w_s - 1]}$ , M2012 express the RHD in terms of  $w_s$  and a single solute specific coefficient,  $\nu_i$ . For a given  $w_s$  and RHD data pair,  $\nu_i$  can be accurately determined if Eq. (A6) is solved with a root-finding method (e.g., bisection). This procedure has been detailed in M2012 and only requires one data-pair. To pre-determine  $\nu_i$  for all salt compounds used in this work, we follow M2012 and use the  $w_s$  and RHD measurements at  $T_o = 298$  [K]. The pre-determined  $\nu_i$  values used are included in Table 1. To solve our mixed solutions framework we assume  $\nu_i$  constant and independent of the temperature. Therefore Eq. (A6) is not needed. It could be used during runtime, e.g., within EQSAM4clim (see Sect. B), to determine  $\nu_i$  for different  $T$ . But this is beyond the scope of this work, since the reference models currently available to evaluate our mixed solution parameterization framework are also based on water activity data at  $T_o$ .

## A5 Kelvin-term

The parameterization of solute molality,  $\mu_s$  (introduced by M2012), depends on the so-called Kelvin-term,  $K_e$  [–] (Eq. A3), which can be expressed in terms of the growth factor,  $g_s$ :

$$K_e = \exp\left(\frac{4 \times M_w \times \sigma_{\text{sol}}}{R \times T \times \rho_w \times D_w}\right) = \exp\left(\frac{4 \times M_w \times \sigma_{\text{sol}}}{R \times T \times \rho_w \times g_s \times D_s}\right) \quad (\text{A7})$$

$\sigma_{\text{sol}}$  [ $\text{J m}^{-2}$ ] denotes the RH dependent surface tension of the solution droplet.  $T$  [K] is the droplet temperature,  $R = 8.314409$  [ $\text{J mol}^{-1} \text{K}^{-1}$ ] the ideal gas constant,  $M_w$  [ $\text{kg mol}^{-1}$ ] the molar mass and  $\rho_w$  [ $\text{kg m}^{-3}$ ] the density of water.  $D_{\text{wet}}$  and  $D_s$  [m] are the ambient and dry droplet diameter, respectively.

## A6 Growth factor

Equation (A7) depends on the RH dependent (mass equivalent) hygroscopic growth factor,  $g_s$  [–]. We assume a geometric diameter = mass equivalent diameter of a compact spherical droplet and a constant surface tension of pure water droplets, i.e.,  $\sigma_{\text{sol}} = 0.0761$  [ $\text{J m}^{-2}$ ]. We further assume that the droplet temperature is in equilibrium with the ambient air, and we consider the widely used “volume-additivity”. Then, the volume of the solution droplet can be expressed as the sum of volumes of the dry solute and that of the associated pure (aerosol) water contained in the droplet. The ambient diameter,  $D_{\text{wet}}$ , of the droplet can therefore be expressed in terms of the solute dry diameter,  $D_s$ , and  $g_s$ :

$$g_s := \frac{D_{\text{wet}}}{D_s} = \left( \frac{V_w + V_s}{V_s} \right)^{1/3} = \left( \frac{V_w}{V_s} + 1 \right)^{1/3} \\ = \left( \frac{\rho_s \times m_w}{\rho_w \times m_s} + 1 \right)^{1/3} = \left( \frac{\rho_s}{M_s \times \rho_w \times \mu_s} + 1 \right)^{1/3} \quad (\text{A8})$$

$V_w + V_s$  [ $\text{m}^3$ ] is the total volume of the wet droplet with  $V_s = m_s / \rho_s = n_s M_s / \rho_s$  and  $V_w = m_w / \rho_w = n_w M_w / \rho_w$  [ $\text{m}^3$ ], i.e., the volumes of the initially dry solute and the associated pure water, respectively.  $m_s$  and  $m_w$  [kg] denote the corresponding solute and water masses,  $M_s$  and  $M_w$  [ $\text{kg mol}^{-1}$ ] the molar masses,  $n_s$  and  $n_w$  [mol] the number of moles, and  $\rho_s$  and  $\rho_w$  [ $\text{kg m}^{-3}$ ] the densities, respectively.

## Appendix B: EQSAM4clim

We apply our new mixed solution parameterization framework (Sect. 2) in the EQUilibrium Simplified Aerosol Model V4 for climate simulations. Selected results are shown in

Sect. 3, which are extended in the Supplement. EQSAM4clim aims at accurate but numerically efficient water uptake calculations that are applicable to high resolution or long-term modeling at climate time scales, i.e., decades to centuries. In contrast to previous EQSAM versions and all other thermodynamic gas-liquid-solid aerosol partitioning models, EQSAM4clim considers a consistent, simplified mixed solution parameterization, which can be solved analytically. Our key equation of solute molality,  $\mu_s$ , (Eq. A3), and the entire mixed solution phase partitioning (Sect. 2) can be solved analytically, even with a pen and pocket calculator as demonstrated in the Supplement (Sect. 1). EQSAM4clim (as all other EQSAM versions) builds on the fact that for atmospheric applications,  $\mu_s$  can be expressed as a function of Relative Humidity (RH); Sect. A2. This was first demonstrated by Metzger et al. (2002a) (based on Metzger et al., 1999; Metzger 2000; PhD Thesis, University of Utrecht, the Netherlands, <http://adsabs.harvard.edu/abs/2000PhDT.....328M>, Provided by the SAO/NASA Astrophysics Data System).

To solve our mixed solution framework, we express  $g_s$  in terms of  $\mu_s$  to reduce the number of unknowns to one, i.e.,  $\nu_i$ ; assuming the aerosol dry size  $D_s$ , temperature ( $T$ ) and relative humidity (RH) are prescribed (e.g., given during run-time as model input). Since  $g_s$  [–] is defined as the ratio of wet to dry droplet diameter, it can be expressed in terms of the solute molality (by using either Eq. A2 or Eq. A3). Due to its implicit character in  $\mu_s$ , solving Eq. (A3) requires iterations. One can apply an efficient root finding algorithm, which converges quickly. Treating  $K_e$  and the  $B$ -term as perturbation, it is possible to truncate after the fourth iteration. Higher accuracy will not improve the results much further. For EQSAM4clim, we solve Eq. (A3) for a given aerosol composition, with  $T$ , RH and  $D_s$  as the unknown variables that are given at model input for each model grid box and time step. Note that we use the  $K_e$ -term for Eq. (A3), so that EQSAM4clim compares to Para1 of M2012 (see their Table 1).

We solve  $\mu_s$  for all compounds listed in Table 1 for a given RH from a two-step approach:

- Step one:  $K_e = 1$ , and  $B = 0$  to obtain the initial  $\mu_s$  from Eq. (A3).

- Step two, repeated three times:  $\mu_s$  from previous iteration is used to calculate  $K_e$  from Eq. (A7),  $\chi_s$  from Eq. (A1),  $B$  from Eq. (A4). Then a new  $\mu_s$  is obtained from Eq. (A3).

Figures A1 and A2 show  $\mu_s$  obtained from Eq. (A3) (applied within EQSAM4clim) as a function of bulk water activity, i.e.,  $K_e = 1$  and  $a_w = \text{RH}$ , for major electrolytes (at  $T = 298.15 \text{ K}$ ). All single solute molalities compare well with the tabulated solute molality data (Sect. A1) used in ISORROPIA II (and other EQMs) for the entire  $a_w$ -range: from the water activity at saturation, i.e., RHD, up to  $a_w = 1$  (pure water). Furthermore, the results of M2012 can be reproduced with Eq. (A3) using the modified  $B$ -term, Eq. (A4) with  $A = 1$ . Figure A3 compares the GF obtained with Eq. (A8) (marked as NEW) for pure  $\text{NaCl}_{(\text{cr})}$  and  $(\text{NH}_4)_2\text{SO}_{4(\text{cr})}$  particles with a dry diameter  $D_s = 0.05 \text{ } [\mu\text{m}]$  and  $D_s = 1 \text{ } [\mu\text{m}]$  against those of M2012 (marked as ACP = Para1) and E-AIM for the subsaturated RH regime with  $\text{RH} \leq 97 \text{ } [\%]$  (upper panels), and the subsequent regime, i.e.,  $97 \leq \text{RH} \leq 100 \text{ } [\%]$  (lower panels). Figure A4 compares the corresponding wet particle diameter,  $D_{\text{wet}}$ , as a function of supersaturation (all at  $T = 298.15 \text{ K}$ ); see description of Figs. 3, 4 and 5 of M2012.

Besides significant computational speed-up, another advantage is that our framework minimizes the number of thermodynamic data that are ~~normally required, and reduces the associated uncertainty, typically required~~, while it enables ~~a larger flexibility with respect~~ greater flexibility with respect to the extension to other compounds, not considered in this evaluation. EQSAM4clim (v09) is limited to the same salt compounds as ISORROPIA II, so that the single solute parameter  $\nu_i$ , which is required to solve the single solute molality,  $\mu_s$  (Eq. A3), can be determined from a single reference data-pair (Sect. A4). In addition, most computations are comprehensive and complex. In contrast, the numerical algorithm of EQSAM4clim is simple and easier to verify, since it does not involve any numerical solution or iteration to solve the gas-liquid-solid partitioning for the reasons summarized in Sect. 2.7.

EQSAM4clim has the advantage of being a short fortran 90 code with approximately 850 lines, including comments (or 8 pages), see Fig. S1 in the Supplement for a ~~sneak preview~~ sample. Figure S2.1 in the Supplement shows the flow chart of processes and operations; the computational algorithm is summarized in the Supplement (Sect. S2). For comparison, the gas-aerosol partitioning routine ISORROPIA II, also used in EMAC counts

roughly 36 300 lines (or approx. 360 pages). For comparison, this is about 1/3 of the source code of the EMAC climate model core (ECHAM5.3.02), which has about 120 000 lines of f90 code (both including comments). Last but not least, due to its analytical structure the additional computational costs of EQSAM4clim are negligible for our climate applications, which will be detailed and presented separately.

### Appendix C: Evaluation metrics

- RMSE – Root Mean Square Error between the model ( $m$ ) and the observations ( $o$ ):

$$RMSE = \sqrt{\frac{1}{N} \sum (X_m - X_o)^2} \quad (C1)$$

- $\sigma$  – Standard deviation of the model ( $\sigma_m$ ) and the observed ( $\sigma_o$ ) value:

$$\sigma = \sqrt{\frac{1}{N} \sum_{i=1}^N (X_i - \bar{X})^2}, \quad \text{where } \bar{X} = \frac{1}{N} \sum_{i=1}^N X_i \quad (C2)$$

- R – Correlation coefficient between the model ( $m$ ) and the observations ( $o$ ):

$$R = \frac{\sum_{i=1}^N (X_i^m - \bar{X}^m)(X_i^o - \bar{X}^o)}{\sqrt{\sum_{i=1}^N (X_i^m - \bar{X}^m)^2 \sum_{i=1}^N (X_i^o - \bar{X}^o)^2}} \quad (C3)$$

- MBE – Mean Bias Error between the model ( $m$ ) and the observations ( $o$ ):

$$MBE = \frac{1}{N} \sum (X_m - X_o) \quad (C4)$$

- r – Geometric mean of the model ( $r_m$ ) and the observations ( $r_o$ ):

$$r = \sqrt[n]{\prod_{i=1}^N X} \quad (C5)$$

- GFE – Growth Factorial Error:

$$GFE = \frac{1}{N} \sum \frac{|(X_m - X_o)|}{X_m + X_o} \quad (C6)$$

- SS1 – Skill score between the model ( $m$ ) and the observations ( $o$ ):

$$SS1 = \frac{4(1 + R)}{(\sigma_f + 1/\sigma_f)^2(1 + R_0)}, \quad \text{where } \sigma_f = \frac{\sigma_o}{\sigma_m} \quad R_0 = 0.0 \quad (\text{C7})$$

PF2 is fraction of the number of points within a factor of two of the observations, PF10 is fraction of the number of points within a factor of ten of the observations, and NPoints is the number of points used.

**The Supplement related to this article is available online at [doi:10.5194/acpd-0-1-2016-supplement](https://doi.org/10.5194/acpd-0-1-2016-supplement).**

*Acknowledgements.* This work was supported the European Research Council under the European Union's Seventh Framework Programme (FP7/2007-2013)–ERC grant agreement no. 226144 through the C8-Project. All EMAC simulations have been carried out on the Cy-Tera Cluster, operated by the Cyprus Institute (Cyl) and co-funded by the European Regional Development Fund and the Republic of Cyprus through the Research Promotion Foundation (Project Cy-Tera NEA-ΥΠΟΔΟΜΗ/ΣΤΡΑΤΗ/0308/31). We thank the measurement and model development teams for providing the observations and reference models used in this study.

The article processing charges for this open-access publication were covered by the Max Planck Society.

## References

- Abdelkader, M., Metzger, S., Mamouri, R. E., Astitha, M., Barrie, L., Levin, Z., and Lelieveld, J.: Dust–air pollution dynamics over the eastern Mediterranean, *Atmos. Chem. Phys.*, 15, 9173–9189, doi:10.5194/acp-15-9173-2015, 2015.
- Amundson, N. R., Caboussat, A., He, J. W., Martynenko, A. V., Savarin, V. B., Seinfeld, J. H., and Yoo, K. Y.: A new inorganic atmospheric aerosol phase equilibrium model (UHAERO), *Atmos. Chem. Phys.*, 6, 975–992, doi:10.5194/acp-6-975-2006, 2006.

- Ansari, A. S. and Pandis, S. N.: An analysis of four models predicting the partitioning of semivolatile inorganic aerosol components, *Aerosol Sci. Tech.*, 31, 129–153, doi:10.1080/027868299304200, 1999.
- 5 Ansari, A. S. and Pandis, S. N.: The effect of metastable equilibrium states on the partitioning of nitrate between the gas and aerosol phases, *Atmos. Environ.*, 34, 157–168, doi:10.1016/S1352-2310(99)00242-3, 2000.
- Bassett, M. and Seinfeld, J. H.: Atmospheric equilibrium model of sulfate and nitrate aerosols, *Atmos. Environ.*, 17, 2237–2252, doi:10.1016/0004-6981(83)90221-4, 1983.
- 10 Bassett, M. E. and Seinfeld, J. H.: Atmospheric equilibrium model of sulfate and nitrate aerosols – II. Particle size analysis, *Atmos. Environ.*, 18, 1163–1170, doi:10.1016/0004-6981(84)90147-1, 1984.
- Binkowski, F. S. and Shankar, U.: The Regional Particulate Matter Model: 1. Model description and preliminary results, *J. Geophys. Res.*, 100, 26191, doi:10.1029/95JD02093, 1995.
- 15 Fountoukis, C. and Nenes, A.: ISORROPIA II: a computationally efficient thermodynamic equilibrium model for  $K^+$ – $Ca^{2+}$ – $Mg^{2+}$ – $NH_4^+$ – $Na^+$ – $SO_4^{2-}$ – $NO_3^-$ – $Cl^-$ – $H_2O$  aerosols, *Atmos. Chem. Phys.*, 7, 4639–4659, doi:10.5194/acp-7-4639-2007, 2007.
- Hauglustaine, D. A., Balkanski, Y., and Schulz, M.: A global model simulation of present and future nitrate aerosols and their direct radiative forcing of climate, *Atmos. Chem. Phys.*, 14, 11031–11063, doi:10.5194/acp-14-11031-2014, 2014.
- 20 Jacobson, M. Z.: Studying the effects of calcium and magnesium on size-distributed nitrate and ammonium with EQUISOLV II, *Atmos. Environ.*, 33, 3635–3649, doi:10.1016/S1352-2310(99)00105-3, 1999.
- Jacobson, M. Z., Lu, R., Turco, R. P., and Toon, O. B.: Development and application of a new air pollution modeling system – part I: Gas-phase simulations, *Atmos. Environ.*, 30, 1939–1963, doi:10.1016/1352-2310(95)00139-5, 1996.
- 25 Kim, Y. P. and Seinfeld, J. H.: Atmospheric gas–aerosol equilibrium: III. Thermodynamics of crustal elements  $Ca^{2+}$ ,  $K^+$ , and  $Mg^{2+}$ , *Aerosol Sci. Tech.*, 22, 93–110, doi:10.1080/02786829408959730, 1995.
- Kim, Y. P., Seinfeld, J. H., and Saxena, P.: Atmospheric gas-aerosol equilibrium II. Analysis of common approximations and activity coefficient calculation methods, *Aerosol Sci. Tech.*, 19, 182–198, doi:10.1080/02786829308959629, 1993a.
- 30 Kim, Y. P., Seinfeld, J. H., and Saxena, P.: Atmospheric gas-aerosol equilibrium I. Thermodynamic model, *Aerosol Sci. Tech.*, 19, 157–181, doi:10.1080/02786829308959628, 1993b.

- Lelieveld, J., Berresheim, H., Borrmann, S., Crutzen, P. J., Dentener, F. J., Fischer, H., Feichter, J., Flatau, P. J., Heland, J., Holzinger, R., Korrmann, R., Lawrence, M. G., Levin, Z., Markowicz, K. M., Mihalopoulos, N., Minikin, A., Ramanathan, V., de Reus, M., Roelofs, G. J., Scheeren, H. A., Sciare, J., Schlager, H., Schultz, M., Siegmund, P., Steil, B., Stephanou, E. G., Stier, P., Traub, M.,  
5 Warneke, C., Williams, J., and Ziereis, H.: Global air pollution crossroads over the Mediterranean, *Science*, 298, 794–799, doi:10.1126/science.1075457, 2002.
- Lide, D. R.: Chemical Rubber Company (CRC): Handbook of Chemistry and Physics, 86th Edn., Taylor and Francis Group LLC, CD-ROM version, 2006, 2004–2005.
- Makar, P., Bouchet, V., and Nenes, A.: Inorganic chemistry calculations using HETV – a vectorized  
10 solver for the  $\text{SO}_4^{2-}$ – $\text{NO}_3^-$ – $\text{NH}_4^+$  system based on the ISORROPIA algorithms, *Atmos. Environ.*, 37, 2279–2294, doi:10.1016/S1352-2310(03)00074-8, 2003.
- Meng, Z., Seinfeld, J. H., Saxena, P., and Kim, Y. P.: Atmospheric gas-aerosol equilibrium: IV. Thermodynamics of carbonates, *Aerosol Sci. Tech.*, 23, 131–154, doi:10.1080/02786829508965300, 1995.
- 15 Metzger, S. and Lelieveld, J.: Reformulating atmospheric aerosol thermodynamics and hygroscopic growth into fog, haze and clouds, *Atmos. Chem. Phys.*, 7, 3163–3193, doi:10.5194/acp-7-3163-2007, 2007.
- Metzger, S., Dentener, F., and Lelieveld, J.: Aerosol multiphase equilibrium composition: results of a parameterization applied to a global chemistry/tracer transport model, *J. Aerosol Sci.*, 30, S877, doi:10.1016/S0021-8502(99)80449-2, 1999.
- 20 Metzger, S., Dentener, F., Pandis, S., and Lelieveld, J.: Gas/aerosol partitioning: 1. A computationally efficient model, *J. Geophys. Res.*, 107, 16-1-24, doi:10.1029/2001JD001102, 2002a.
- Metzger, S., Dentener, F., Krol, M., Jeurken, A., and Lelieveld, J.: Gas/aerosol partitioning: 2. Global modeling results, *J. Geophys. Res.*, 107, ACH 17-1–ACH 17-23, doi:10.1029/2001JD001103, 2002b.
- 25 Metzger, S., Mihalopoulos, N., and Lelieveld, J.: Importance of mineral cations and organics in gas-aerosol partitioning of reactive nitrogen compounds: case study based on MINOS results, *Atmos. Chem. Phys.*, 6, 2549–2567, doi:10.5194/acp-6-2549-2006, 2006.
- Metzger, S., Steil, B., Xu, L., Penner, J. E., and Lelieveld, J.: New representation of water activity  
30 based on a single solute specific constant to parameterize the hygroscopic growth of aerosols in atmospheric models, *Atmos. Chem. Phys.*, 12, 5429–5446, doi:10.5194/acp-12-5429-2012, 2012.
- Nenes, A., Pandis, S. N., and Pilinis, C.: ISORROPIA: a new thermodynamic equilibrium model for multiphase multicomponent inorganic aerosols, *Aquat. Geochem.*, 4, 123–152, 1998.

- Nenes, A., Pandis, S. N., and Pilinis, C.: Continued development and testing of a new thermodynamic aerosol module for urban and regional air quality models, *Atmos. Environ.*, **33**, 1553–1560, doi:10.1016/S1352-2310(98)00352-5, 1999.
- Pilinis, C. and Seinfeld, J. H.: Continued development of a general equilibrium model for inorganic multicomponent atmospheric aerosols, *Atmos. Environ.*, **21**, 2453–2466, doi:10.1016/0004-6981(87)90380-5, 1987.
- Pilinis, C., Capaldo, K. P., Nenes, A., and Pandis, S. N.: MADM-A New Multicomponent Aerosol Dynamics Model, *Aerosol Sci. Tech.*, **32**, 482–502, doi:10.1080/027868200303597, 2000.
- Pringle, K. J., Tost, H., Message, S., Steil, B., Giannadaki, D., Nenes, A., Fountoukis, C., Stier, P., Vignati, E., and Lelieveld, J.: Description and evaluation of GMXe: a new aerosol submodel for global simulations (v1), *Geosci. Model Dev.*, **3**, 391–412, doi:10.5194/gmd-3-391-2010, 2010.
- Pringle, K. J., Tost, H., Metzger, S., Steil, B., Giannadaki, D., Nenes, A., Fountoukis, C., Stier, P., Vignati, E., and Lelieveld, J.: Corrigendum to “Description and evaluation of GMXe: a new aerosol submodel for global simulations (v1)” published in *Geosci. Model Dev.*, **3**, 391–412, 2010, *Geosci. Model Dev.*, **3**, 413–413, doi:10.5194/gmd-3-413-2010, 2010.
- Salisbury, G., Williams, J., Holzinger, R., Gros, V., Mihalopoulos, N., Vrekoussis, M., Sarda-Estève, R., Berresheim, H., von Kuhlmann, R., Lawrence, M., and Lelieveld, J.: Ground-based PTR-MS measurements of reactive organic compounds during the MINOS campaign in Crete, July–August 2001, *Atmos. Chem. Phys.*, **3**, 925–940, doi:10.5194/acp-3-925-2003, 2003.
- Saxena, P., Belle Hudischewskyj, A., Seigneur, C., and Seinfeld, J. H.: A comparative study of equilibrium approaches to the chemical characterization of secondary aerosols, *Atmos. Environ.*, **20**, 1471–1483, doi:10.1016/0004-6981(86)90019-3, 1986.
- Seinfeld, J. H. and Pandis, S. N.: *Atmospheric Chemistry and Physics: From Air Pollution to Climate Change*, 1st edn., J. Wiley, Hoboken, N.J., 1998.
- Seinfeld, J. H. and Pandis, S. N.: *Atmospheric Chemistry and Physics: From Air Pollution to Climate Change*, 2nd Edn., J. Wiley, Hoboken, N.J., 2006.
- Topping, D. O., McFiggans, G. B., and Coe, H.: A curved multi-component aerosol hygroscopicity model framework: Part 1 – Inorganic compounds, *Atmos. Chem. Phys.*, **5**, 1205–1222, doi:10.5194/acp-5-1205-2005, 2005.
- Topping, D. O., McFiggans, G. B., and Coe, H.: A curved multi-component aerosol hygroscopicity model framework: Part 2 – Including organic compounds, *Atmos. Chem. Phys.*, **5**, 1223–1242, doi:10.5194/acp-5-1223-2005, 2005.

- Wexler, A. and Potukuchi, S.: Kinetics and thermodynamics of tropospheric aerosols, in: Atmospheric Particles, edited by: Harrison, R. M. and Van Grieken, R., Wiley, Sussex, England, 203–231, 1998.
- 5 Wexler, A. S. and Clegg, S. L.: Atmospheric aerosol models for systems including the ions  $H^+$ ,  $NH_4^+$ ,  $N^+$ ,  $SO_4^{2-}$ ,  $NO_3^-$ ,  $Cl^-$ ,  $Br^-$ , and  $H_2O$ , *J. Geophys. Res.*, 107, ACH 14-1–ACH 14-14, doi:10.1029/2001JD000451, 2002.
- Wexler, A. S. and Seinfeld, J. H.: Second-generation inorganic aerosol model, *Atmos. Environ. A-Gen.*, 25, 2731–2748, doi:10.1016/0960-1686(91)90203-J, 1991.
- 10 Xu, L., Penner, J. E., Metzger, S., and Lelieveld, J.: A comparison of water uptake by aerosols using two thermodynamic models, *Atmos. Chem. Phys. Discuss.*, 9, 9551–9595, doi:10.5194/acpd-9-9551-2009, 2009.
- Zaveri, R. A., Easter, R. C., and Wexler, A. S.: A new method for multicomponent activity coefficients of electrolytes in aqueous atmospheric aerosols, *J. Geophys. Res.*, 110, D02201, doi:10.1029/2004JD004681, 2005.
- 15 Zhang, K. and Wexler, A.: Modeling urban and regional aerosols – Development of the UCD Aerosol Module and implementation in CMAQ model, *Atmos. Environ.*, 42, 3166–3178, doi:10.1016/j.atmosenv.2007.12.052, 2008.
- 20 Zuend, A., Marcolli, C., Booth, A. M., Lienhard, D. M., Soonsin, V., Krieger, U. K., Topping, D. O., McFiggans, G., Peter, T., and Seinfeld, J. H.: New and extended parameterization of the thermodynamic model AIOMFAC: calculation of activity coefficients for organic-inorganic mixtures containing carboxyl, hydroxyl, carbonyl, ether, ester, alkenyl, alkyl, and aromatic functional groups, *Atmos. Chem. Phys.*, 11, 9155–9206, doi:10.5194/acp-11-9155-2011, 2011.

**Table 1.** Thermodynamic data ~~–Units see text–~~ (Sect. 2.1): Stoichiometric coefficient  $\nu_s$  [–], the ion-pair charge  $Z_s$  [–], the single solute parameter  $\nu_i$  [–], the mass fraction solubility in percent  $W_s$  [%] ( $w_s = W_s/100$ ), the molar masses  $M_s$  [ $\text{kg mol}^{-1}$ ], the densities  $D_s$  [ $\text{kg m}^{-3}$ ],  $\text{RHD}(T_o)$  [–] at reference temperature  $T_o = 298.15$  [K], and the corresponding temperature coefficients,  $T_{\text{coef(RHD)}}$  [–]. The  $\nu_i$  values have been obtained from the RHD and  $W_s$  values (at  $T_o = 298$  [K]) following the method described in Metzger et al. (2012). The RHD values are taken from Fountoukis and Nenes (2007); the  $W_s$  and all other values are taken from the Handbook of Chemistry and Physics (Lide, 2005).

Species 01–05	H <sub>2</sub> O	H <sub>2</sub> SO <sub>4</sub>	HNO <sub>3</sub>	HCl	NH <sub>3</sub>
$\nu_s   Z_s$	2   1	3   2	2   1	2   1	1   1
$\nu_i$	–	–	–	–	–
$W_s$	–	–	–	–	–
$M_s$	0.018020	0.098090	0.063020	0.036460	0.017040
$D_s$	997	1830	1513	1490	696
RHD	–	–	–	–	–
$T_{\text{coef}}$	–	–	–	–	–
Species 06–10	(NH <sub>4</sub> ) <sub>3</sub> H(SO <sub>4</sub> ) <sub>2</sub>	(NH <sub>4</sub> ) <sub>2</sub> SO <sub>4</sub>	NH <sub>4</sub> HSO <sub>4</sub>	NH <sub>4</sub> NO <sub>3</sub>	NH <sub>4</sub> Cl
$\nu_s   Z_s$	5   3	3   2	2   1	2   1	2   1
$\nu_i$	1.616356	1.274822	1.253573	1.051480	1.243054
$W_s$	53.30	43.31	76.00	68.05	28.34
$M_s$	0.247300	0.132170	0.115130	0.080060	0.053500
$D_s$	1775	1770	1780	1720	1519
RHD	0.6900	0.7997	0.4000	0.6183	0.7710
$T_{\text{coef}}$	186.00	80.00	384.00	852.00	239.00
Species 11–15	Na <sub>3</sub> H(SO <sub>4</sub> ) <sub>2</sub>	Na <sub>2</sub> SO <sub>4</sub>	NaHSO <sub>4</sub>	NaNO <sub>3</sub>	NaCl
$\nu_s   Z_s$	5   3	3   2	2   1	2   1	2   1
$\nu_i$	–	1.278762	1.293906	1.160345	1.358377
$W_s$	–	21.94	66.18	47.70	26.47
$M_s$	0.262120	0.142050	0.120070	0.085000	0.058440
$D_s$	2565	2700	2430	2260	2170
RHD	–	0.9300	0.5200	0.7379	0.7528
$T_{\text{coef}}$	–	80.00	–45.00	304.00	25.00

**Table 1.** Continued.

Species 16–20	$K_3H(SO_4)_2$	$K_2SO_4$	$KHSO_4$	$KNO_3$	KCl
$\nu_s   Z_s$	5   3	3   2	2   1	2   1	2   1
$\nu_i$	–	1.286445	1.308499	1.014102	1.256989
$W_s$	–	10.71	33.60	27.69	26.23
$M_s$	0.310444	0.174266	0.136178	0.101108	0.074548
$D_s$	2490	2660	2320	2110	1988
RHD	–	0.9750	0.8600	0.9248	0.8426
$T_{coef}$	–	35.60	0	0	159.00
Species 21–25	n/a	$CaSO_4$	n/a	$Ca(NO_3)_2$	$Ca(Cl)_2$
$\nu_s   Z_s$	– / –	2   2	– / –	3   2	3   2
$\nu_i$	–	1.271828	–	1.586562	2.024869
$W_s$	–	0.21	–	59.02	44.84
$M_s$	–	0.136150	–	0.164100	0.110980
$D_s$	–	2960	–	2500	2150
RHD	–	0.9900	–	0.4906	0.2830
$T_{coef}$	–	0	–	509.40	551.10
Species 25–30	n/a	$MgSO_4$	n/a	$Mg(NO_3)_2$	$Mg(Cl)_2$
$\nu_s   Z_s$	– / –	2   2	– / –	3   2	3   2
$\nu_i$	–	1.435281	–	1.878693	2.107772
$W_s$	–	26.31	–	41.59	35.90
$M_s$	–	0.120375	–	0.148325	0.095205
$D_s$	–	2660	–	2300	2325
RHD	–	0.8613	–	0.5400	0.3284
$T_{coef}$	–	–714.45	–	230.20	42.23

**Table 2.** Chemical domains (introduced in Sect. 2.2).

D4	SULFURIC ACID ONLY	$t\text{CAT} < \text{MIN}$	AND	$t\text{HSO}_4 \geq \text{MIN}$
D3	SULFATE VERY RICH	$t\text{CAT} \geq \text{MIN}$	AND	$t\text{CAT} < t\text{HSO}_4$
D2	SULFATE RICH	$t\text{CAT} \geq t\text{HSO}_4$	AND	$t\text{CAT} < t\text{SO}_4$
D1	SULFATE NEUTRAL	$t\text{CAT} \geq t\text{SO}_4$		

**Table 3.** Neutralization reaction order for Table 2 (introduced in Sect. 2.3).

D1			= Sulfate Neutral
1. CaSO <sub>4</sub>	2. MgSO <sub>4</sub>	3. K <sub>2</sub> SO <sub>4</sub>	
4. Na <sub>2</sub> SO <sub>4</sub>	5. (NH <sub>4</sub> ) <sub>2</sub> SO <sub>4</sub>	6. Ca(NO <sub>3</sub> ) <sub>2</sub>	
7. Mg(NO <sub>3</sub> ) <sub>2</sub>	8. KNO <sub>3</sub>	9. NaNO <sub>3</sub>	
10. NH <sub>4</sub> NO <sub>3</sub>	11. Ca(Cl) <sub>2</sub>	12. Mg(Cl) <sub>2</sub>	
13. KCl	14. NaCl	15. NH <sub>4</sub> Cl	
D2			= Sulfate Rich
1. CaSO <sub>4</sub>	2. MgSO <sub>4</sub>	3. K <sub>2</sub> SO <sub>4</sub>	
4. KHSO <sub>4</sub>	5. Na <sub>2</sub> SO <sub>4</sub>	6. NaHSO <sub>4</sub>	
7. (NH <sub>4</sub> ) <sub>2</sub> SO <sub>4</sub>	8. NH <sub>4</sub> HSO <sub>4</sub>		
D3			= Sulfate Very Rich
1. CaSO <sub>4</sub>	2. MgSO <sub>4</sub>	3. KHSO <sub>4</sub>	
4. NaHSO <sub>4</sub>	5. NH <sub>4</sub> HSO <sub>4</sub>	6. H–HSO <sub>4</sub>	
D4			= Sulfuric Acid
1. H <sub>2</sub> SO <sub>4</sub>			

**Table 4.** Equilibrium dissociation constants [ppbv<sup>2</sup>] and *T*-coefficients [–]; from Fountoukis and Nenes (2007).

NH <sub>4</sub> NO <sub>3</sub>	$K_p^\circ = 57.46$	$a = -74.38$	$b = 6.120$
NH <sub>4</sub> Cl	$K_p^\circ = 1.086$	$a = -71.00$	$b = 2.400$

**Table 5.** MINOS aerosol statistics (see Figs. 8, 9 of Sec. 3.4; Appendix C for the evaluation metrics): EQSAM4clim (EQ4c) and ISORROPIA II (ISO2) versus MINOS observations (Aug 2001).

	Aerosol Fine Mode							
	HNO <sub>3</sub>		NH <sub>3</sub>		HCl		PM	
	EQ4c	ISO2	EQ4c	ISO2	EQ4c	ISO2	EQ4c	ISO2
Mean <sub>m</sub>	19.86 ± 12.89	20.17 ± 13.05	74.16 ± 63.93	74.91 ± 63.41	69.86 ± 42.81	70.08 ± 42.55	0.13 ± 0.05	0.13 ± 0.10
Mean <sub>o</sub>	19.56 ± 13.17	19.56 ± 13.17	41.13 ± 40.55	41.13 ± 40.55	78.26 ± 38.36	78.26 ± 38.36	0.17 ± 0.08	0.17 ± 0.08
r <sub>m</sub>	16.81 ± 0.24	17.01 ± 0.25	37.35 ± 1.48	51.10 ± 0.43	44.75 ± 0.62	44.80 ± 0.62	0.13 ± 0.15	0.09 ± 0.46
r <sub>o</sub>	16.15 ± 0.26	16.15 ± 0.26	32.33 ± 0.27	32.33 ± 0.27	69.89 ± 0.21	69.89 ± 0.21	0.15 ± 0.21	0.15 ± 0.21
RMSE	2.56	2.02	58.99	59.02	3.89	4.41	0.06	0.07
R	0.98	0.99	0.65	0.65	0.99	0.99	0.89	0.80
MBE	0.30	0.61	33.07	33.78	0.22	0.47	-0.03	-0.04
GFE	0.04	0.05	0.34	0.34	0.02	0.02	0.11	0.26
SS1	0.99	0.99	0.67	0.68	0.99	0.99	0.68	0.88
PF2	1.00	1.00	0.52	0.52	1.00	1.00	0.99	0.66
PF10	1.00	1.00	0.96	0.96	1.00	1.00	1.00	0.85
NPOINTS	124	124	122	122	110	110	124	124
	Aerosol Coarse Mode							
	HNO <sub>3</sub>		NH <sub>3</sub>		HCl		PM	
	EQ4c	ISO2	EQ4c	ISO2	EQ4c	ISO2	EQ4c	ISO2
Mean <sub>m</sub>	13.39 ± 13.73	9.55 ± 12.34	43.57 ± 40.39	40.76 ± 41.05	57.58 ± 41.57	38.29 ± 41.11	0.23 ± 0.11	0.23 ± 0.14
Mean <sub>o</sub>	19.56 ± 13.17	19.56 ± 13.17	41.13 ± 40.55	41.13 ± 40.55	78.26 ± 38.36	78.26 ± 38.36	0.19 ± 0.10	0.19 ± 0.10
r <sub>m</sub>	5.79 ± 0.76	0.00 ± 12.54	35.09 ± 0.27	27.97 ± 0.46	39.17 ± 0.48	0.00 ± 11.11	0.20 ± 0.22	0.18 ± 0.36
r <sub>o</sub>	16.15 ± 0.26	16.15 ± 0.26	32.33 ± 0.27	32.33 ± 0.27	69.89 ± 0.21	69.89 ± 0.21	0.17 ± 0.24	0.17 ± 0.24
RMSE	28.87	17.68	6.73	8.67	32.91	43.90	0.05	0.08
R	0.47	0.34	0.99	0.98	0.82	0.80	0.97	0.86
MBE	-2.09	-10.01	3.08	0.24	-20.58	-35.75	0.04	0.04
GFE	0.05	0.59	0.07	0.13	0.22	0.49	0.10	0.18
SS1	0.73	0.67	0.99	0.99	0.91	0.90	0.98	0.84
PF2	0.02	0.37	0.99	0.91	0.66	0.45	0.98	0.86
PF10	0.06	0.58	1.00	0.98	0.86	0.75	1.00	0.97
NPOINTS	124	124	122	122	110	110	124	124

**Table A1.** List of names and abbreviations.

Abbreviation	Name
AOD	Aerosol Optical Depth
AERONET	AERosol RObotic NETwork ( <a href="http://aeronet.gsfc.nasa.gov">http://aeronet.gsfc.nasa.gov</a> )
CNN	Cloud Condensation Nuclei
CPU	Computational Performance Unit
EQMs	Thermodynamic equilibrium models
E-AIM	(Wexler and Clegg, 2002), <a href="http://www.aim.env.uea.ac.uk/aim/aim.php">http://www.aim.env.uea.ac.uk/aim/aim.php</a>
EQSAM	Equilibrium Simplified Aerosol Model (Metzger et al., 2002b)
EQSAM4clim	Equilibrium Simplified Aerosol Model (Version 4) for Climate Simulations (this work)
EQUISOLV II	Jacobson (1999)
EMAC	Atmospheric Chemistry-climate model
GMXe	Global Modal-aerosol eXtension (Pringle et al., 2010)
ISORROPIA II	Fountoukis and Nenes (2007)
MODIS	satellite data ( <a href="http://modis-atmos.gsfc.nasa.gov/">http://modis-atmos.gsfc.nasa.gov/</a> )
MISR	global satellite data ( <a href="http://disc.sci.gsfc.nasa.gov/giovanni">http://disc.sci.gsfc.nasa.gov/giovanni</a> )
MINOS	Mediterranean INTensive Oxidant Study (Lelieveld et al., 2002; Salisbury et al., 2003)
NRO	neutralization reaction order (Sect. 2.3)
M2012	Metzger et al. (2012)
SP2006	Seinfeld and Pandis (2006)

**Table A2.** List of greek symbols.

Greek Symbol	Name	Unit
$\nu_i$	solute specific constant (introduced by M2012)	[-]
$\nu_s$	stoichiometric coefficient of solute ( $\pm$ ion-pair)	[-]
$\mu_s$	molality of solute	[mol kg <sup>-1</sup> (H <sub>2</sub> O)]
$\mu_s^o$	reference molality of 1 mole of solute (considering stoichiometry)	[mol kg <sup>-1</sup> (H <sub>2</sub> O)]
$\mu_s^{\text{sat}}$	saturation molality of solute	[mol kg <sup>-1</sup> (H <sub>2</sub> O)]
$\rho_s$	density of solute	[kg m <sup>-3</sup> ]
$\rho_w$	density of water	[kg m <sup>-3</sup> ]
$\sigma_{\text{sol}}$	surface tension of the solution droplet	[J m <sup>-2</sup> ]
$\chi_s$	solute mass fraction, referring to the solute's dry mass	[-]
$\chi_s^{\text{sat}}$	solute mass fraction, referring to the solute's dry mass at saturation	[-]
sat	superscript, indicator for saturation	
(cr)	subscript, phase indicator for anhydrous (solid = crystalline = cr) phase	
(aq)	subscript, phase indicator for aqueous phase	
(g)	subscript, phase indicator for gas phase	

**Table A3.** List of symbols.

Symbol	Name	Unit
$A$	$A$ -term of Eq. (A4), introduced with Sect. A3	[-]
$B$	$B$ -term of Eq. (A4), introduced with Sect. A3	[-]
$a_w$	water activity (Raoult-term)	[-]
$D_s$	dry droplet diameter of the solute	[m]
$D_{wet}$	wet droplet diameter of the solution	[m]
$K_e$	surface or Kelvin-term of the solution	[-]
$m_s$	crystalline mass of solute	[kg]
$m_w$	aqueous mass of water (solvent)	[kg]
$M_s$	molar mass of solute	[kg mol <sup>-1</sup> ]
$M_w$	molar mass of water	[kg mol <sup>-1</sup> ]
$n_s$	moles of solute	[mol]
$\sum_i n_i$	summation over all moles of solutes	[mol]
$n_w$	moles of water	[mol]
GF	Growth Factor	[-]
RH	relative humidity in percent (as used in the text)	[%]
RH	fractional relative humidity (as used in equations)	[-]
RHD	fractional relative humidity of deliquescence	[-]
$s$	saturation ratio	[-]
$S$	supersaturation	[-]
$S_c$	critical supersaturation in percent	[%]
$T_{coef}$	dimensionless temperature coefficients for the RHD	[-]
$T_o$	reference temperature in Kelvin	[298.15 K]
$T$	temperature in Kelvin	[K]
$w_s$	mass fraction solubility, referring to the solute's dry mass required for saturation	[-]
$W_s$	mass fraction solubility, referring to the solute's dry mass required for saturation	[%]
tCAT	total cations (for chemical domains; Sect. 2.2)	[mol m <sup>-3</sup> (air)]

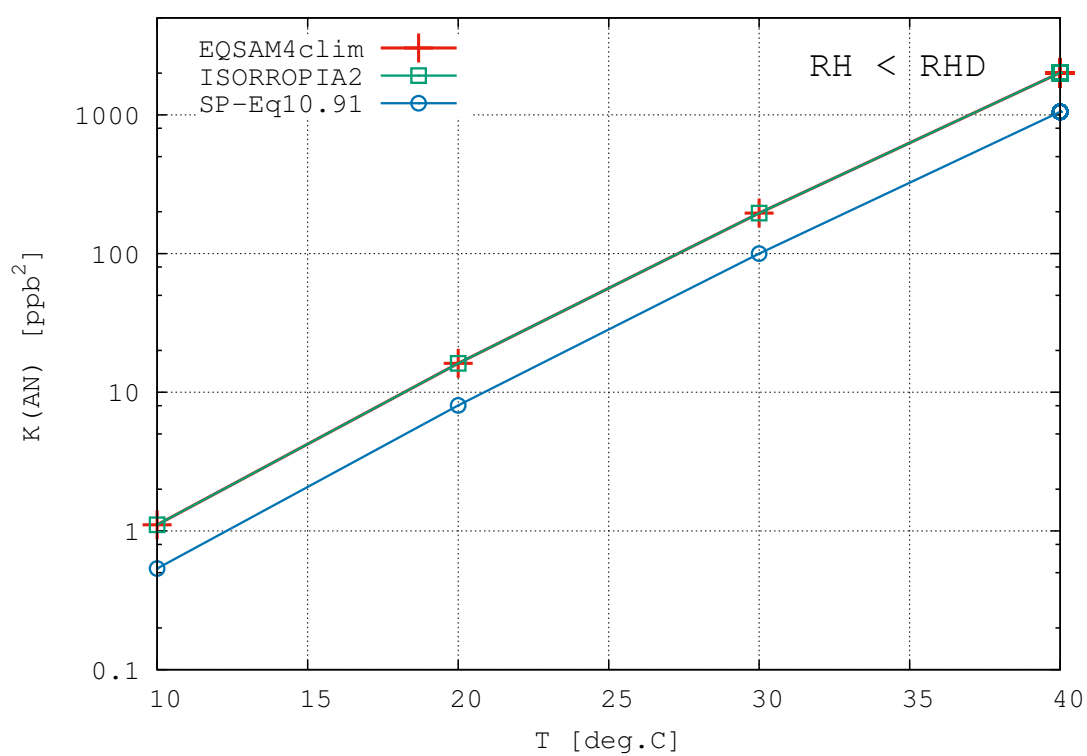


**Figure 1.**  $\text{NH}_4\text{NO}_3$  equilibrium dissociation constant as function of  $T$  at  $\text{RH} < \text{RH}(\text{AN})$ . Red crosses show the values of EQSAM4clim, green squares refer to ISORROPIA II and the blue circles show Eq. (10.91) of Seinfeld and Pandis (2006); see their Fig. 10.19, respectively.

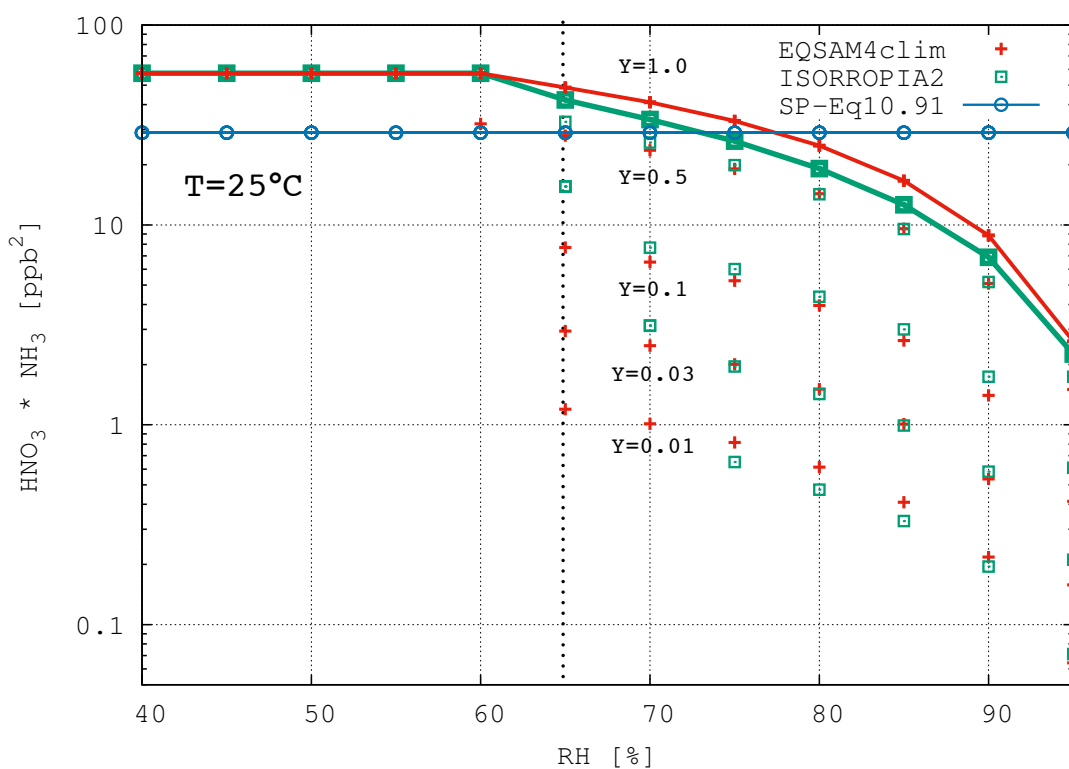


**Figure 2.**  $\text{NH}_4\text{NO}_3$  equilibrium dissociation constant as function of RH (at  $T = 298.15$  [K]) for various ionic strength factors ( $Y$ ) defined in Seinfeld and Pandis (2006); see their Fig. 10.21, respectively. Red crosses show the results of EQSAM4clim, green squares those of ISORROPIA II. The line-points refer to pure ammonium nitrate ( $Y = 1$ ). The vertical line at  $\text{RH} = 65$  [%] indicates the solid-liquid phase partitioning threshold for the mixed solution, shown in Seinfeld and Pandis (2006). The ordinate values refer to the product of  $[\text{NH}_3]_{(\text{g},\text{AN})} \times [\text{HNO}_3]_{(\text{g},\text{AN})}$  that are obtained at end of the gas-liquid-solid  $\text{NH}_4\text{NO}_3$ -partitioning of ISORROPIA II, and by Eq. (9) for EQSAM4clim.

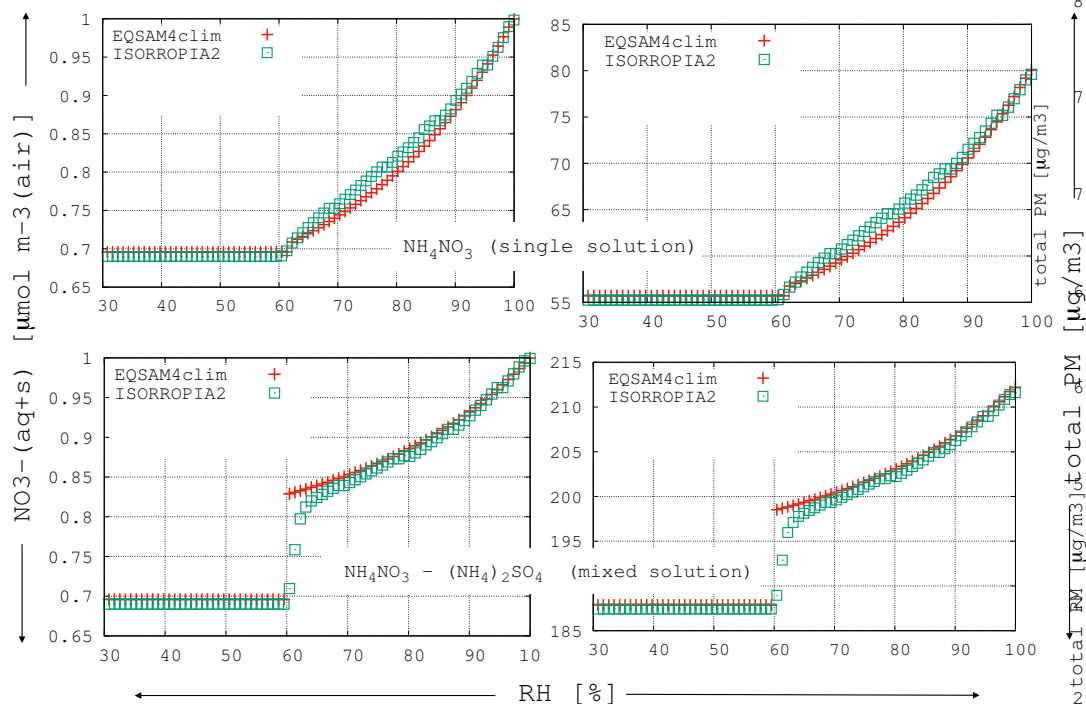


**Figure 3.** Results of EQSAM4clim (red crosses) and ISORROPIA II (green squares) for two idealized gas-liquid-solid partitioning examples: Single solute (binary) solution of pure  $\text{NH}_4\text{NO}_3$  (upper panels) and mixed solution of  $\text{NH}_4\text{NO}_3$  and  $(\text{NH}_4)_2\text{SO}_4$  with the concentration of each compound fixed to  $1 \mu\text{mol m}^{-3}(\text{air})$  at  $T = 298.15\text{K}$ . The left panels show the  $\text{NH}_4\text{NO}_3$  concentration in  $\mu\text{mol m}^{-3}(\text{air})$ , the right panels show the corresponding particulate mass  $\mu\text{g m}^{-3}(\text{air})$ . The mixed solution RHD described in Sect. 2.6 has been neglected for EQSAM4clim for this case, since this figure presents only an example for Sects. 2.4 and 2.5 (Sect. 2.6 is considered below).

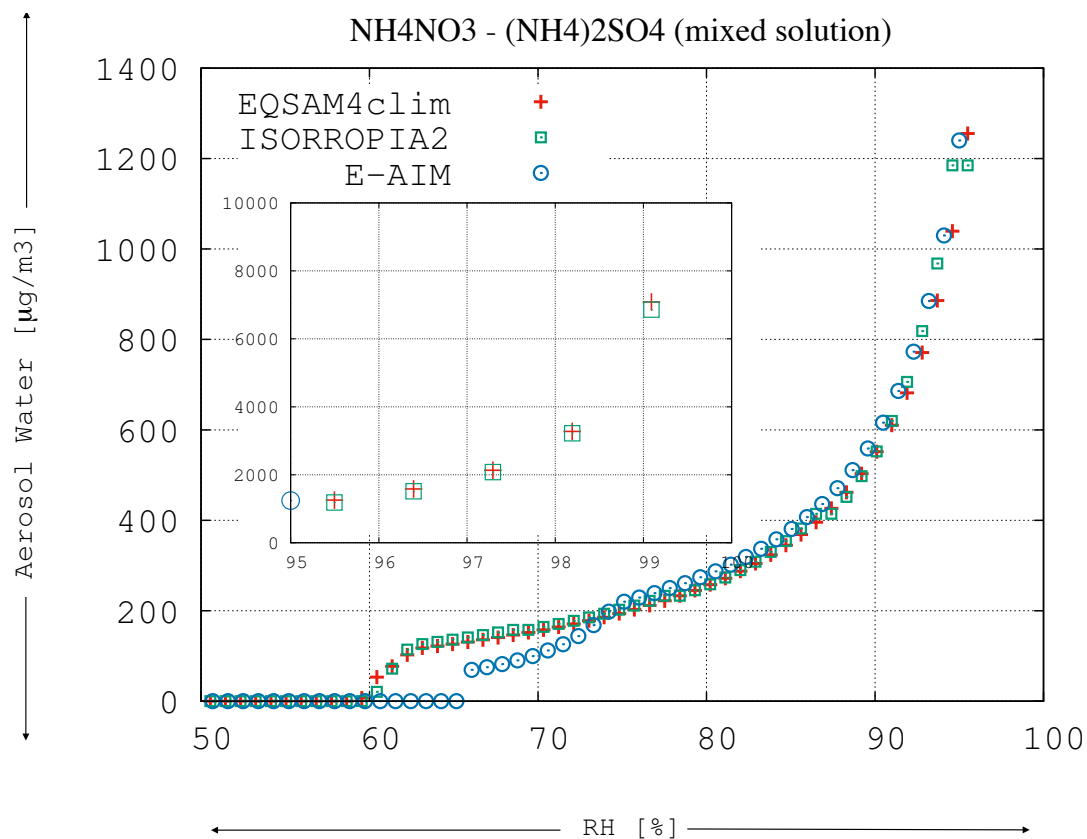


**Figure 4.** Results of EQSAM4clim (red crosses) and ISORROPIA II (green squares) for the total aerosol water mass  $m_{w,mix}$  [ $\text{kg m}^{-3}(\text{air})$ ] obtained by Eq. (22) for the mixed solution of  $\text{NH}_4\text{NO}_3$  and  $(\text{NH}_4)_2\text{SO}_4$  shown in Fig. 3 (lower panels). The results are shown for  $\text{RH} = 50\text{--}97$  [%] (large panels) and for the  $\text{RH} = 95\text{--}99.5$  [%] (small panel). The results of E-AIM (web version) (blue circles) are included for comparison. The mixed solution RHD has been obtained for EQSAM4clim from Eqs. (13)–(22) and are based on measured MDRH values for ISORROPIA II. The mutual deliquescence range of EQSAM4clim and ISORROPIA II (described in Sect. 2.6) differs from those of E-AIM (web version: <http://www.aim.env.uea.ac.uk/aim/aim.php>). This figure is extended by Fig. S3.

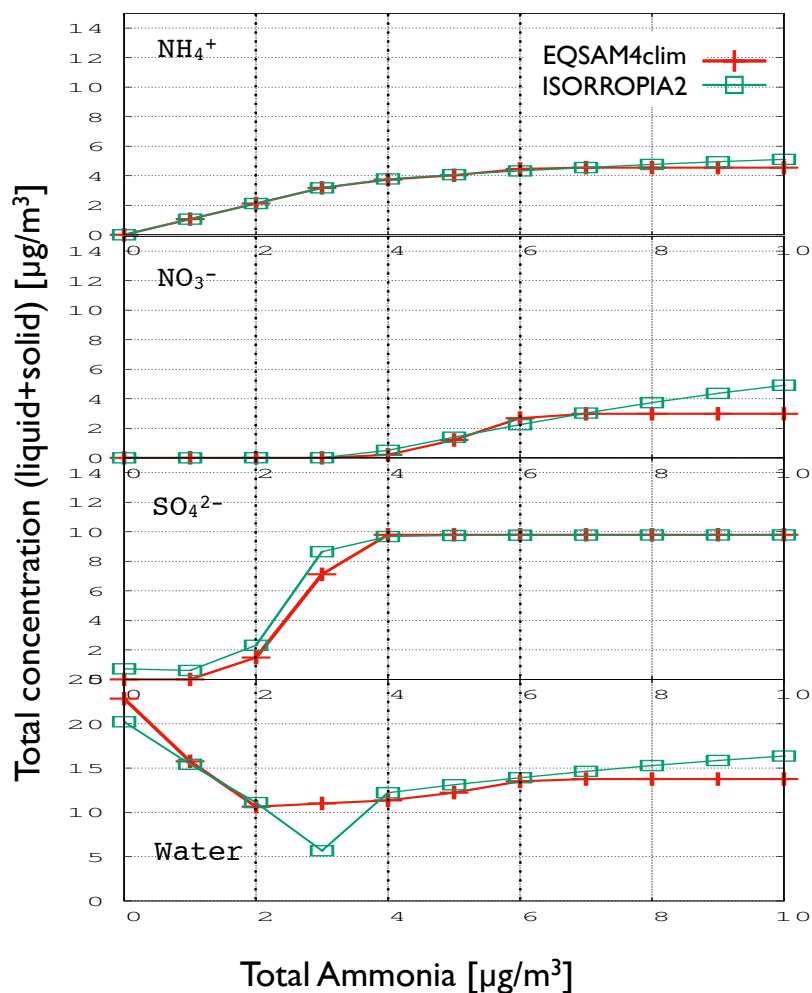


**Figure 5.** Mixed solution composition of  $\text{NH}_4\text{NO}_3$  and  $(\text{NH}_4)_2\text{SO}_4$  as a function of total ammonia at  $T = 298.15$  [K] and  $\text{RH} = 70$  [%], as defined in Seinfeld and Pandis (2006) for their Fig. 10.23. EQSAM4clim (red crosses) and ISORROPIA II (green squares) for  $[\text{TS}] = [\text{TN}] = 10$  [ $\mu\text{g m}^{-3}$ (air)]. This figure Note that at zero ammonia,  $\text{H}_2\text{SO}_4$  is extended by at a maximum; shown in Fig. S4.

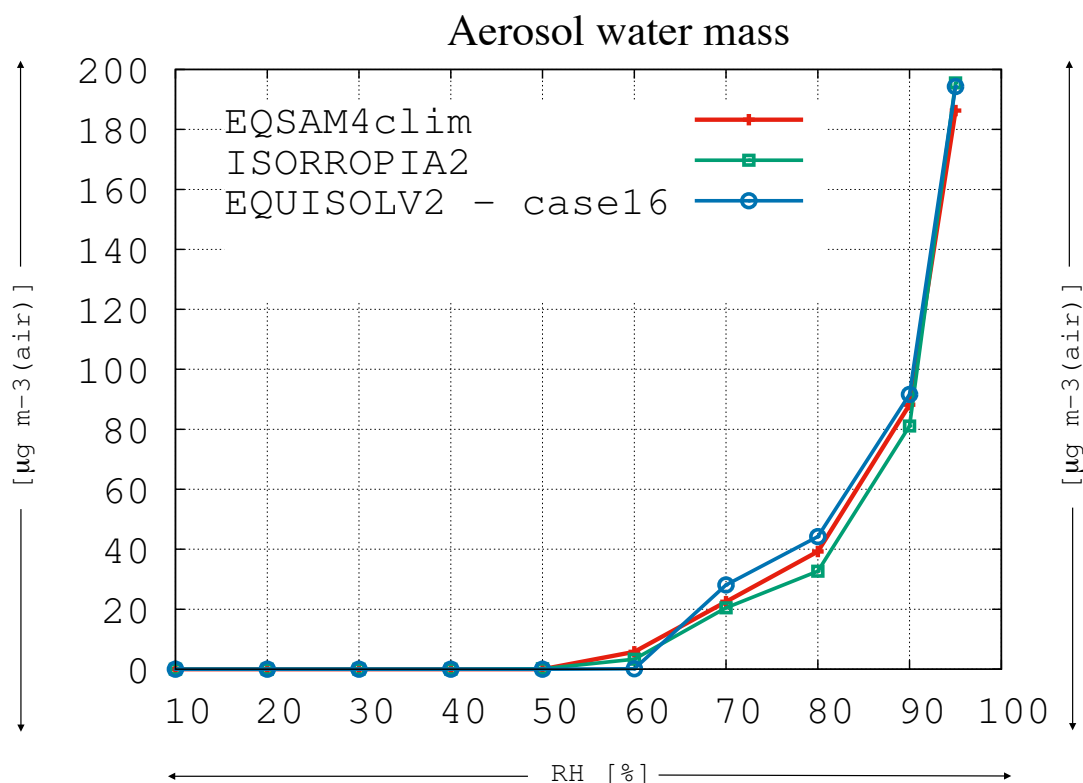


**Figure 6.** 20-Cases-EQUISOLV II Comparison – case 16. Bulk aerosol water mass as a function of RH for various-different sulfate molar ratios, fixed for the entire RH range (at constant  $T = 298.15$  K). The dry concentration ratios of sulfate are,  $\frac{t_{\text{NH}_4}}{t_{\text{SO}_4}} = 2.0$ ,  $\frac{t_{\text{NO}_3}}{t_{\text{SO}_4}} = 1.0$ ,  $\frac{t_{\text{NaCl}}}{t_{\text{SO}_4}} = 0.5$ ,  $\frac{t_{\text{K}}}{t_{\text{SO}_4}} = 0.04$ ,  $\frac{t_{\text{Ca}}}{t_{\text{SO}_4}} = 0.02$ ,  $\frac{t_{\text{Mg}}}{t_{\text{SO}_4}} = 0.01$  and corresponds to domain 1 of Table 2. This figure is extended to various (20 cases) sulfate molar ratios that are shown in Fig. S5 and correspond to Table 3 of Xu et al. (2009).

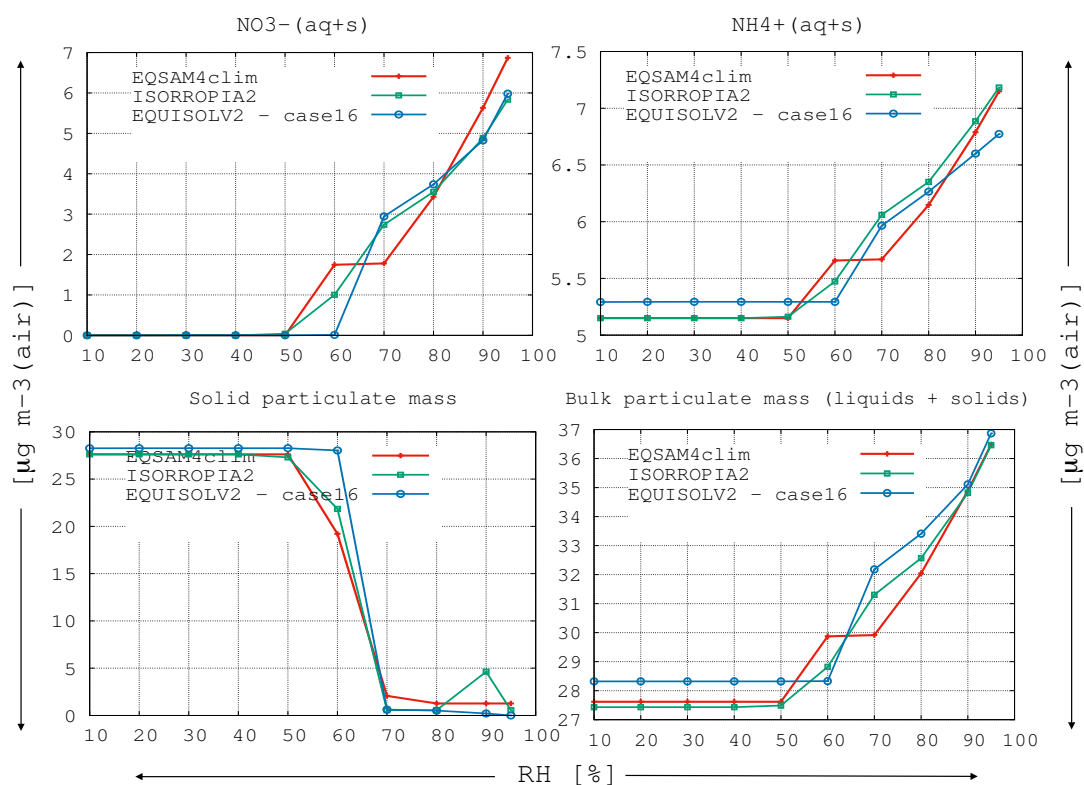


**Figure 7.** ~~20 Cases~~ EQUISOLV II Comparison – case 16. Bulk aerosol nitrate (ul), ammonium (ur), total solid PM (ll), liquid + solid PM (lr) as a function of RH for the sulfate molar ratios shown in Fig. 6. This figure is extended by Figs. S6 and S7.

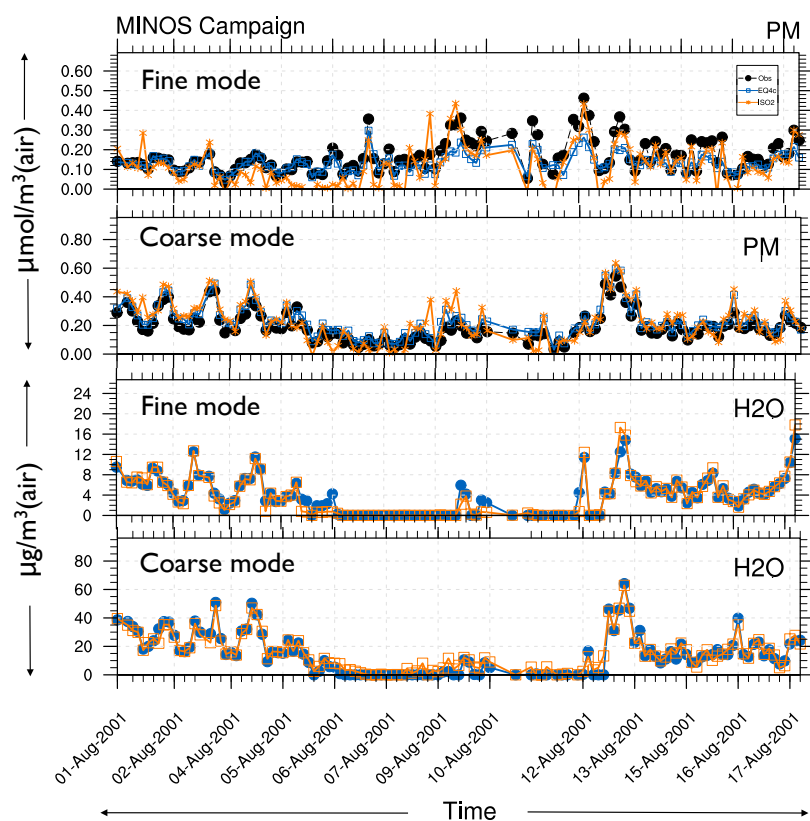


**Figure 8.** Observed and simulated total particulate matter [ $\mu\text{mol m}^{-3}(\text{air})$ ] and the predicted associated water mass [ $\mu\text{g m}^{-3}(\text{air})$ ] for the observed aerosol fine and coarse modes; EQSAM4clim (EQ4c), ISORROPIA II (ISO2), MINOS observations (black circles). This figure is extended to various other aerosol properties by Figs. S8 and S9 in the Supplement.

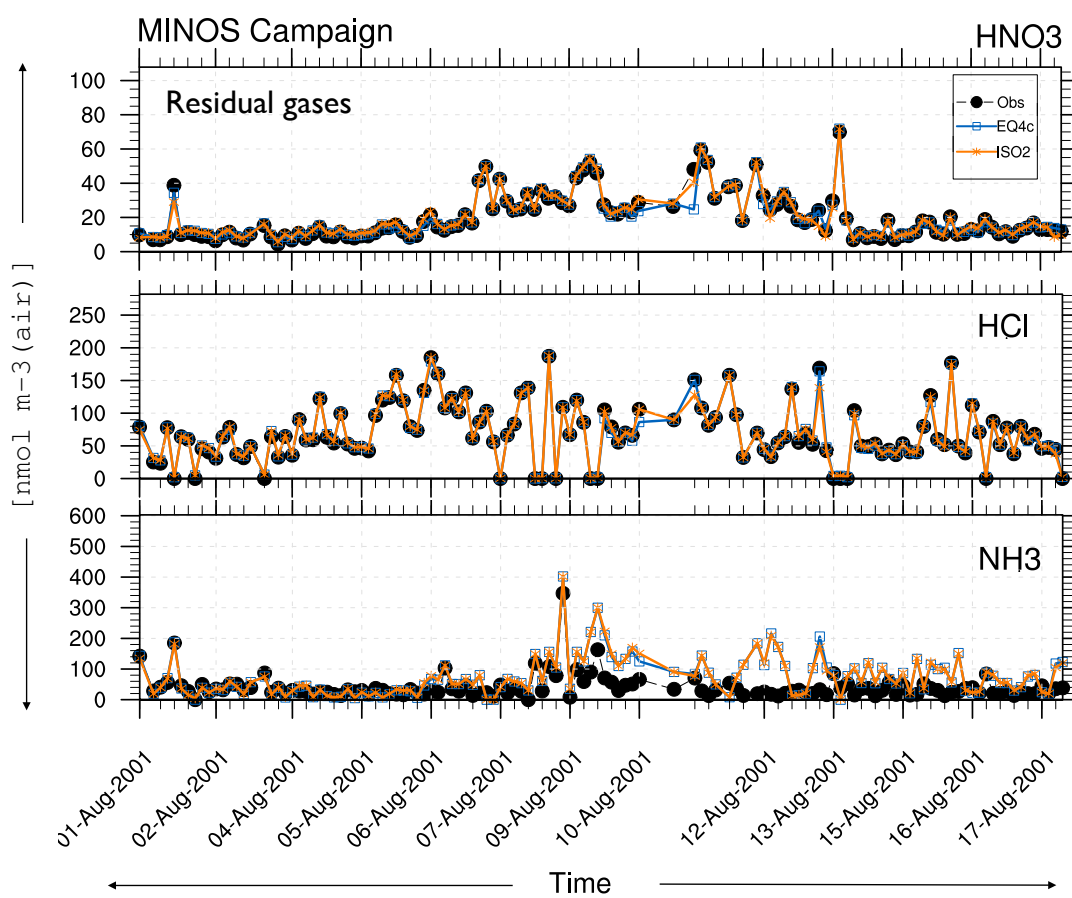


**Figure 9.** Residual gases [ $\mu\text{mol m}^{-3}(\text{air})$ ] corresponding to Fig. 8.

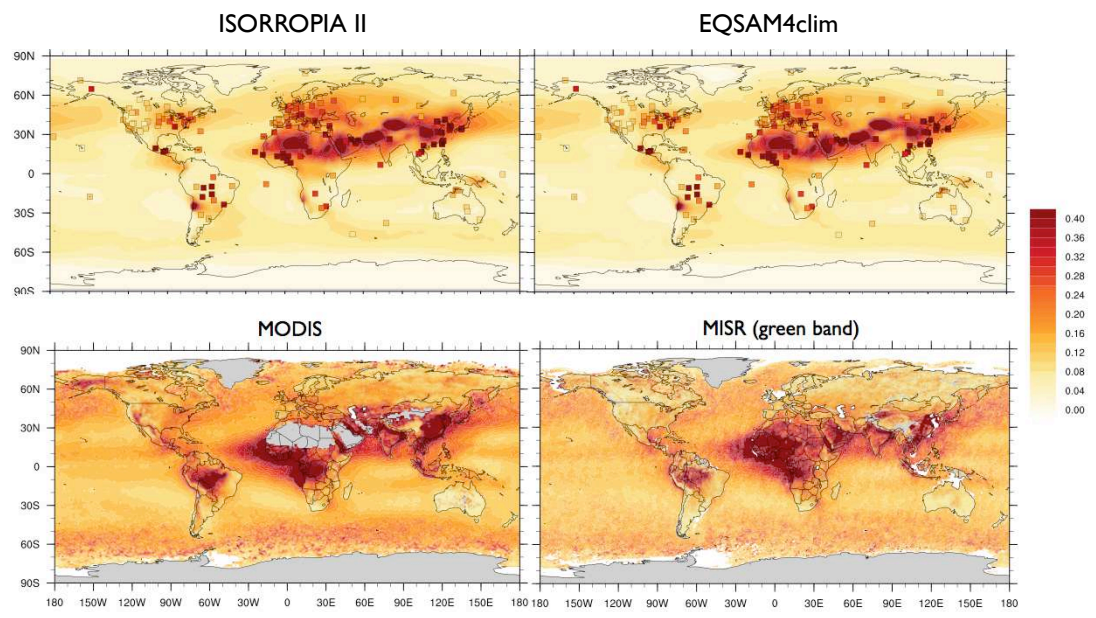


**Figure 10.** EMAC AOD vs. MODIS, MISR and AERONET (550 nm, annual mean 2005).

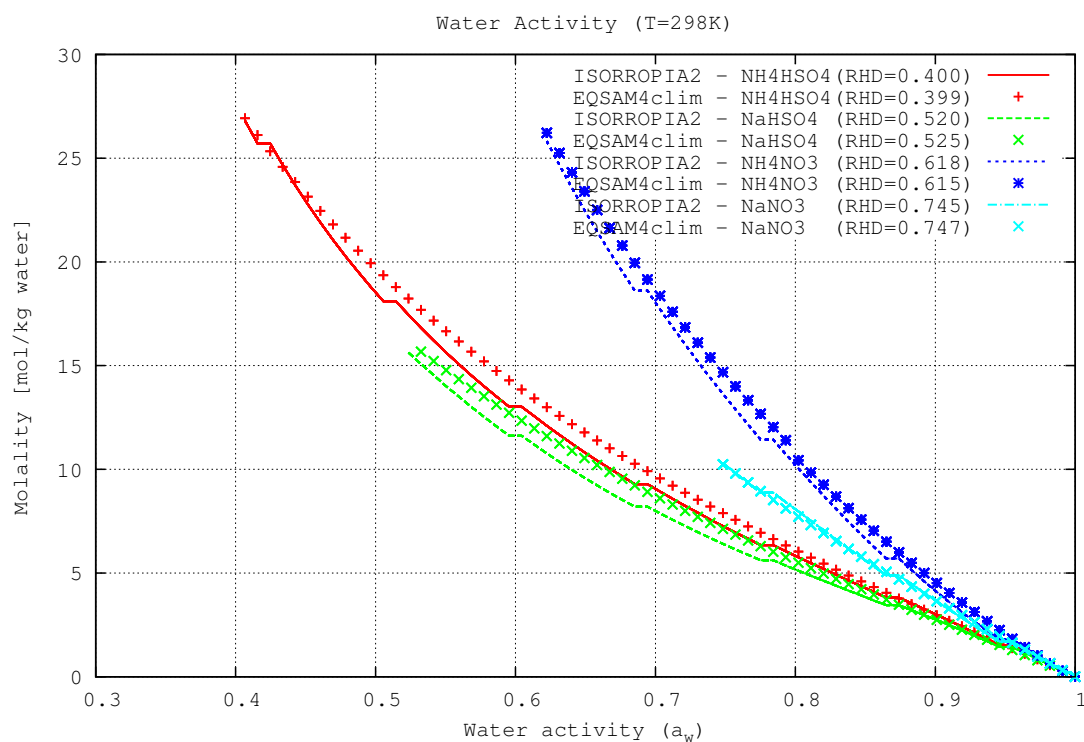


**Figure A1.** Single solute molality as a function of water activity for several electrolytes: (NH<sub>4</sub>)HSO<sub>4</sub>, NaHSO<sub>4</sub>, NH<sub>4</sub>NO<sub>3</sub>, NaNO<sub>3</sub> (at  $T = 298.15$  K) calculated with EQSAM4clim from Eqs. (A3) and (A6) compared to tabulated molality and RHD measurements of ISORROPIA II used to determine  $\nu_i$ .

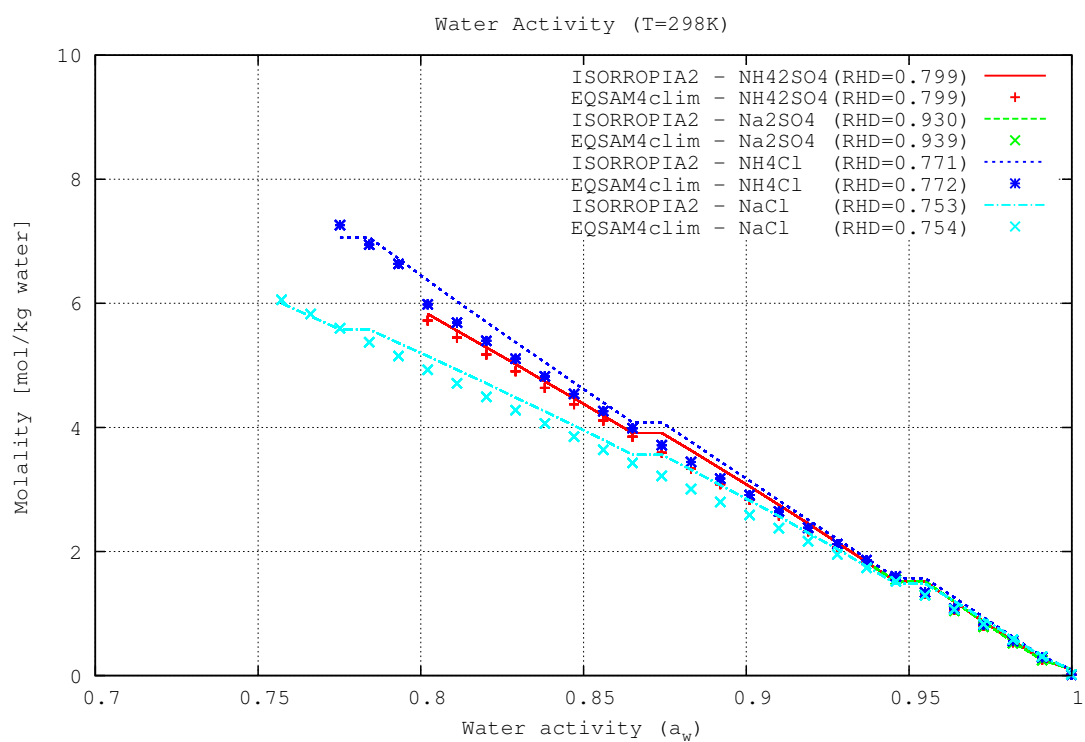


**Figure A2.** Fig. A1 continued for  $(\text{NH}_4)_2\text{SO}_4$ ,  $\text{Na}_2\text{SO}_4$ ,  $\text{NH}_4\text{Cl}$ ,  $\text{NaCl}$  (at  $T = 298.15\text{ K}$ ).

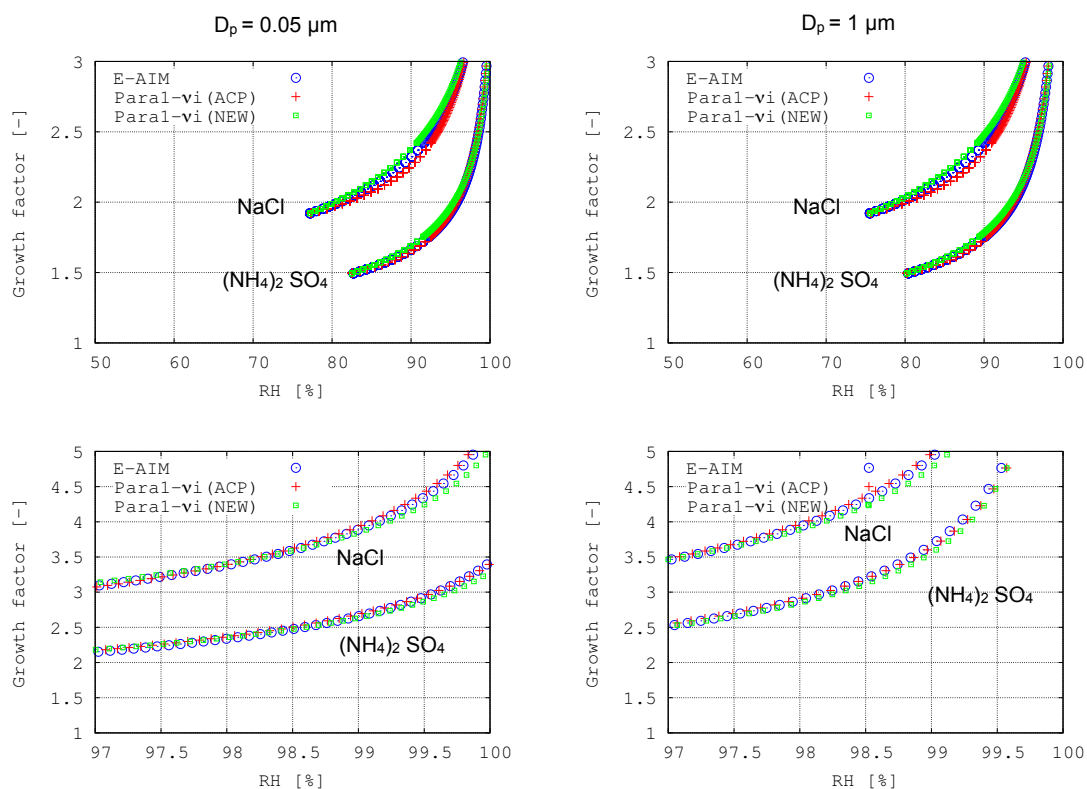


**Figure A3.** Growth factor of pure  $\text{NaCl}_{(cr)}$  and  $(\text{NH}_4)_2\text{SO}_{4(cr)}$  particles with a dry diameter  $D_s = 0.05 [\mu\text{m}]$  (UL) and  $D_s = 1 [\mu\text{m}]$  (UR) for  $\text{RH} \leq 97 [\%]$ . Lower panels show the corresponding values within the subsaturated regime, i.e.  $97 \leq \text{RH} \leq 100 [\%]$ . The results of the parameterization used by EQSAM4clim (labeled NEW) are compared to our ACP 2012 water activity,  $a_w$ -parameterization (labeled ACP, i.e., Para1 of Table 1 in M2012). The comparison includes the results of E-AIM and extends the corresponding figures of M2012.

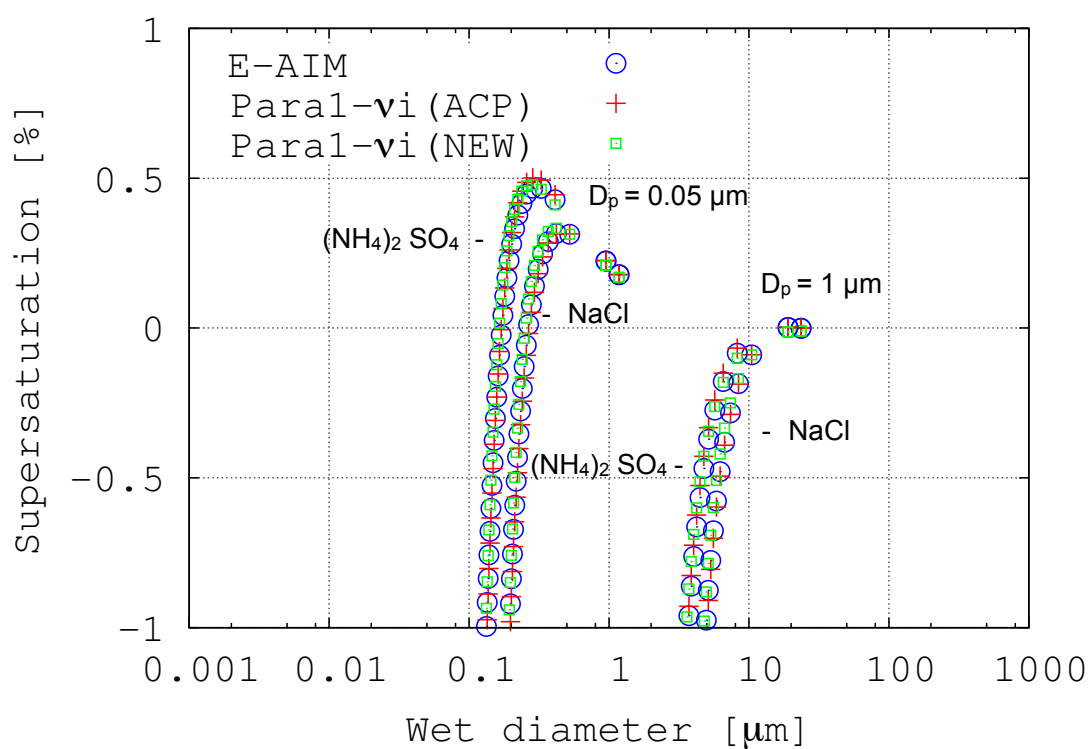


**Figure A4.** Wet particle diameter,  $D_{\text{wet}}$ , as a function of supersaturation for pure NaCl and  $(\text{NH}_4)_2\text{SO}_4$  aerosols with different dry diameters, i.e.  $D_s = 0.05$  and  $D_s = 1$  [ $\mu\text{m}$ ] as shown in Fig. 5 of M2012.  $S$  is defined as  $S = (s - 1) \times 100$  [%];  $s$  is the saturation = fractional RH.

# 1 S1 Examples – Semi-volatile compounds

2 The following three sub-sections provide detailed examples for semi-volatile compounds,  
 3 described in Sec. 2.4 (main text). The analytical solution is part of our new single  
 4 parameter gas-liquid-solid partitioning framework and applied in Sec. 3 to mixed aerosol  
 5 salt solutions through EQSAM4clim (see Appendix B and Sec. S2).

## 6 S1.1 Pure $\text{NH}_4\text{NO}_3$ –gas-solid equilibrium ( $\text{RH} < \text{RHD}$ )

7 Gas-solid equilibrium of pure ammonium nitrate;  $\text{NH}_4\text{NO}_3$  (index  $_{AN}$ ) with  $\text{RH} = 50\%$   
 8 and below the  $\text{RHD}_{AN} = 61.83\%$  (Table 1), as illustrated in Fig. 3. The partial pres-  
 9 sure product of gaseous ammonia,  $\text{NH}_3(\text{g})$ , and nitric acid,  $\text{HNO}_3(\text{g})$  must equal or exceed  
 10  $K_p(T)$  to allow the formation of solid ammonium nitrate,  $\text{NH}_4\text{NO}_3(\text{s})$ . This is described  
 11 by (R1) and the system can be solved with Eqs. (6–12). Note that in this case, only the  
 12 gas phase concentrations are required to solve (R1), since the concentrations of solids  
 13 are treated as unity. Here, all concentrations denoted by  $[\ ]$  are given in  $[\mu\text{mol}/\text{m}^3(\text{air})]$ ;  
 14 the EQSAM4clim computations (see Sec. S2) are performed in  $[\text{mol}/\text{m}^3(\text{air})]$ . For com-  
 15 parison with SP2006, we use ppbv. Units, e.g., in  $[\mu\text{mol}/\text{m}^3(\text{air})]$  can be converted to  
 16 ppbv by multiplication with the molar volume  $24.465 [\text{L}/\text{mol}]$ , and from  $[\mu\text{g}/\text{m}^3(\text{air})]$  by  
 17 additional division with the compounds molar mass,  $M_s$ .

18 At  $T_o = 298.15 \text{ K}$ ,  $P_o = 1 \text{ atm}$  and  $\text{RH} = 50\%$  (i.e.,  $\text{RH} < \text{RHD}_{AN}$ ), with  $M_s$  in  
 19 units of  $[\text{g}/\text{mol}]$  (and  $1 \text{ ppbv} = 1 \text{ nano Liter gas per 1 Liter air} = 1 \text{ micro Liter(gas) per}$   
 20  $\text{m}^3(\text{air})$ ), the unit conversion to  $[\text{ppbv}]$  from concentrations in  $[\mu\text{g}(\text{gas})/\text{m}^3(\text{air})]$  yields,  
 21 e.g., for  $\text{NH}_3(\text{g})=17.04$  and  $\text{HNO}_3(\text{g})=63.02$  (see example on p474 of SP2006):

- 22 •  $\text{NH}_3(\text{g}) : 17.04 [\mu\text{g}(\text{gas})/\text{m}^3(\text{air})]/17.04 [\text{g}/\text{mol}] \cdot 24.465 [\text{L}/\text{mol}] = 24.465 [\text{ppbv}]$
- 23 •  $\text{HNO}_3(\text{g}) : 63.02 [\mu\text{g}(\text{gas})/\text{m}^3(\text{air})]/63.02 [\text{g}/\text{mol}] \cdot 24.465 [\text{L}/\text{mol}] = 24.465 [\text{ppbv}]$

24 The partial pressure product is  $24.465^2 \approx 600 [\text{ppbv}^2]$  and at this  $T$  well above the  
 25 equilibrium value of  $K_{p,AN}(T) = 57.5 [\text{ppbv}^2]$  (Table 4; Fig. 1), but lower than the value  
 26 of  $655 [\text{ppbv}^2]$  given in SP2006, which corresponds to  $T = 308 [\text{K}]$ .

27 Following SP2006 for this dry case, the amount  $x [\text{ppbv}]$  of the gaseous concentration  
 28  $C_i [\text{ppbv}]$ , which could form a solid, can be directly computed by solving the equation:

$$\prod_{i=1}^n (C_i - x) = K_p(T) \quad (\text{S1})$$

29 For ammonium nitrate, (R1) yields a quadratic equation (with  $a \cdot x^2 - 2 \cdot b \cdot x + c = 0$ )  
 30  $(24.5 - x)(24.5 - x) = 57.5 [\text{ppbv}^2]$ , i.e.,  $x^2 - 49x + 543 = 0$ . And, upon solving (with  
 31  $x_{1,2} = 0.5 \cdot (-b \pm \sqrt{(b^2 - 4 \cdot a \cdot c)})/a$ ), i.e.,:  $x_1 = 0.5 \cdot (49 - \sqrt{(2401 - 4 \cdot 543)}) \approx 16.9 [\text{ppbv}]$ .  
 32 Note that the second solution ( $x_2 \approx 32.1$ ) is to be discarded, since its value is larger than  
 33 the actual  $C_i$  concentrations. Thus, an equal amount of  $16.9 [\text{ppbv}]$  of each  $\text{NH}_3(\text{g})$  and  
 34  $\text{HNO}_3(\text{g})$  and solid  $\text{NH}_4\text{NO}_3(\text{s})$  would be in equilibrium at this temperature and RH.  
 35 In terms of mass loadings, this corresponds to  $11.8$  and  $43.5$  and  $55.2 [\mu\text{g}/\text{m}^3(\text{air})]$ ,  
 36 respectively. The mass loadings of the corresponding residual (free) acids are:  $\text{NH}_3(\text{g}) =$   
 37  $(24.5 - 16.9)/24.5 \cdot 17 = 5.3$  and  $\text{HNO}_3(\text{g}) = (24.5 - 16.9)/24.5 \cdot 63 = 19.5 [\mu\text{g}/\text{m}^3(\text{air})]$ ,  
 38 respectively. This case is illustrated in Fig. 3 (see upper panels); Sec. 2.4.1 and 2.5.

## 39 S1.2 Pure $\text{NH}_4\text{NO}_3$ -gas-liquid equilibrium ( $\text{RH} \geq \text{RHD}$ )

40 Same as the first example, but with  $\text{RH} = 80\%$  and above the  $\text{RHD}_{\text{AN}}$ . In line with  
 41 the dry case (Sec. 2.4.1 and S1.1), the amount  $x$  [ppbv] of the gaseous concentration  
 42  $C_i$  [ppbv], which could form aqueous ammonium nitrate, can be directly computed with  
 43 Eqs. (6–12), if Eqs. (2–3) are used to solve  $K_p(T, \text{RH})$  (see Sec. 2.4.2). Then, (R-1) can  
 44 be analogously solved by using Eq. (S1) of the above dry case (Sec. S1.1):

$$\prod_{i=1}^n (C_i - x) = K_p(T, \text{RH}) \quad (\text{S2})$$

45 For instance, considering the gas-aqueous phase equilibrium of ammonium nitrate at  
 46  $\text{RH} = 80\%$ , by assuming that the water activity  $a_w$  equals  $\text{RH}/100$ , we can obtain a  
 47 value of 10 [ $\text{mol}_{\text{AN}}/\text{kg}(\text{H}_2\text{O})$ ] of the corresponding solute molality,  $\mu_{\text{AN}}(a_w = 0.8)$ , from  
 48 measurements, or from Eq. (A3) of Sec. A2; both are shown in Fig. A1 (in Sec. B). Using  
 49 Eq. (S2), with  $M_s = 0.08$  [ $\text{kg}/\text{mol}$ ] (of Table 1), we find for the solute mass fraction  
 50 (using Eq. A1) the corresponding value of:  $\chi_{\text{AN}}(a_w = 0.8) = (\frac{1}{0.08 \cdot 10} + 1)^{-1} = 0.44$ . And  
 51 from Eq. (3) we obtain,  $\text{COEF}_{\text{AN}}(\text{RH} = 80\%) = 2 \cdot 0.44^2 = 0.39$ , so that we can directly  
 52 obtain the required value for the T- and RH-dependent ammonium nitrate equilibrium  
 53 dissociation constant from Eq. (S2). At  $T = 298$  (using the value given in Table 4) we  
 54 accordingly find  $K_{p,\text{AN}}(T = 298, \text{RH} = 80\%) = 57.5 \cdot 0.39 \approx 22$  [ppbv<sup>2</sup>].

55 Mozurkewich (1993) gives a  $K_p^o(T_o)$  value of 42 [ppbv<sup>2</sup>], for which we would obtain at  
 56  $\text{RH} = 80\%$ ,  $41.9 \cdot 0.39 \approx 16$  [ppbv<sup>2</sup>] and accordingly  $\approx 12$  [ppbv<sup>2</sup>] for the value 29.9 [ppbv<sup>2</sup>],  
 57 which was originally given by Pilinis and Seinfeld (1987) (e.g., for use in the thermo-  
 58 dynamic model SEQUILIB). For EQSAM4clim, either  $K_p^o(T_o)$  value can be used. The  
 59 corresponding value of SP2006 (given in their example below Eq. (10.99)) is  $\approx 15$  [ppbv<sup>2</sup>].

60 Thus, knowing  $K_{p,\text{AN}}(T, \text{RH})$  one can directly solve the quadratic equation Eq. (S2)  
 61 for the aqueous phase analogously to Eq. (S1) for the dry case, without any iterations.  
 62 Using  $K_{p,\text{AN}}(T = 298, \text{RH} = 80\%) \approx 22$  [ppbv<sup>2</sup>] and the gas concentration for the solid  
 63 example given for Eq. (S1), we obtain for the equilibrium concentrations at  $\text{RH} = 80\%$ :  
 64  $(24.5 - x)(24.5 - x) = 57.5 \cdot 0.39 \approx 22$ , i.e.,  $x^2 - 49x + 578 = 0$ . And, upon solving the  
 65 quadratic equation  $x_1 = 0.5 \cdot (49 - \sqrt{(2401 - 4 \cdot 578)}) = 19.8$  [ppbv] (the second solution  
 66 has to be discarded, since its value is always larger than the actual  $C_i$  concentrations).  
 67 Using  $K_{p,\text{AN}}(T = 298, \text{RH} = 80\%) \approx 16$  [ppbv<sup>2</sup>] yields  $x = 20.5$  [ppbv], while using the ppb  
 68 values of the example of SP2006 gives  $(5 - x)(6 - x) = 15$ , i.e.,  $x^2 - 11x + 15 = 0$ , which  
 69 yields  $x_1 = 0.5 \cdot (11 - \sqrt{(121 - 4 \cdot 15)}) = 1.6$  [ppbv]. Thus, an equal amount 19.8 (20.5, 1.6)  
 70 [ppbv] of each  $\text{NH}_3(\text{g})$  and  $\text{HNO}_3(\text{g})$  and aqueous  $\text{NH}_4\text{NO}_3(\text{aq})$  would be in equilibrium at  
 71 this temperature and RH. The corresponding mass loadings of the residual (free) acids  
 72 are:  $(24.5 - 19.8)/24.5 \cdot 17 = 3.3$  and  $(4.7)/24.5 \cdot 63 = 12.1$  [ $\mu\text{g}/\text{m}^3(\text{air})$ ], respectively,  
 73 and those of the aqueous cation and anion are:  $\text{NH}_4^+(\text{aq}) = 19.8/24.5 \cdot 18 = 14.6$ , and  
 74  $\text{NO}_3^-(\text{aq}) = 19.8/24.5 \cdot 62 = 50.1$  [ $\mu\text{g}/\text{m}^3(\text{air})$ ]. The sum,  $14.6 + 50.1 = 64.7$  [ $\mu\text{g}/\text{m}^3(\text{air})$ ]  
 75 forms  $\text{NH}_4\text{NO}_3(\text{aq})$  and would be in equilibrium with  $\text{NH}_3(\text{g}) = 17.04$  and  $\text{HNO}_3(\text{g}) = 63.02$   
 76 [ $\mu\text{g}/\text{m}^3(\text{air})$ ] at  $T = 298.15$  [K] and  $\text{RH} = 80$  [%], while respectively 3.3 and 12.1  
 77 [ $\mu\text{g}/\text{m}^3(\text{air})$ ] of  $\text{NH}_3(\text{g})$  and  $\text{HNO}_3(\text{g})$  remain in the gas phase.

78 Compared to the solid case, the additional formation of  $64.7 - 55.2 \approx 9.5$  [ $\mu\text{g}/\text{m}^3(\text{air})$ ]  
 79  $\text{NH}_4\text{NO}_3$  corresponds to a change in RH from 50 to 80 [%]. Fig. 10.21 of SP2006 de-  
 80 picts the situation of the RH-dependent equilibrium partitioning. For comparison Fig. 2  
 81 (see line-points) and Fig. 3 (left part of the upper panels) reveals the situation for our  
 82 EQSAM4clim and the ISORROPIA II applications.

### 83 S1.3 EQSAM4clim algorithm: $\text{NH}_4\text{NO}_3$ -equilibrium

84 To provide a complete example for mixed solution cases with an analytical solution of  
 85 EQSAM4clim (Sec. 2.5), we consider Fig. 3 (Sec. S1.1–S1.2) in terms of the notation  
 86 of SP2006. For EQSAM4clim, we obtain the  $\text{NH}_4\text{NO}_3$ (*nro*) equilibrium concentration by  
 87 solving Eqs. (6–12), based on chemical domains (Table 2, Sec. 2.2) and the neutralization  
 88 reaction order (NRO, Table 3, Sec. 2.3).

#### 90 I. Single Solution, Dry/Wet Case (Fig. 3, upper panels)

91  
 92 For the single solution case shown in Fig. 3, we assume for the EQSAM4clim computa-  
 93 tions a total (gas+aerosol) cation and anion input concentration of 1 [ $\mu\text{mol}/\text{m}^3(\text{air})$ ], i.e.,  
 94 total ammonium  $[TA] = [\text{NH}_4^+]_{(nro,free)} = 1$  and total nitrate  $[TN] = [\text{NO}_3^-]_{(nro,free)} = 1$ .  
 95 For this sulfate neutral case (all other ions are zero), we apply domain D1. Solving  
 96 the NRO for D1 automatically yields only a single reaction, i.e., for  $\text{NH}_4\text{NO}_3$ , since all  
 97 other cation and anion products are zero, so that just one ion-pair combination can  
 98 exist. Considering the ion charge,  $[ZN] = [ZA] = 1$ , we can obtain from the prod-  
 99 uct  $[TA] \cdot [ZA]$  and  $[TN] \cdot [ZN]$  the corresponding maximum ammonium nitrate con-  
 100 centration  $[\text{NH}_4\text{NO}_3]_{(nro,max)} := \text{MIN}([TA] \cdot [ZA], [TN] \cdot [ZN]) = 1$  [ $\mu\text{mol}/\text{m}^3(\text{air})$ ],  
 101 which is possible for the input concentration with  $K_p(T, RH, Y) := 1$  (Sec. 2.5),  $T$   
 102 and  $RH$ . The temperature is fixed to  $T = 298.15$  K, the RH varies from  $RH = 30$   
 103 to  $RH = 100$  [%]. After solving the NRO, [TA] and [TN] are zero over the entire  
 104  $RH$ -range, since here the input concentrations are fixed to 1 [ $\mu\text{mol}/\text{m}^3(\text{air})$ ] for this  
 105 pure  $\text{NH}_4\text{NO}_3$  case (binary solution, upper left panel of Fig. 3). To solve a dry and  
 106 wet case, we again consider  $RH = 50$  [%] and  $RH = 80$  [%]. According to Table 1,  
 107 the  $RHD = 61.83$  [%] for  $\text{NH}_4\text{NO}_3$  so that at  $RH = 50$  [%] only the gas-solid equi-  
 108 librium partitioning needs to be considered, i.e., (R1), while at  $RH = 80$  [%] the  
 109 gas-liquid equilibrium partitioning, i.e., (R2), is relevant. In EQSAM4clim we solve  
 110 the equilibrium in molal scale. At  $T = 298.15$  K and  $RH = 50$  [%], conversion of  
 111  $K_p(T) = 57.46$  [ $\text{ppbv}^2$ ] (Table 4) to the molal scale yields (with  $K_p/(RT/P)^2$ ), i.e.,  
 112  $57.46$  [ $\text{ppbv}^2$ ]  $\cdot 10^{-18}/(8.314409/101325$  [ $\text{m}^3(\text{air})/\text{mol}/\text{K}$ ]  $\cdot 298.15$  [K]) $^2 = 57.46 \cdot 1.67^{-15} =$   
 113  $9.6 \cdot 10^{-14}$  [ $\text{mol}/\text{m}^3(\text{air})$ ] $^2$ . Solving Eqs. (6–12), we then obtain for the evaporative loss  
 114  $[x]$  [ $\mu\text{mol}/\text{m}^3(\text{air})$ ] of  $[\text{NH}_4\text{NO}_3]_{(nro,max)}$ :

115  $x = 0.5 \cdot \sqrt{(4 \cdot 9.6 \cdot 10^{-14})} = 0.31$  [ $\mu\text{mol}/\text{m}^3(\text{air})$ ], with  $[TA] = [TN] = 0$ . Thus, at  
 116  $RH = 50$  [%],  $\text{NH}_4\text{NO}_3(s,nro) = 1 - 0.31 \approx 0.69$  [ $\mu\text{mol}/\text{m}^3(\text{air})$ ], or  $0.69$  [ $\mu\text{mol}/\text{m}^3(\text{air})$ ]  
 117  $\cdot 80$  [ $\text{g}/\text{mol}$ ]  $\approx 55.2$  [ $\mu\text{g}/\text{m}^3(\text{air})$ ] for the total particulate matter (PM). For the aque-  
 118 ous phase at  $RH = 80$  [%], we analogously obtain  $\text{NH}_4\text{NO}_3(aq,nro)$ . According to the  
 119 above example (Sec. S1.2),  $K_{p,AN}(T = 298, RH = 80\%) = 57.5 \cdot 0.39 \approx 22$  [ $\text{ppbv}^2$ ], so  
 120 that we get;  $= 22 \cdot 1.67^{-15} = 3.7 \cdot 10^{-14}$  [ $\text{mol}/\text{m}^3(\text{air})$ ] $^2$  and  $x = 0.5 \cdot \sqrt{(4 \cdot 3.7 \cdot 10^{-14})}$   
 121  $\approx 0.19$  [ $\mu\text{mol}/\text{m}^3(\text{air})$ ]. This yields  $\text{NH}_4\text{NO}_3(aq,nro) \approx 0.81$  [ $\mu\text{mol}/\text{m}^3(\text{air})$ ], or for the  
 122 total PM  $\approx 0.81$  [ $\mu\text{mol}/\text{m}^3(\text{air})$ ]  $\cdot 80$  [ $\text{g}/\text{mol}$ ]  $\approx 64.6$  [ $\mu\text{g}/\text{m}^3(\text{air})$ ]. These values refer  
 123 respectively to the (upper) left and right panels of Fig. 3, and are close to the values of  
 124 ISORROPIA II, which are independently computed with a different approach.

#### 126 II. Mixed Solution, Dry/Wet Case (Fig. 3, lower panels)

127  
 128 For the mixed solution case shown in Fig. 3, we assume for the EQSAM4clim com-  
 129 putations a total (gas+aerosol) cation and anion input concentration ( $[\mu\text{mol}/\text{m}^3(\text{air})]$ )

130 of total ammonium  $[TA] = [NH_4^+]_{(nro,free)} = 3$ , total nitrate  $[TN] = [NO_3^-]_{(nro,free)} = 1$ ,  
 131 and total sulfate  $[TS] = [SO_4^{2-}]_{(nro,free)} = 1$ . This sulfate case also falls into domain D1,  
 132 since other ions are zero. Solving the NRO for D1 yields two reactions. Considering the  
 133 ion charge,  $[ZN] = [ZA] = 1$  and  $[ZS] = 2$ , we can directly obtain from the NRO and  
 134 the products  $[TA] \cdot [ZA]$ ,  $[TN] \cdot [ZN]$  and  $[TS] \cdot [ZS]$  the corresponding maximum  
 135 concentrations of ammonium sulfate and ammonium nitrate, which is possible for the  
 136 input concentration with  $K_p(T, RH, Y) := 1$  (Sec. 2.5 and S1.3-I):

- 137 1.  $[TA] \cdot [ZA] = 3$  and  $[TS] \cdot [ZS] = 2$ :  
 138  $[(NH_4)_2SO_{4(nro,max)}] := MIN([3], [2]) = 1$
- 139 2.  $[TA = 3 - 2 = 1] \cdot [ZA = 1] = 1$  and  $[TN = 1] \cdot [ZN = 1] = 1$ :  
 140  $[NH_4NO_{3(nro,max)}] := MIN([1], [1]) = 1$

141 Extending our above example calculation (Sec. S1.3-I) to the mixture of  $NH_4NO_3$  of  
 142  $1 \mu mol/m^3(air)$  of each  $NH_4NO_3$  and  $(NH_4)_2SO_4$  (lower left panel of Fig. 3), we compute  
 143 the dry ( $RH = 50$  [%]) and wet ( $RH = 80$  [%]) case. For  $NH_4NO_3$ , the RHD= 61.83 [%]  
 144 and for  $(NH_4)_2SO_4$  the RHD= 79.97 [%] (Table 1), so that at  $RH = 50$  [%] again only  
 145 the gas-solid equilibrium partitioning needs to be considered. Note that mixed solution  
 146 effects described in Sec. 2.6 are not considered for the RHD in this example, but they  
 147 are considered for the gas-liquid and liquid-solid equilibrium partitioning and associated  
 148 aerosol water uptake examples presented in Sec. 3.

149 For the mixed solution case, the computation is similar to that discussed above  
 150 (Sec. S1.3-I), only the ionic strength factor needs to be included for the wet case. For the  
 151 dry case, the solid equilibrium concentration,  $NH_4NO_{3(s,nro)}$ , is identical, since  $Y := 1$   
 152 (the ionic strength correction factor is defined only for solutions). The total dry aerosol  
 153 mass therefore is the sum of the  $NH_4NO_{3(s,nro)}$  (from above) and  $(NH_4)_2SO_{4(s,nro)}$  masses,  
 154 i.e.,  $PM \approx 55.2 + 132.2 = 187.4 \mu g/m^3(air)$ . For the aqueous case, we obtain  $Y$  from  
 155 Eq. (4) (as used for Eq. 5), i.e., we obtain for  $1 \mu mol/m^3(air)$  of each,  $NH_4NO_{3(aq,max,nro)}$   
 156 and  $(NH_4)_2SO_{4(aq,eq)}$ ,  $Y = \frac{1}{1+3 \cdot 1} = 0.25$ . Using further the above (Sec. S1.2) value  
 157 for  $\mu_{AN}(a_w = 0.8) \approx 10 [mol_{AN}/kg(H_2O)]$  (Fig. A1), we compute the solute mass frac-  
 158 tion again from Eq. (A1) as  $\chi_{AN}(a_w = 0.8) = (\frac{1}{0.08 \cdot 10} + 1)^{-1} = 0.44$ . Then, Eqs. (3)  
 159 and (5) yield  $COEF(RH, Y) = 2 \cdot 0.44^2 \approx 0.39$  and  $Y^{0.8} = 0.25^{0.8} = 0.33$ , so that  
 160  $K_{p,AN}(T = 298, RH = 80\%, Y = 0.25) = 57.5 \cdot 0.39 \cdot 0.33 = 7.4 [ppbv^2]$ , or  $7.4 \cdot 1.67^{-15}$   
 161  $= 1.24 \cdot 10^{-14} [mol/m^3(air)]^2$ . Solving Eqs. (6–12), we then again obtain for the evapo-  
 162 rative loss  $[x] \mu mol/m^3(air)$  of  $[NH_4NO_{3(nro,max)}]$ :

163  $x = 0.5 \cdot \sqrt{4 \cdot 1.24 \cdot 10^{-14}} \approx 0.11 \mu mol/m^3(air)$ , with  $[TA] = [TN] = 0$ . Thus,  
 164 at  $RH = 80$  [%],  $NH_4NO_{3(aq,nro)} = 1 - 0.11 \approx 0.89 \mu mol/m^3(air)$ , or for the total (dis-  
 165 solved)  $PM \approx 0.89 \mu mol/m^3(air) \cdot 80 [g/mol] + 132.2 \mu g/m^3(air) = 203.4 \mu g/m^3(air)$ .  
 166 These values refer to the (lower) left and right panels of Fig. 3, respectively, and are also  
 167 close to the results of ISORROPIA II, despite the distinctly different approaches.

## 168 S2 Computational algorithm of EQSAM4clim

169 The EQSAM4clim computational algorithm is summarized as follows (see Fig. S2.2-S1):

- 170 • EQSAM4clim (v09), described in Sec. B, considers the salt compounds listed in Ta-  
 171 ble 1. To calculate the gas-liquid-solid partitioning, a pre-calculated (constant)  $\nu_i$

172 coefficient is used for each compound (ion-pair), which is obtained from a small set  
 173 of thermodynamic data: stoichiometric coefficient  $\nu_s$  [-], the ion-pair charge  $Z_s$  [-],  
 174 the single solute parameter  $\nu_i$  [-], the mass fraction solubility  $W_s$  [%], the molar  
 175 mass  $M_s$  [kg/mol], the density  $D_s$  [kg/m<sup>3</sup>], the RHD( $T_o$ ) [-] at reference tempera-  
 176 ture  $T_o = 298.15$  [K] and the corresponding temperature coefficients,  $T_{coef(RHD)}$  [-].  
 177 For all salt compounds,  $\nu_i$  has been pre-determined with the bi-section method by  
 178 the procedure of solving Eq. (5b) of M2012 (Eq. A6 in Appendix A4), using mea-  
 179 surements of  $W_s$ -RHD( $T_o$ ) (single data pairs) at  $T_o$ , which are listed with  $\nu_i$  in  
 180 Table 1. The required RHD values, including T-coefficients, have been taken from  
 181 ISORROPIA II for a consistent comparison (Fountoukis and Nenes, 2007). All  
 182 other data of Table 1 have been taken from the CRC Handbook of Chemistry and  
 183 Physics (2006).

184 • The EQSAM4clim algorithm starts with the assignment of two internal loop param-  
 185 eters: An outermost loop, considering e.g., vertical model levels, and an innermost  
 186 vector loop for e.g., the longitude-latitude grid box that contains the input-data  
 187 for a given time-step. Both loops are scalable and can be externally determined  
 188 depending on the climate model set-up, e.g., to best match the cache of the com-  
 189 pute nodes. The consideration is optional and can be controlled in the subroutine  
 190 call. The actual computations are structured in blocks, which are fully sequen-  
 191 tial. Each computational block has its own vector loop with the compound specific  
 192 logic around it, so that loops can be fully optimized by the compiler and iterations  
 193 between different computational blocks are avoided. All computational blocks are  
 194 within an outermost loop (for this version).

195 • The first two computational blocks (out of 15) assign the T [K] and RH [0–1] data,  
 196 as well as the lumped cations and anion concentrations [mol/m<sup>3</sup>(air)]. Further, the  
 197 total cation and anion concentration charge is computed and a logical switch for each  
 198 compound is defined. Thus, we assume that a compound can be formed only, if the  
 199 product of the required cation and anion concentration is non-zero. This compound  
 200 specific flag is subsequently used to skip the computation of individual compounds,  
 201 which may not be present at the considered model time step. The flag is applied  
 202 to all computational blocks which have an outer compound loop. In case all cation  
 203 and anion concentrations are zero, i.e., the total cation charge equals (or is below)  
 204 REALZERO = tiny(0.\_dp) (with dp = SELECTED\_REAL\_KIND(12,307)), none of  
 205 the compounds could form and we therefore skip all computations. Depending on  
 206 the EMAC model set-up and the number of compounds considered, this may happen  
 207 for instance in remote locations such as the upper stratosphere. Both options are  
 208 merely included to minimize the overall computational burden.

209 • To further minimize the CPU time, the next computational block (3) defines:

- 210 – Whether solids are excluded or included, i.e., the hysteresis loop. The criteria  
 211 depend on the presence of aerosol water of the previous time step. In case  
 212 aerosol water is not present, the aerosol is assumed to be dry and the water  
 213 uptake is calculated based on RH and RHD thresholds. Otherwise, gas-liquid  
 214 partitioning is considered and the water uptake is calculated without RHD  
 215 thresholds, assuming the aerosol phase to be metastable.
- 216 – The domain that needs to be considered. Similar to ISORROPIA II, we con-  
 217 sider a domain approach (Sec. 2.2). But the approach used here only depends

218 on the input concentration ratio of total cations (tCAT) to total sulfate anions  
219 (tSO<sub>4</sub>), which is more elementary compared to the domain approach used in  
220 ISORROPIA II and is similar to the one used in the original EQSAM code  
221 (Metzger et al., 2002). Table 2 lists the domains used to characterize the  
222 potential sulfate aerosol neutralization levels.

- 223 • The next two computational blocks initialize the internal arrays, including all out-  
224 put fields, while block (5) defines the neutralization reaction order for all com-  
225 pounds that may form for a given domain during the cation-anion neutralization.  
226 The compound’s indices are ranked according to a preferred neutralization (from  
227 left to right). The domain dependent neutralization order is shown in Table 3.
- 228 • Computational block (6) solves the compound’s solute molality  $\mu_s$  from Eq. (A3),  
229 by optionally including the Kelvin-term. To avoid iteration, we take a two-step  
230 approach / approximation (see Appendix B):
  - 231 – Step one:  $K_e = 1$ , and  $B = 0$  to obtain the initial  $\mu_s$  from Eq. (A3).
  - 232 – Step two, repeated three times:  $\mu_s$  from previous iteration is used to calculate  
233  $K_e$  from Eq. (A7),  $\chi_s$  from Eq. (A1),  $B$  from Eq. (A4). Then a new  $\mu_s$  is  
234 obtained from Eq. (A3).

235 Note that we sequentially solve the equations three times, whereby we only loop  
236 over those compounds of Table 1 that are allowed to form and those compounds  
237 that have a non-zero input ion-pair concentration (determined by block 2).

- 238 • The next computational block (7) calculates the temperature dependency of the  
239 RHD from Eq. (A5) and optionally considers the Kelvin effect according to Eq. (A7).
- 240 • In computational block 8, the actual cation-anion neutralization reactions are solved  
241 assuming chemical equilibrium. Based on the pre-defined reaction order the input  
242 cation and anion concentrations are balanced (neutralized) by looping over all com-  
243 pounds those cation-anion product is above REALZERO. As a result, the cation  
244 and anion concentrations subsequently decrease in favor of the concentrations of  
245 the corresponding compounds, independent of any solvent and solute activity.  
246 Within the same loop, we calculate the total solute activity and store the RHD val-  
247 ues only for the compound’s that have a non-zero concentration. This information  
248 is subsequently used to analytically solve the liquid-solid partitioning.
- 249 • Computational block 9 approximates the mixed solution RHD from Eqs. (18-21).
- 250 • Thus far, all compounds have been treated as non-volatile and are assumed to reside  
251 in the aqueous phase. Computational block (10) solves the gas-liquid or gas-solid  
252 partitioning for the two semi-volatile compounds, NH<sub>4</sub>NO<sub>3</sub> and NH<sub>4</sub>Cl, that may  
253 be present in the sulfate neutral / poor (D1) domain (Sec. 2.4). Within one loop,  
254 Eqs. (2-5) are computed and the reactions (Eq. R2) are sequentially solved. In case  
255 the RH is below the semi-volatile compound’s RHD, Eq. 1 is used.
- 256 • The liquid-solid partitioning is calculated for all salt compounds in computational  
257 block 11 from the weighted mixed solution approach, Eqs. (13-21), described in  
258 Sec. 2.6. Each compound is treated as solid (instantaneously precipitated from the

259 solution) in case the RH is below the compound's RHD (binary solution), or in case  
260 of mixed solutions below the weighted RHD.

- 261 • Within computational block 12 all partial aerosol water mass are calculated from  
262 Eq. (22) for those compounds with a non-zero aqueous phase concentration. The  
263 total water mass is obtained from the sum of all partial water masses (Sec. 2.7).
- 264 • Computational block 13 estimates the final  $H^+$  concentration  $[mol]$  from the dif-  
265 ference of the total anion and cation concentrations. Within EMAC/GMXe the  
266  $H^+$  concentration is recalculated for both EQSAM4clim and ISORROPIA II to ac-  
267 count for the changes in the aerosol precursor gas concentrations, which may result  
268 from the size-dependent condensation of  $HNO_3$ ,  $HCl$  and  $NH_3$  and  $H_2SO_4$  on the  
269 pre-existing aerosol surfaces (see Pringle et al., 2010a).
- 270 • Finally, the residual gases are calculated within computational block 14 from the  
271 remaining ion concentrations based on the implicit assumptions that: (i) Unneu-  
272 tralized  $NH_4^+$  will instantaneously be fully vaporized to yield  $NH_3$ , unneutralized  
273  $NO_3^-$  yields  $HNO_3$  and unneutralized  $Cl^-$  yields  $HCl$ . (ii) In addition, unneutral-  
274 ized  $SO_4^{2-}$  is assumed to yield  $H_2SO_4$ , which is however treated as non-volatile;  
275 vaporization of  $H_2SO_4$  is considered within GMXe (Brühl et al., 2012).  $H_2SO_4$   
276 contributes to the water uptake (assuming the solute molality of  $(NH_4)_3H(SO_4)_2$ ).
- 277 • The last computational block (15) prepares the model output, which is user specific  
278 and can be individually extended or configured to write out all aerosol properties.

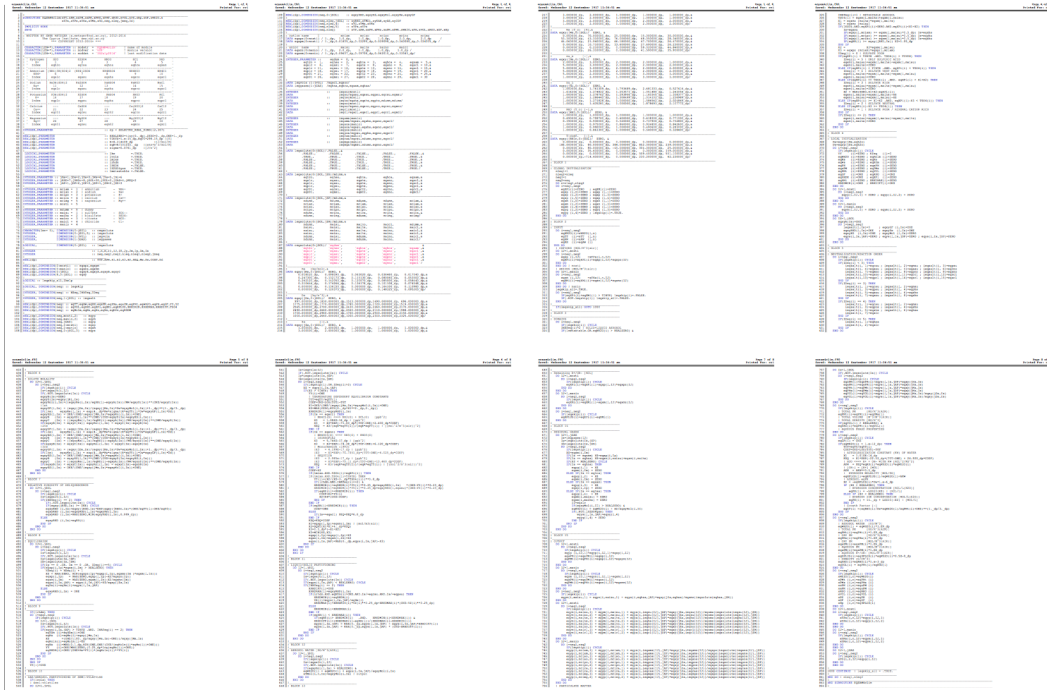


Figure S1: EQSAM4clim computational algorithm (code length overview, no details).

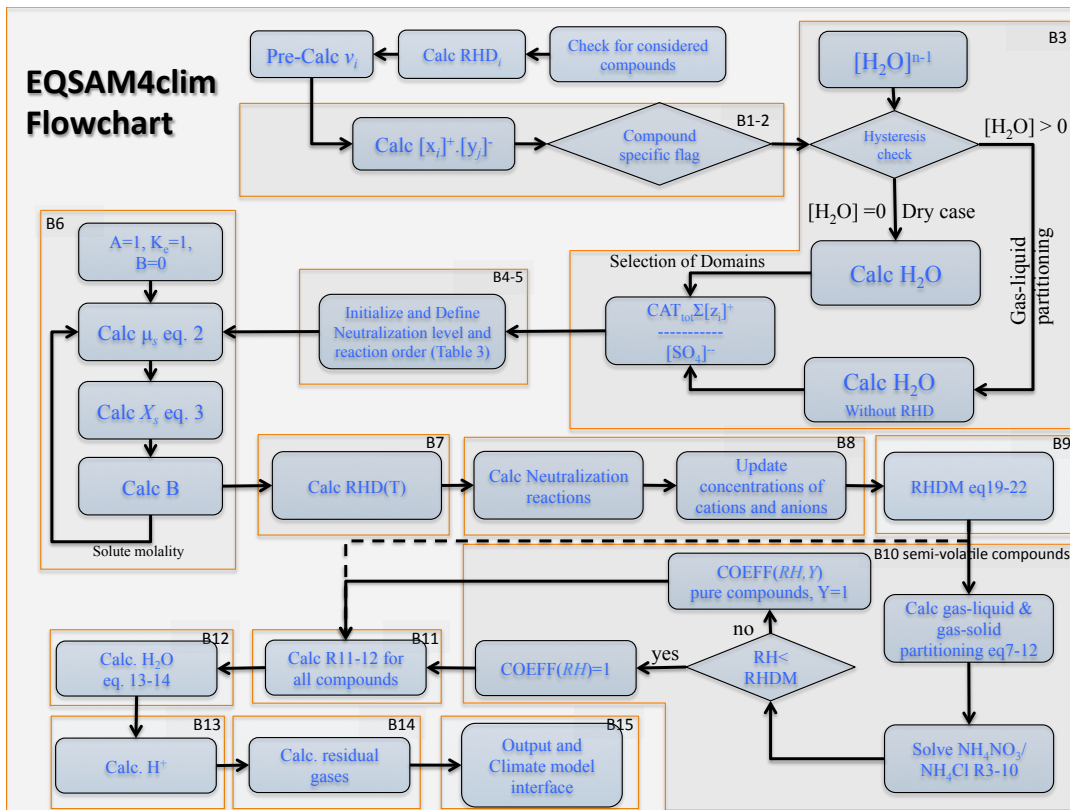


Figure S2.1: EQSAM4clim flowchart.

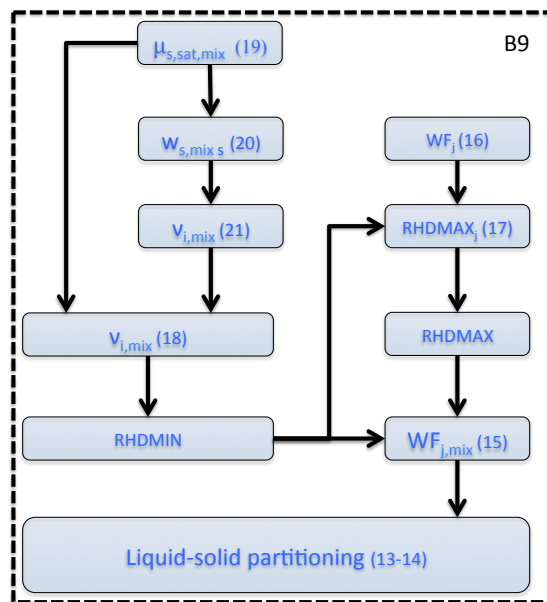


Figure S2.2: EQSAM4clim flowchart (B9): Calculation of mixed solution RHD (Sect. 2.6).

## 279 **S3 Extended Applications**

280 This section extends/complements the results shown in Sec. 3:

- 281 1. Fixed solute concentrations (9 cases): ISORROPIA II and E-AIM  
282 (see main text, Sec. 3.1)
- 283 2. Variable ammonia concentration: ISORROPIA II and Seinfeld and Pandis (2006)  
284 (see main text, Sec. 3.2)
- 285 3. Variable solute concentrations (20 cases): ISORROPIA II and EQUISOLV II  
286 (see main text, Sec. 3.3)
- 287 4. Field observations (MINOS campaign, 184 cases): ISORROPIA II  
288 (see main text, Sec. 3.4)

### 289 **S3.1 Fixed solute concentrations**

290 Figure S3 extends the aerosol water mass calculations shown in Figure 4 (see Sec. 3.1) to 9  
291 binary and mixed solution cases with fixed aerosol concentrations. The results are based  
292 on the full gas-liquid-solid partitioning and compare the calculations of EQSAM4clim  
293 with ISORROPIA II and E-AIM, with each (dry) compound concentration fixed to  
294  $1 \mu\text{mol}/\text{m}^3(\text{air})$ . The panels of Figure S3 show (from left to right, top-down):

- 295 • single solute solutions:  
296 (1.) NaCl; (2.)  $(\text{NH}_4)_2\text{SO}_4$ ; (3.)  $\text{NH}_4\text{NO}_3$ ;
- 297 • mixed solutions:  
298 (4.)  $\text{NH}_4\text{HSO}_4 / (\text{NH}_4)_3\text{H}(\text{SO}_4)_2$ ;  
299 (5.)  $\text{NaHSO}_4 / \text{Na}_3\text{H}(\text{SO}_4)_2$ ;  
300 (6.)  $\text{NH}_4\text{NO}_3 - (\text{NH}_4)_2\text{SO}_4$ ;  
301 (7.)  $\text{NaNO}_3 - \text{NaCl} / \text{NaCl}$ ;  
302 (8.)  $(\text{NH}_4)_2\text{SO}_4 - \text{NH}_4\text{Cl} - \text{Na}_2\text{SO}_4$ ;  
303 (9.)  $\text{NH}_4\text{NO}_3 - (\text{NH}_4)_2\text{SO}_4 - \text{NH}_4\text{Cl} - \text{Na}_2\text{SO}_4$

304 The large panels show the aerosol water mass predictions for the RH range = 50 – 97 [%],  
305 while the small inserted panels expand the range to RH = 95 – 99.5 [%].

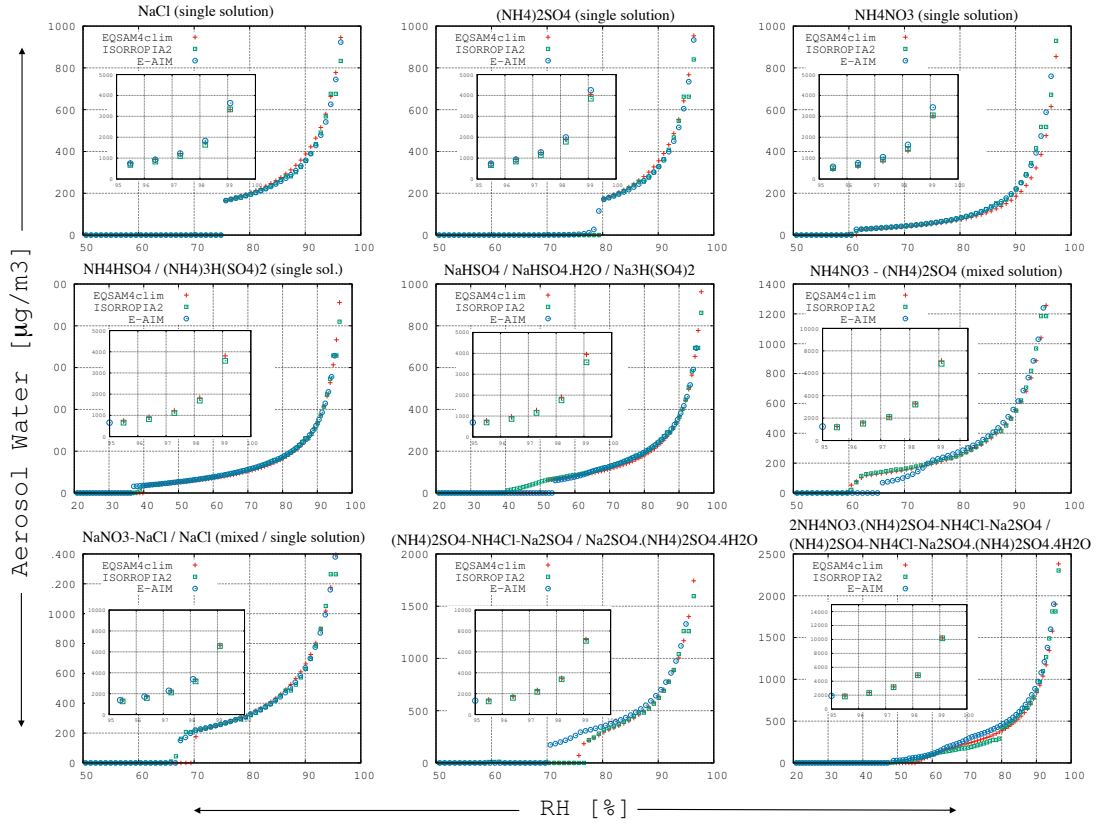


Figure S3: Extension of Figure 4 (main text): The bulk comparison of the total aerosol water mass,  $m_{w,mix} [kg/m^3(air)]$  obtained by Eq. (22) for EQSAM4clim, is shown for various single and mixed solutions. The dry concentration of each compound is fixed to  $1 [\mu mol/m^3(air)]$  at  $T = 298.15 K$ . Results of EQSAM4clim (red crosses) and ISORROPIA II (green squares) are shown for  $RH = 50 - 97 [\%]$  (large panels) and for the  $RH = 95 - 99.5 [\%]$  (small panel). The results of E-AIM (web version) (blue circles) are included for comparison. The mixed solution RHD has been obtained for EQSAM4clim from Eq. (13–22) and are based on measured MDRH values for ISORROPIA II. The mutual deliquescence range of EQSAM4clim and ISORROPIA II (described in Sec. 2.6) differ from those of AIM (web version: <http://www.aim.env.uea.ac.uk/aim/aim.php>). Each panel is shown in the following for better reading.

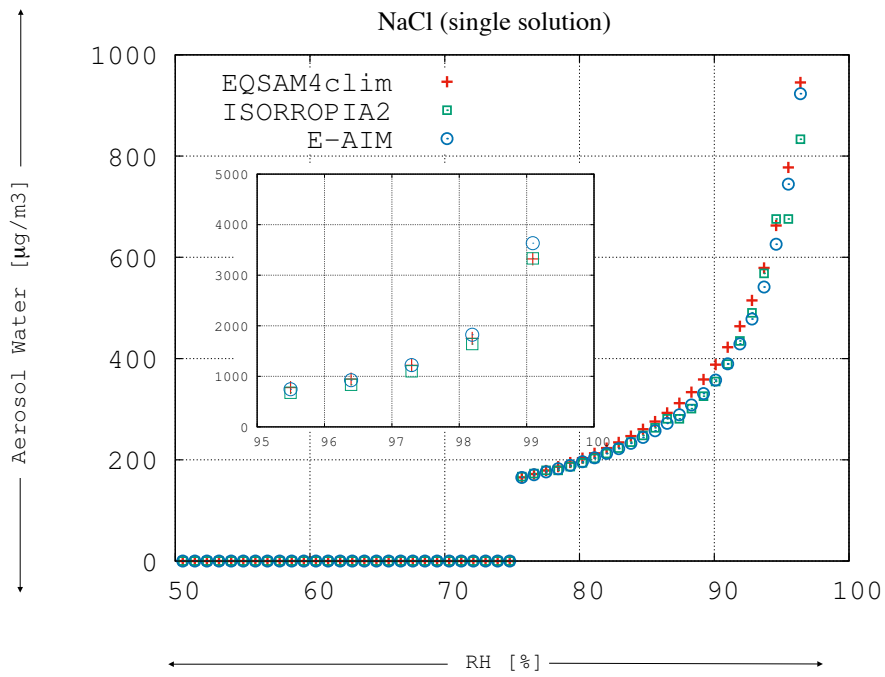


Figure S3.1: Panel 1 of Figure S3 (Supplement).

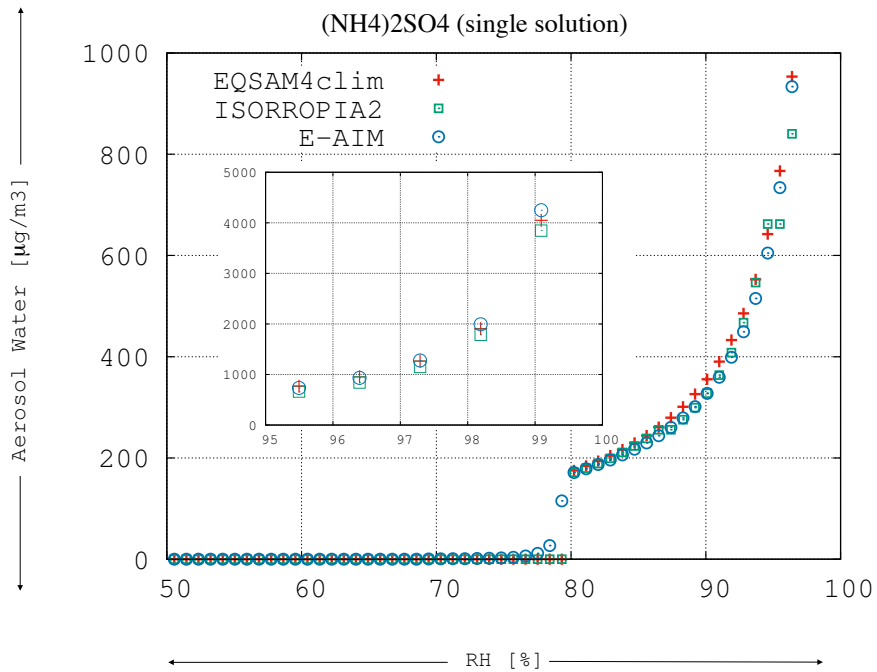


Figure S3.2: Panel 2 of Figure S3 (Supplement).

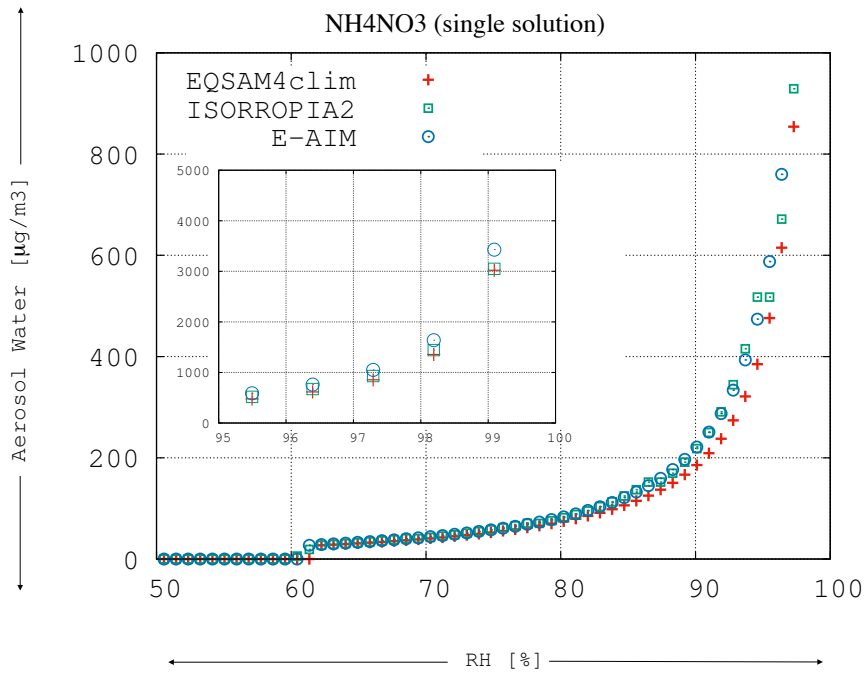


Figure S3.3: Panel 3 of Figure S3 (Supplement).

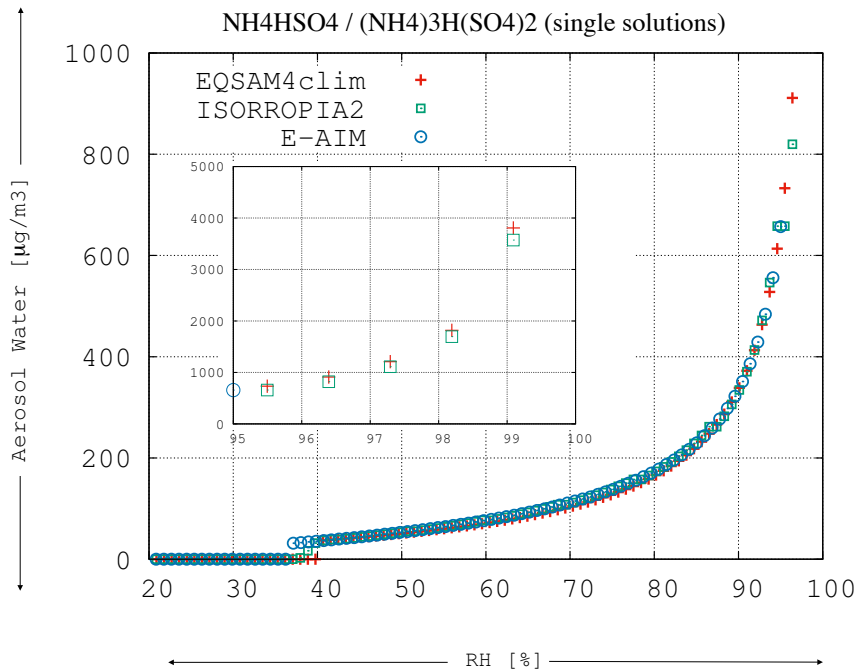


Figure S3.4: Panel 4 of Figure S3 (Supplement).

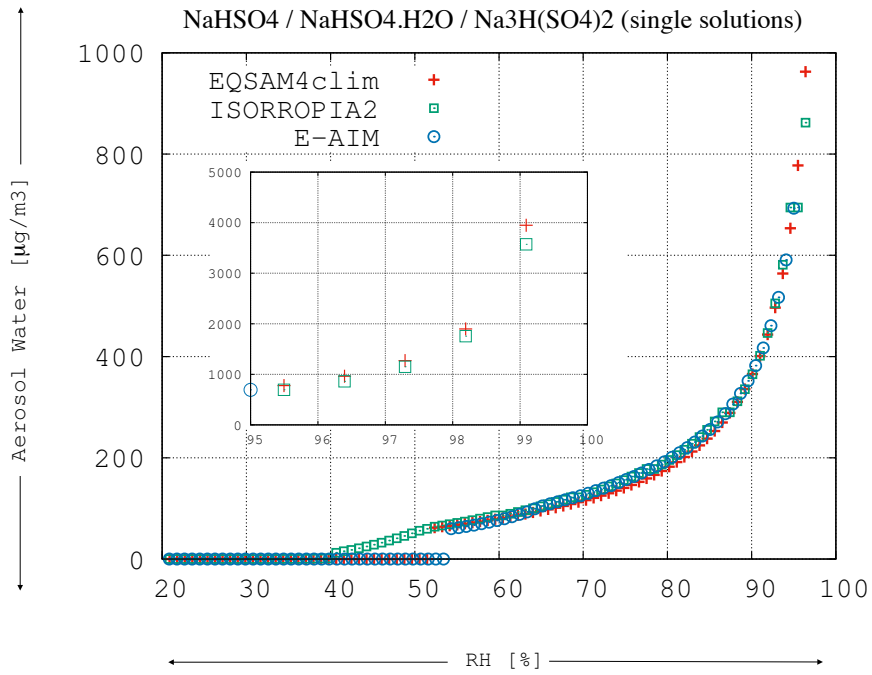


Figure S3.5: Panel 5 of Figure S3 (Supplement).

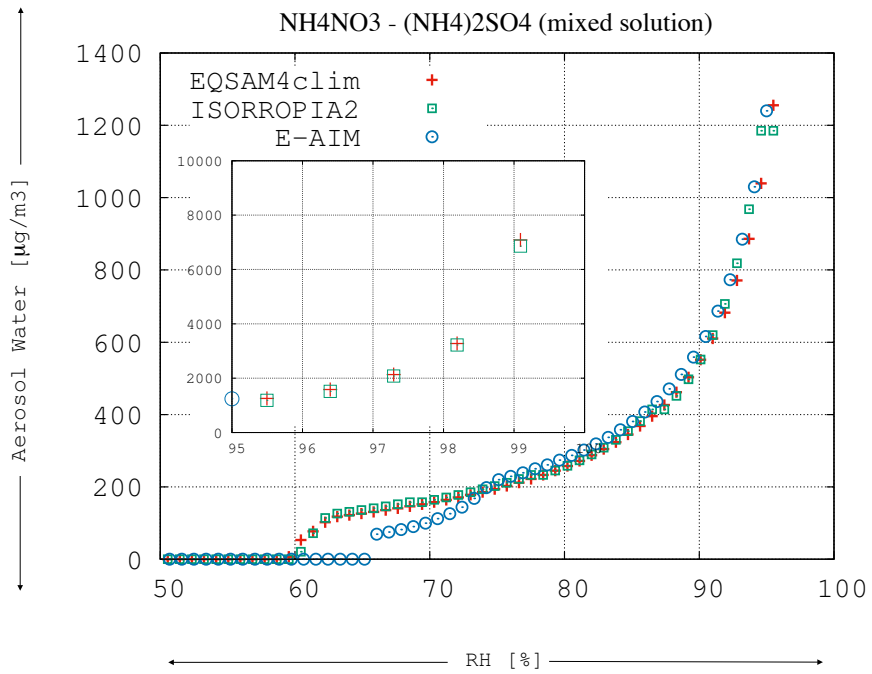


Figure S3.6: Panel 6 of Figure S3 (Supplement).

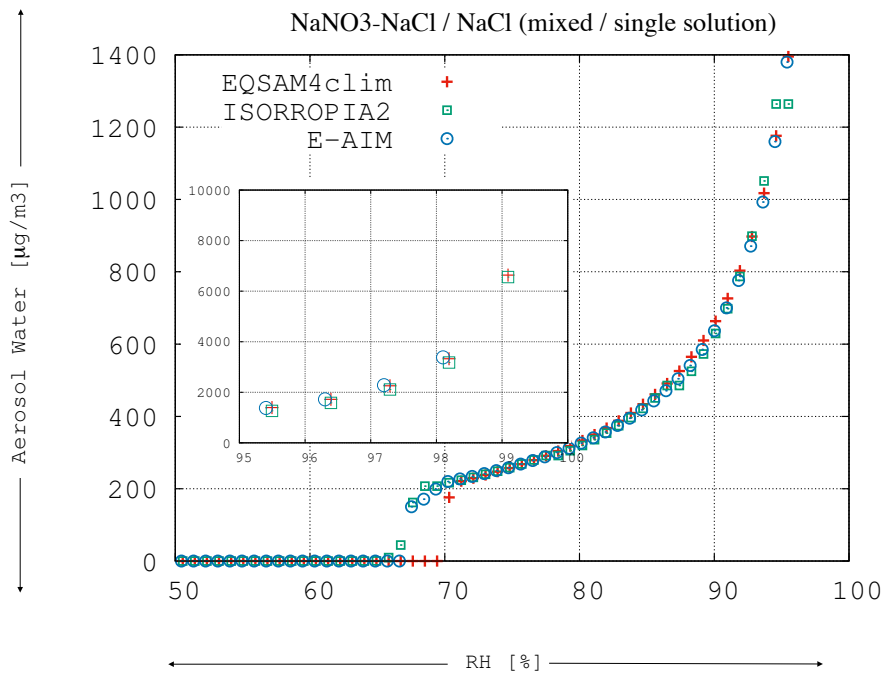


Figure S3.7: Panel 7 of Figure S3 (Supplement).

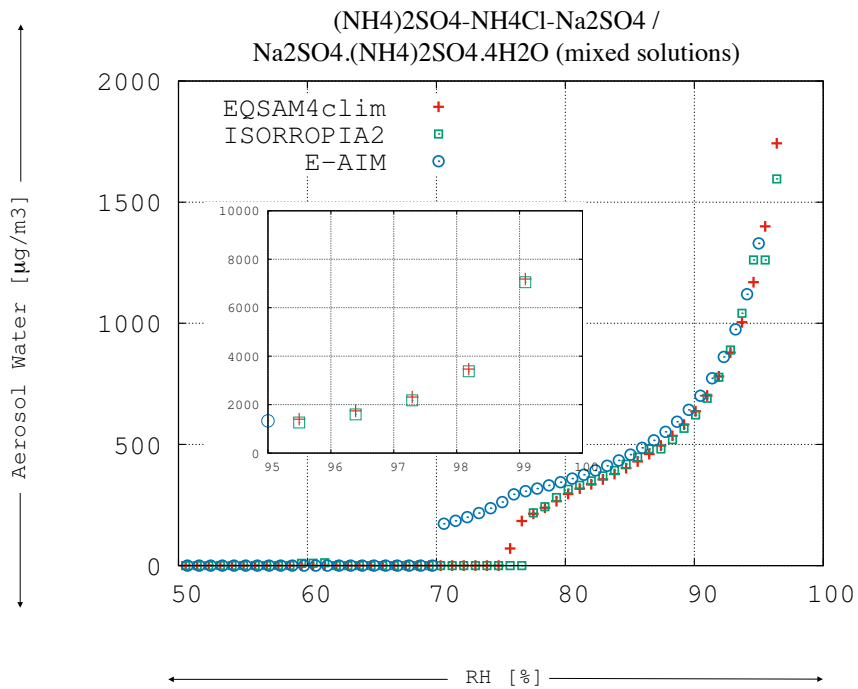


Figure S3.8: Panel 8 of Figure S3 (Supplement).

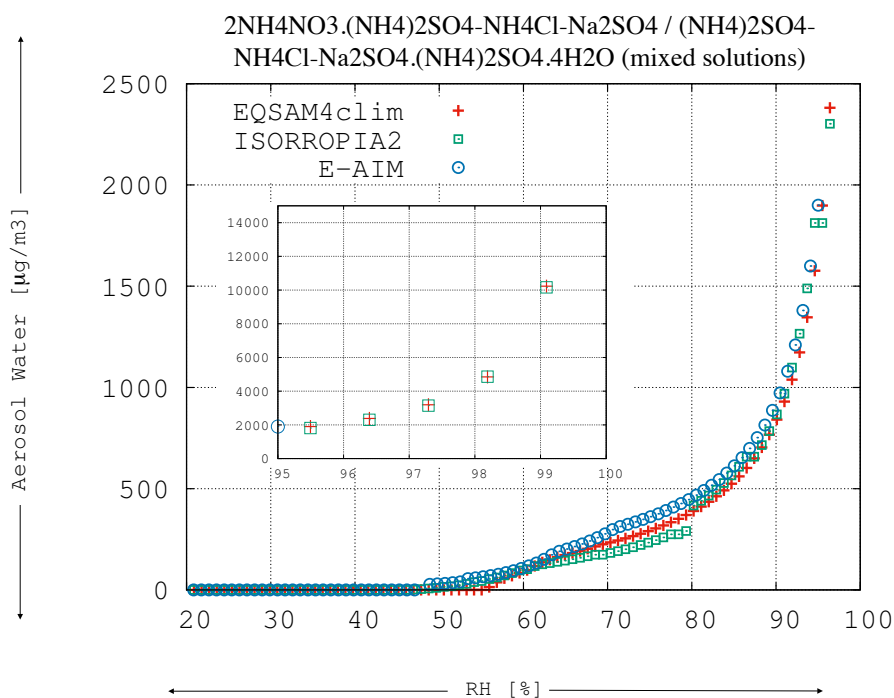


Figure S3.9: Panel 9 of Figure S3 (Supplement).

### 306 S3.2 Variable $\text{NH}_3$ concentration – SP2006

307 Figure S4 extends the Fig. 5 (main text) to bi-sulfate and sulfuric acid. Both, the  
 308 gaseous uptake of  $\text{NH}_3$  and  $\text{HNO}_3$  on saturated solutions and the weak dissociation of,  
 309 e.g.,  $\text{H}_2\text{SO}_4$  and  $\text{HSO}_4^-$ , are not considered for EQSAM4clim (see Sec. S2). Therefore  
 310 differences occur for bi-sulfate, sulfate and water in the concentration range of ammonia,  
 311 i.e., within  $2 - 4 [\mu\text{g}/\text{m}^3(\text{air})]$ . At lower ammonia concentrations, where the sulfates are  
 312 less neutralized, the bi-sulfate concentration increases and the sulfate concentration ac-  
 313 cordingly decreases, until only free sulfuric acid exists. Note that the differences between  
 314 EQSAM4clim and ISORROPIA II are for ammonia concentrations below  $2 [\mu\text{g}/\text{m}^3(\text{air})]$   
 315 only a matter of naming definition – the version of ISORROPIA II used considers all  
 316 unneutralized sulfate simply as sulfate, an output variable sulfuric acid does not exist,  
 317 since sulfuric acid has such a low vapor pressure that it practically only exists in the  
 318 aerosol phase. EQSAM4clim has an option to treat it either way.

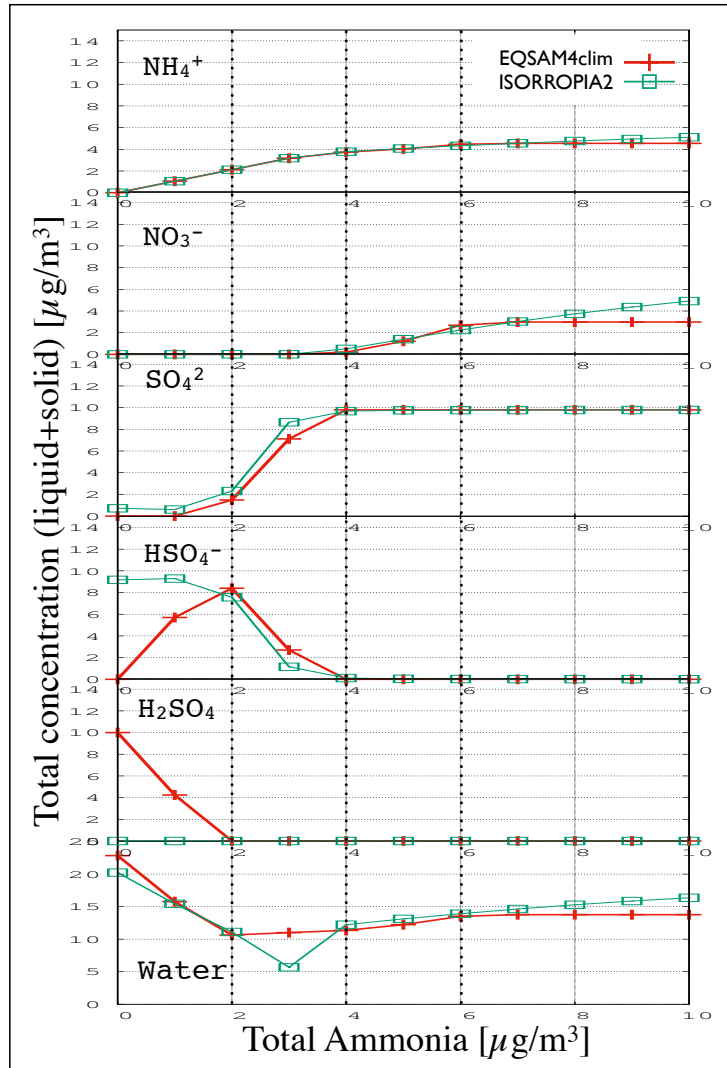


Figure S4: Extension of Figure 5 (main text): Mixed solution composition of  $NH_4NO_3$  and  $(NH_4)_2SO_4$  as a function of total ammonia at  $T = 298.15 [K]$  and  $RH = 70 [\%]$ , as defined in SP2006 for their Figure 10.23.  $[TS] = [TN] = 10 [\mu g/m^3(air)]$  showing EQSAM4clim (red crosses) and ISORROPIA II (green squares). Each panel is shown in the following for better reading.

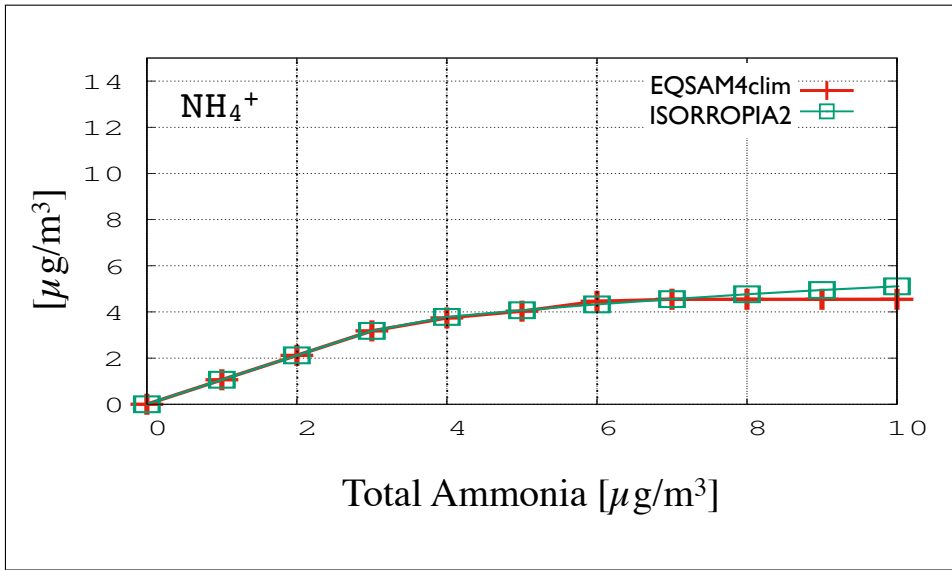


Figure S4.1: Panel 1 of Figure S4 (Supplement).

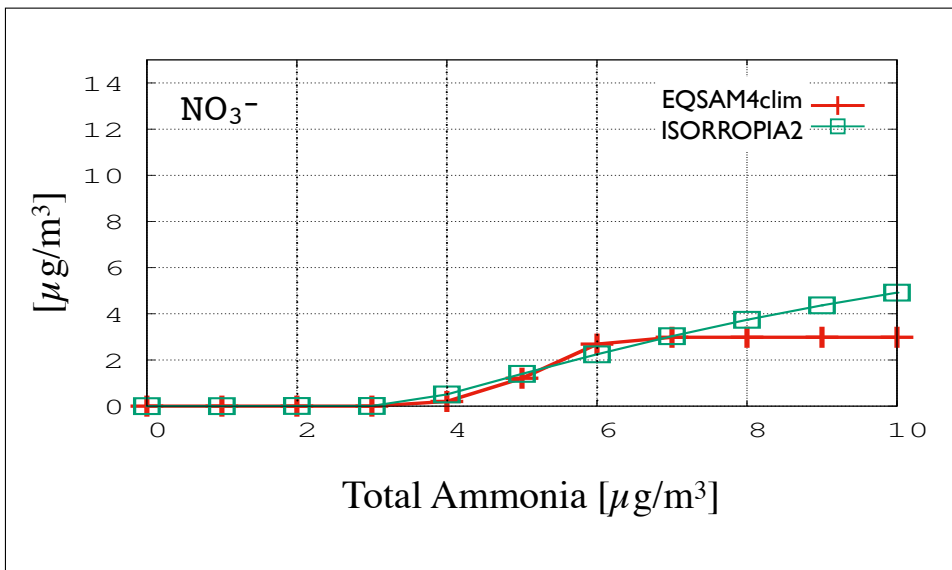


Figure S4.2: Panel 2 of Figure S4 (Supplement).

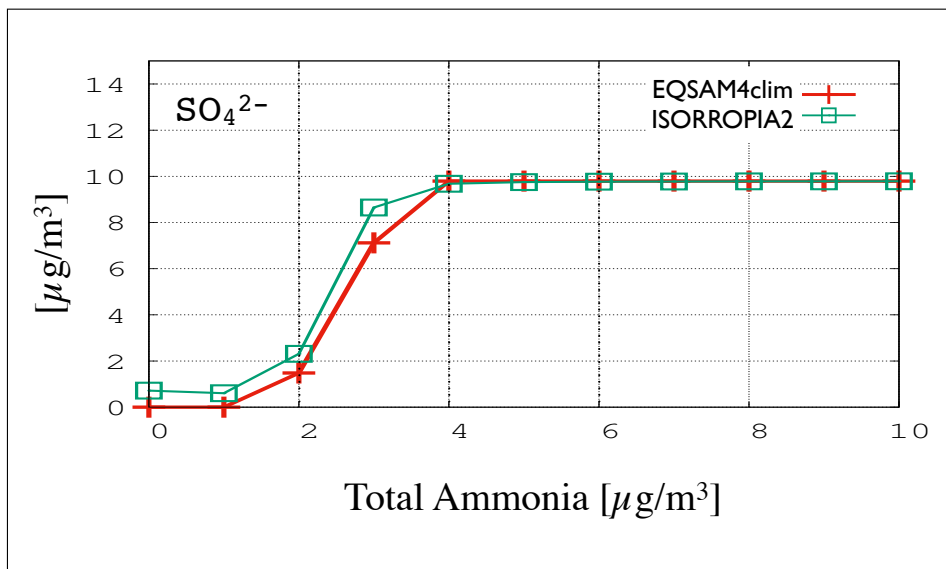


Figure S4.3: Panel 3 of Figure S4 (Supplement).

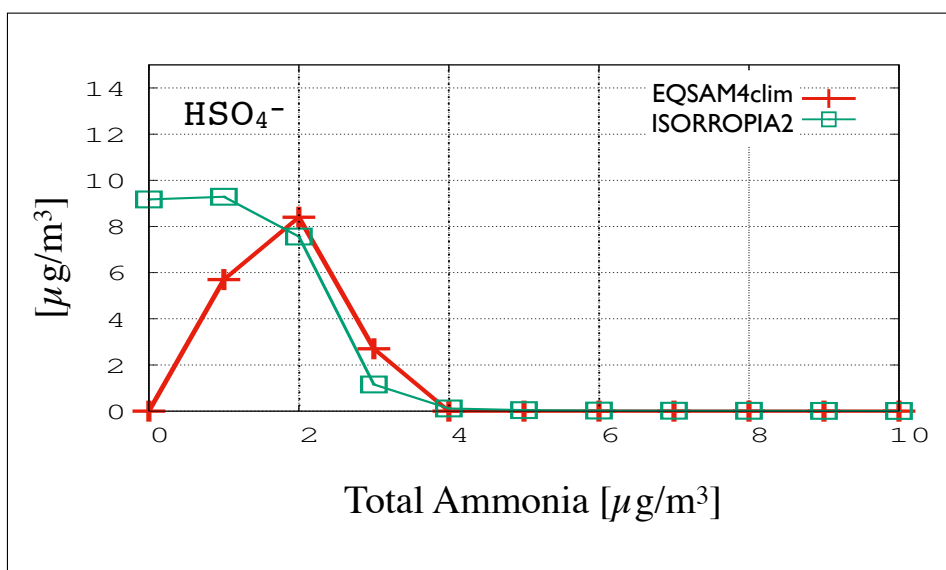


Figure S4.4: Panel 4 of Figure S4 (Supplement).

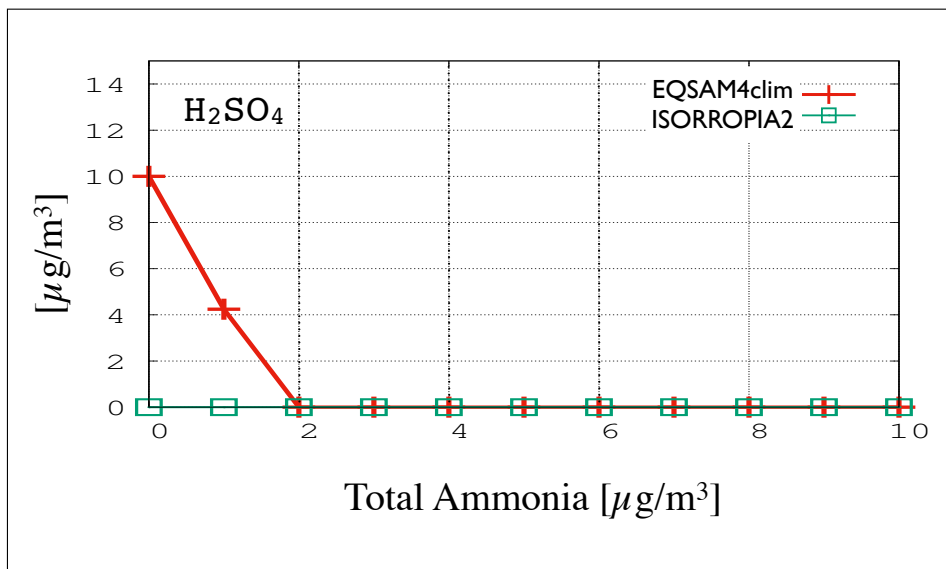


Figure S4.5: Panel 5 of Figure S4 (Supplement).

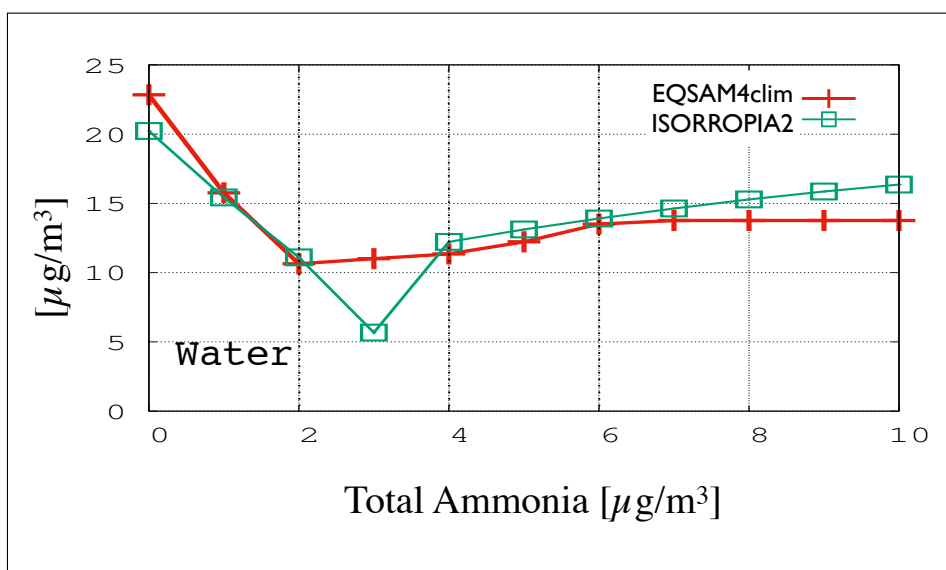


Figure S4.6: Panel 6 of Figure S4 (Supplement).

### 319 S3.3 Variable solute concentrations (20 cases)

320 Extension of Figure 6 and 7 to 20 aerosol composition cases. Cases 1–5 refer to the sulfate  
 321 very rich regime, cases 6–10 to sulfate rich, and 11–20 to sulfate neutral and poor regimes  
 322 (see Sec. 2.2). The concentrations of all aerosol components only depend on fixed molar  
 323 ratios with respect to the total sulfate concentration, which is fixed to 20 [ $\mu\text{g}/\text{m}^3(\text{air})$ ]  
 324 for all 20 cases. The ratios are shown in Table 3 of Xu et al. (2009). Note that some of  
 325 the cases are the same as in the model inter-comparison of Zhang et al. (2000), so that  
 326 a direct comparison can be made to a wider range of equilibrium models, including AIM  
 327 (the case number in the parenthesis in Table 3 of Xu et al., 2009, refers to the cases in  
 328 the study by Zhang et al., 2000). Here, Figures S5–S7 show the corresponding results  
 329 of EQSAM4clim, ISORROPIA II and EQUISOLV II for these 20 cases as a function of  
 330 RH: 10, 20, 30, 40, 50, 60, 70, 80, 90, 95 [%]. The aerosol composition is calculated for each  
 331 model from the gas-liquid-solid equilibrium partitioning, assuming deliquescence.

332 Figure S5 shows for the cases 1-20 (from left to right and top to bottom), the bulk  
 333 aerosol water mass as a function of RH at  $T = 298.15$  [K]. Fig. S6 shows the corresponding  
 334 solid particulate matter (cases 11-20 in panels 1-10), panels 11-20 show the corresponding  
 335 total dry particulate matter (PM), i.e., the sum of the liquid and solid aerosol mass  
 336 (without aerosol water). Panels 1-10 of Fig. S7 show the total aerosol nitrate, while the  
 337 panels 11-20 the aerosol ammonium concentration (both show cases 11-20).

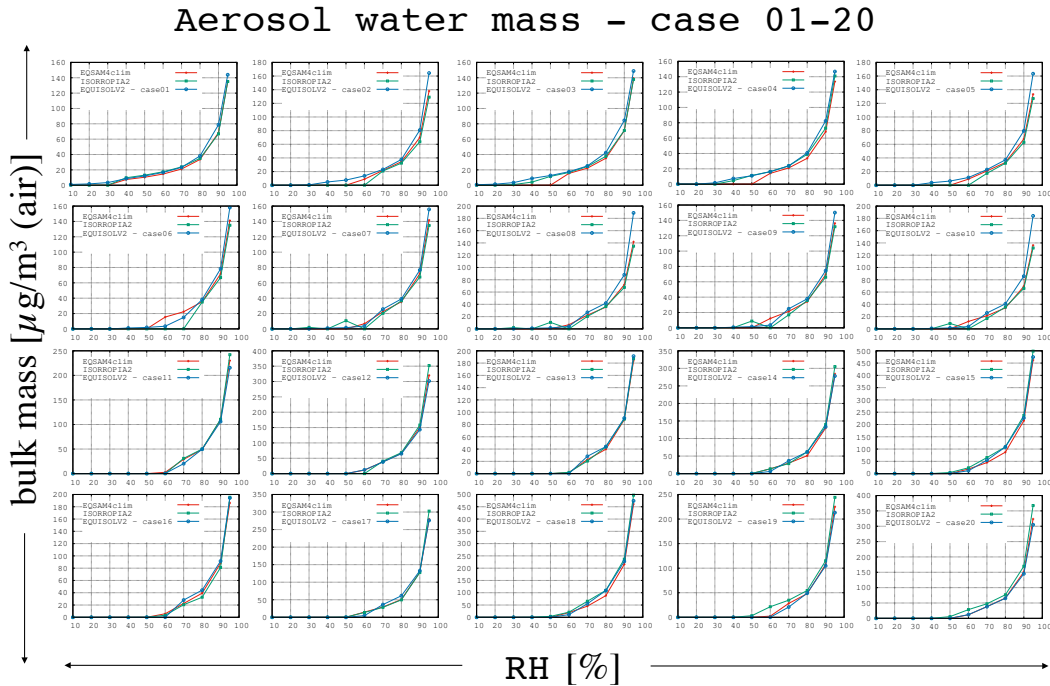


Figure S5: Extension of Figure 6 (main text): Bulk aerosol water mass as a function of RH for various sulfate molar ratios, fixed for the entire RH range (at constant  $T = 298.15$  K). Only the dry concentration ratio varies from case to case to match the domains of Table 2. The 20 aerosol composition cases refer to Table 3 of Xu et al. (2009). A subset of four panels is shown in the following for better reading.

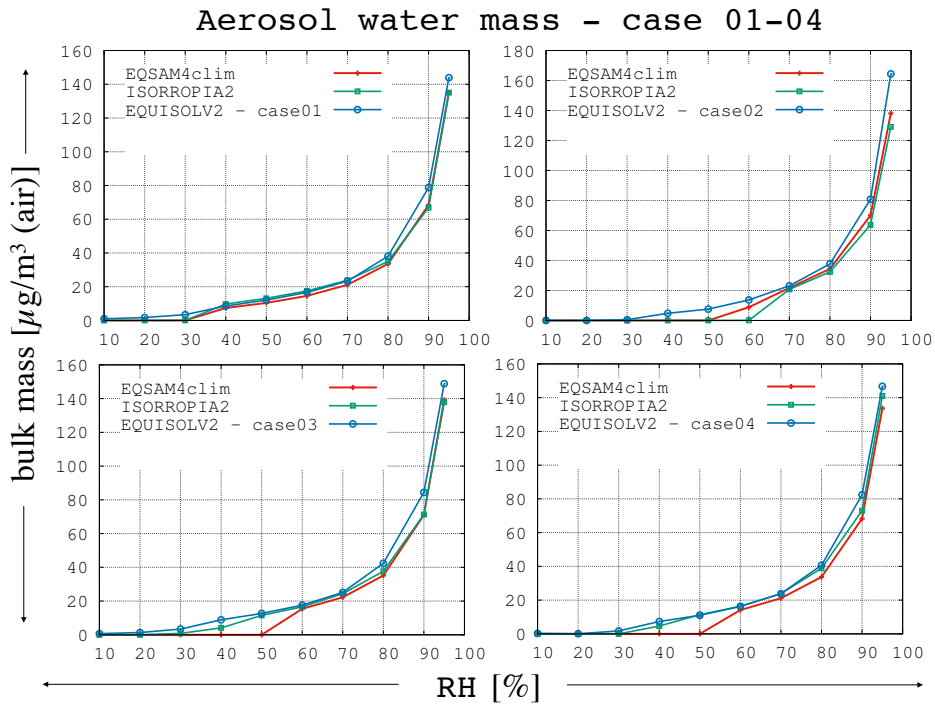


Figure S5.1: Case 1-4 of Figure S5 (Supplement).

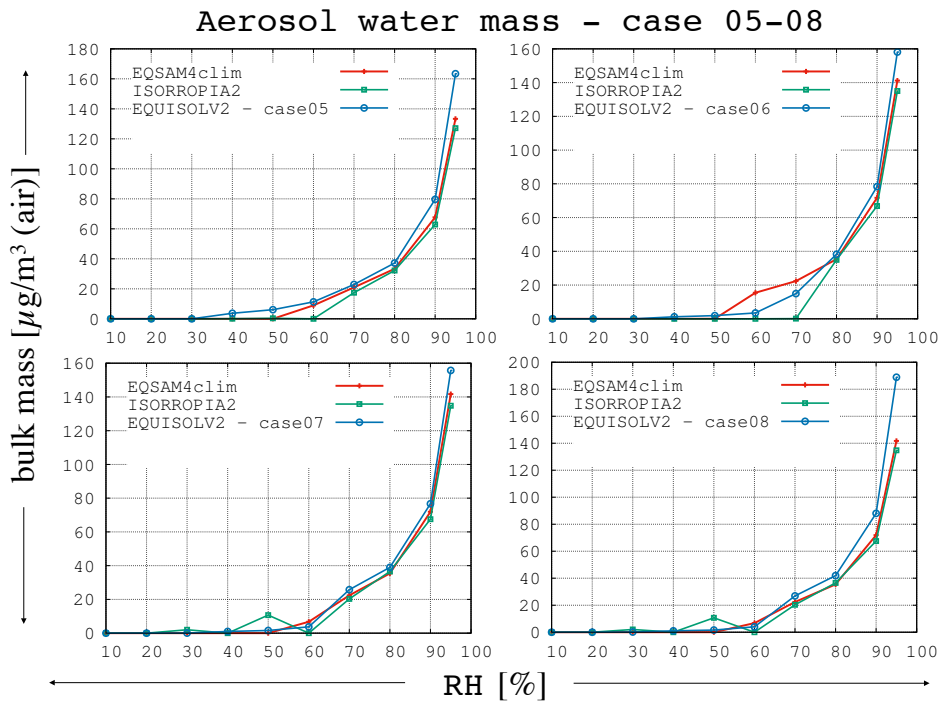


Figure S5.2: Case 5-8 of Figure S5 (Supplement).

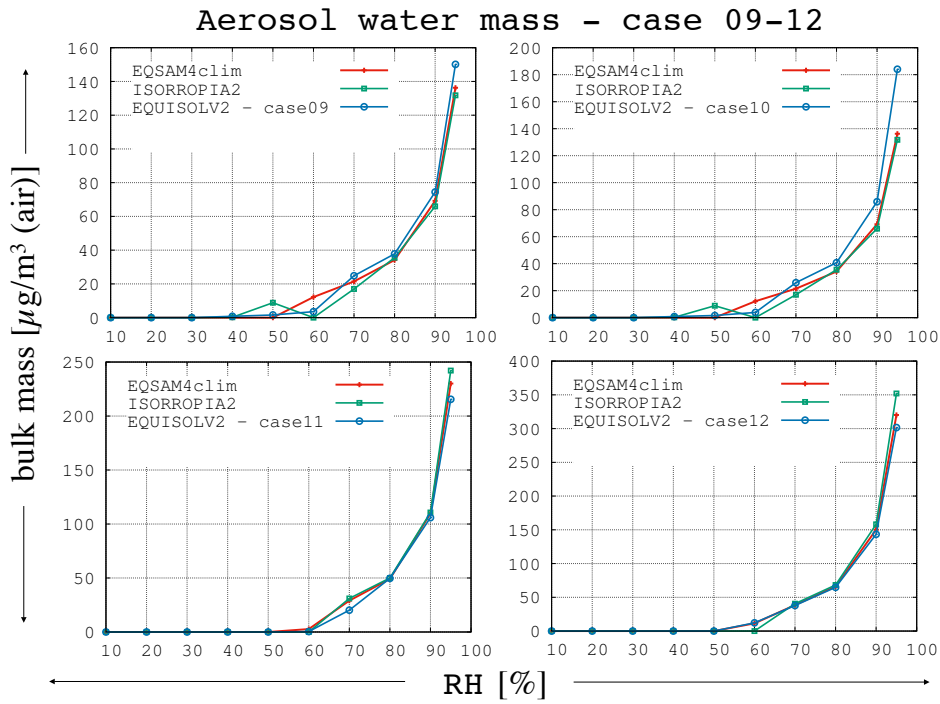


Figure S5.3: Case 9-12 of Figure S5 (Supplement).

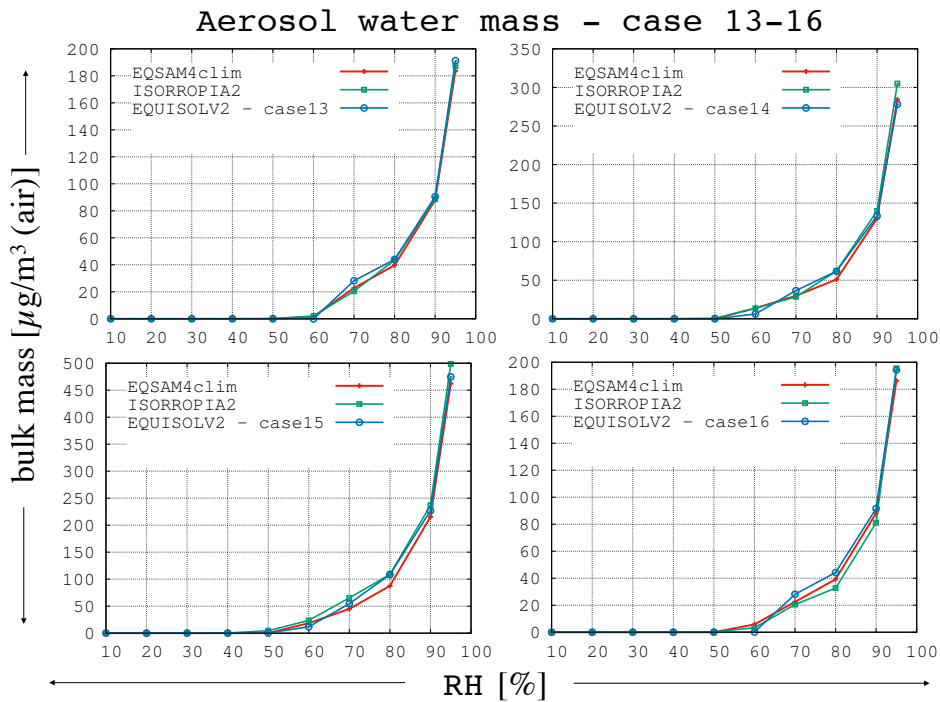


Figure S5.4: Case 13-16 of Figure S5 (Supplement).

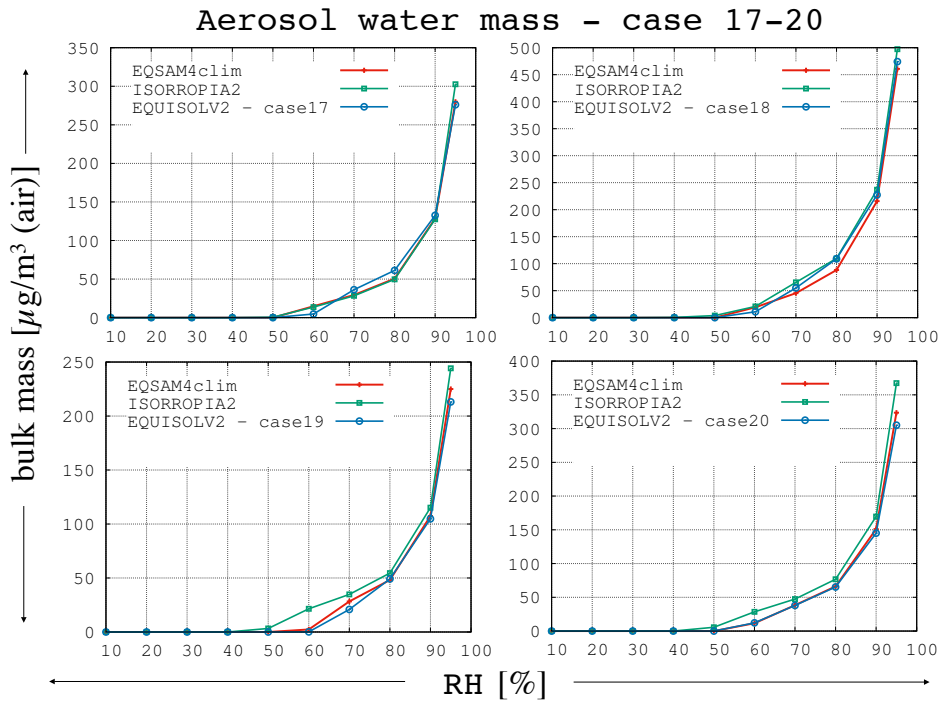


Figure S5.5: Case 17-20 of Figure S5 (Supplement).

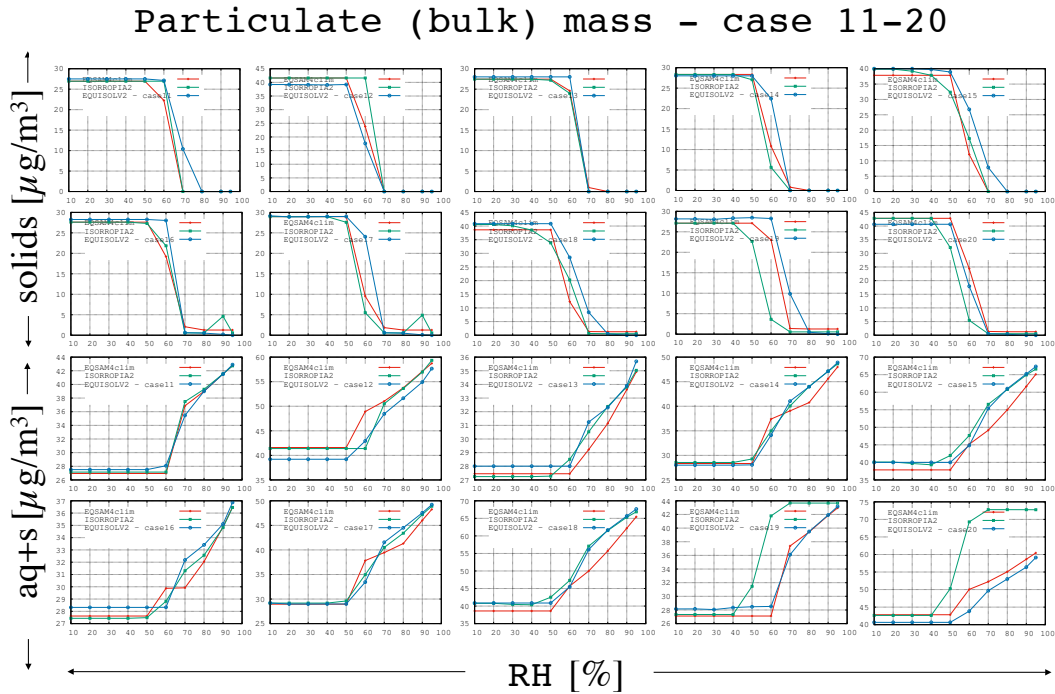


Figure S6: Extension of Figure 7 (main text): Total solid PM and liquid+solid PM.

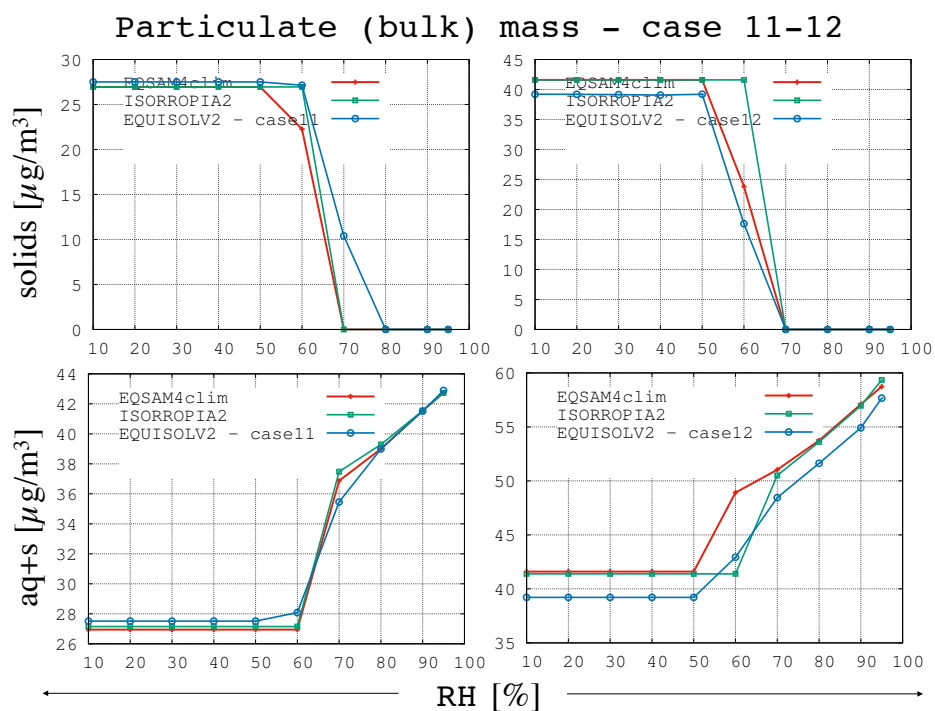


Figure S6.1: Case 11-12 of Figure S6 (Supplement).

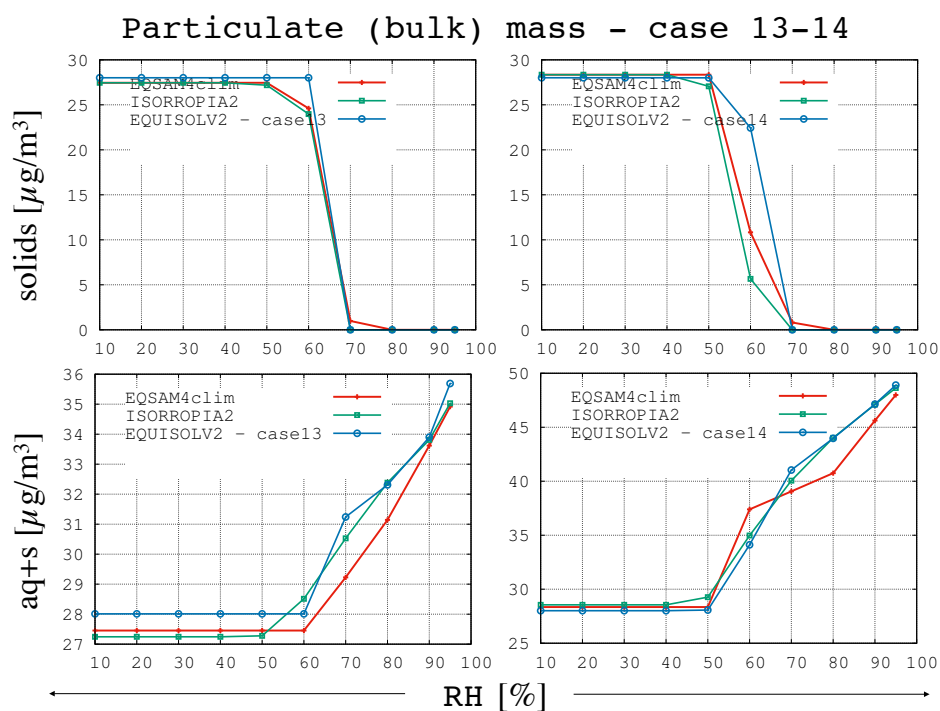


Figure S6.2: Case 13-14 of Figure S6 (Supplement).

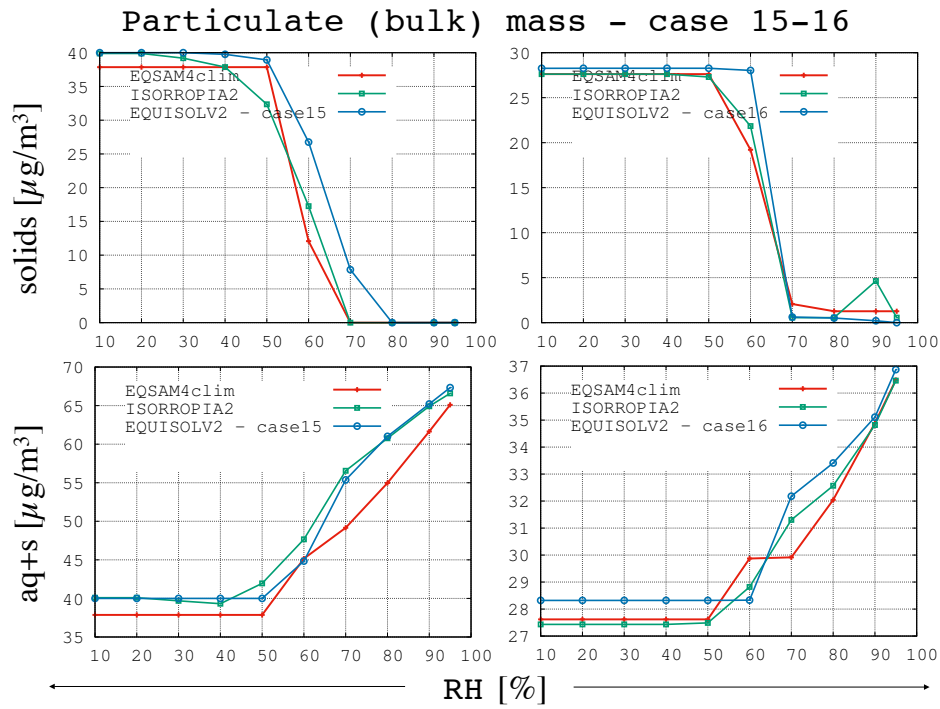


Figure S6.3: Case 15-16 of Figure S6 (Supplement).

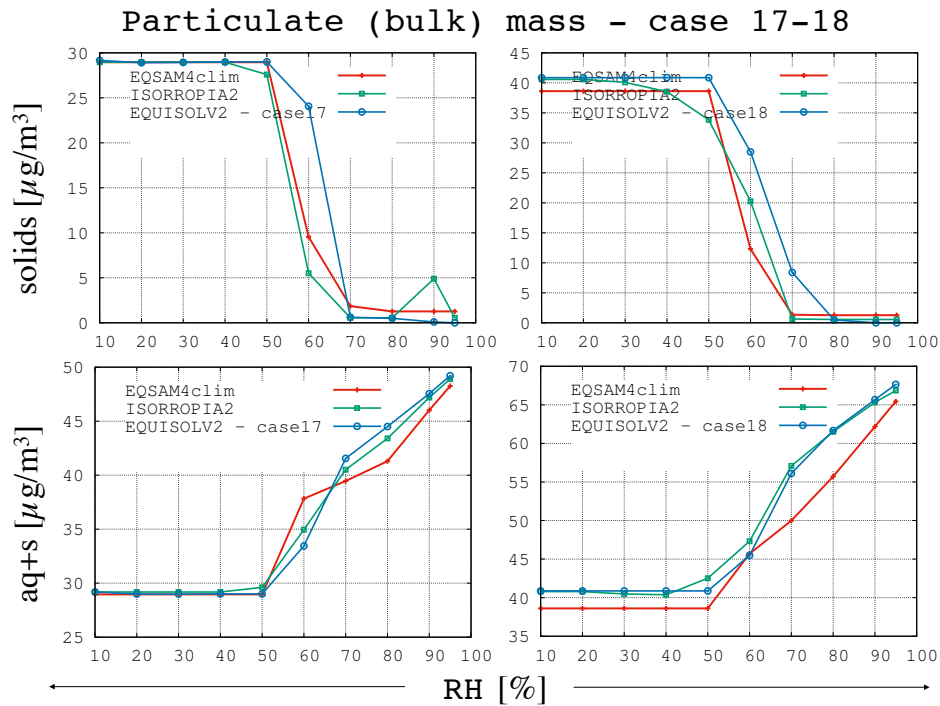


Figure S6.4: Case 17-18 of Figure S6 (Supplement).

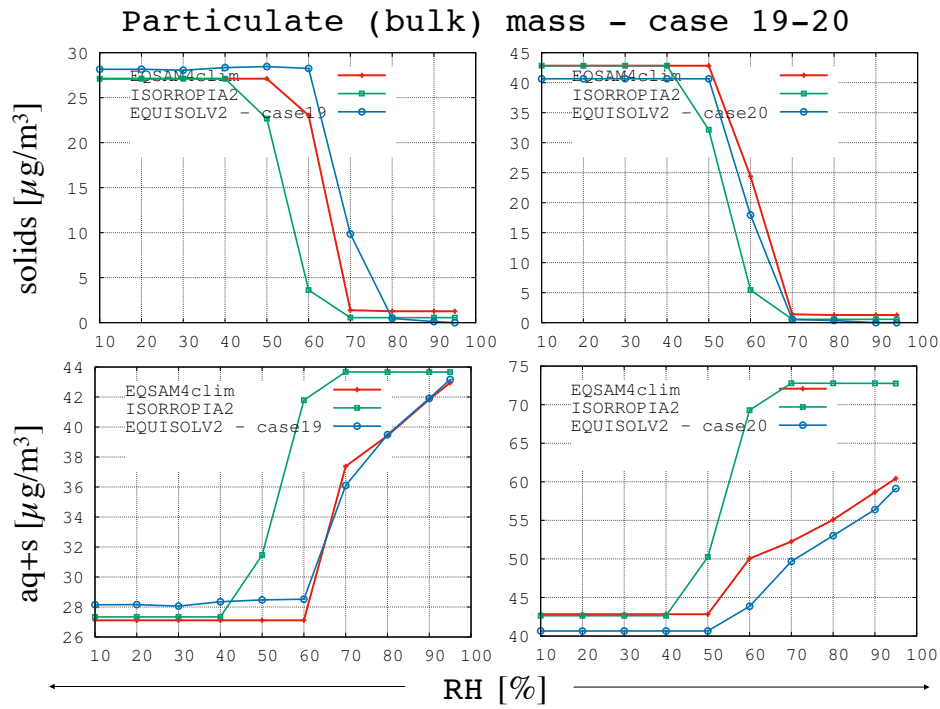


Figure S6.5: Case 19-20 of Figure S6 (Supplement).

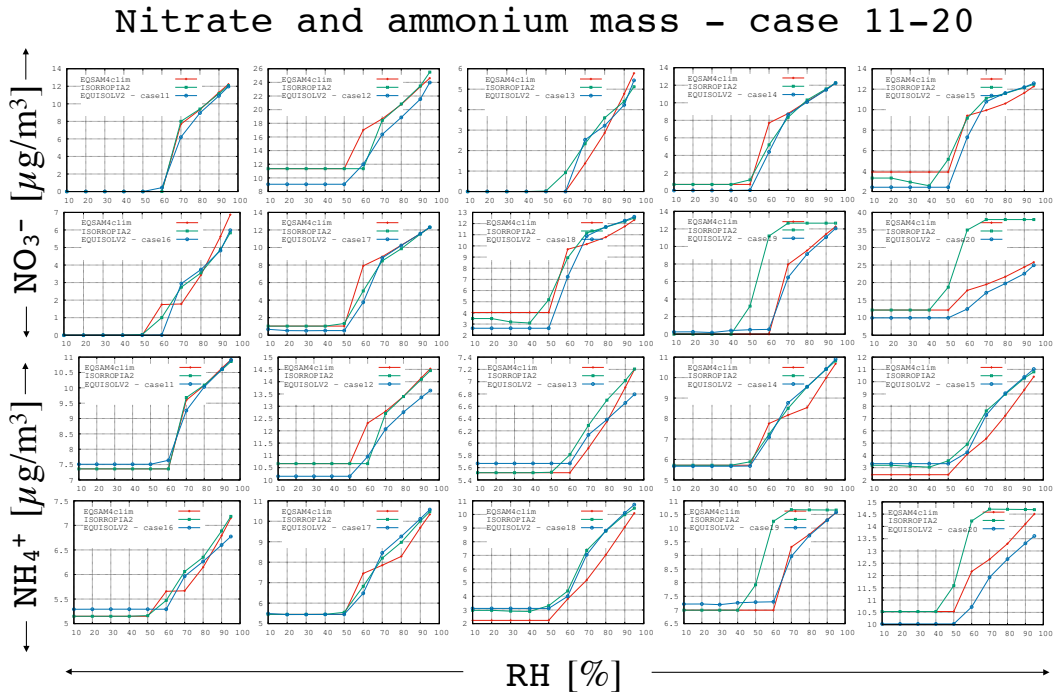


Figure S7: Extension of Figure 7 (main text): Bulk aerosol nitrate and ammonium.

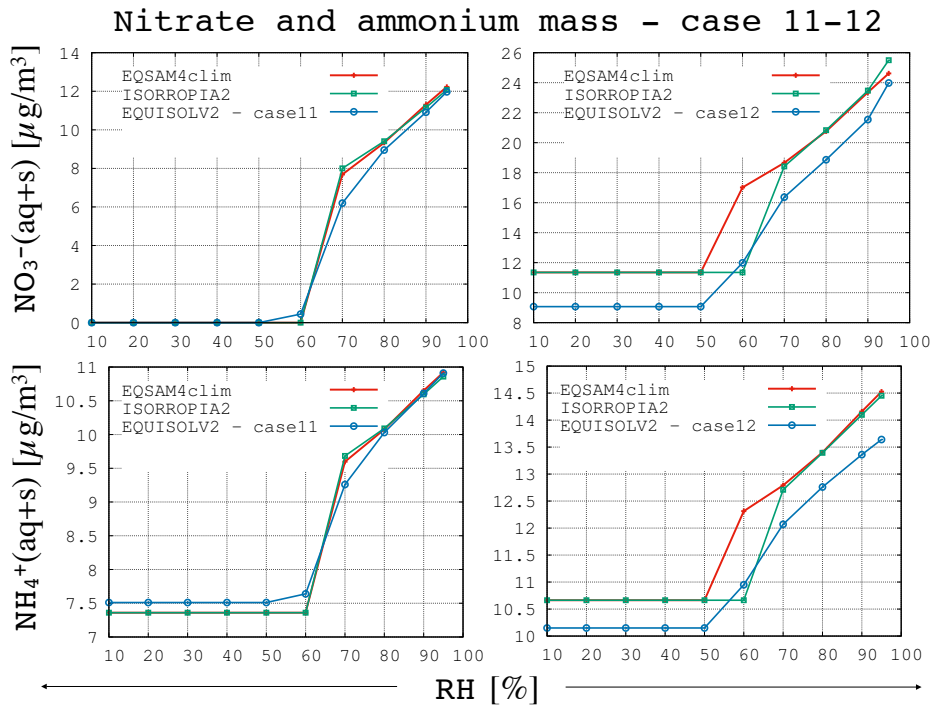


Figure S7.2: Case 11-12 of Figure S7 (Supplement).

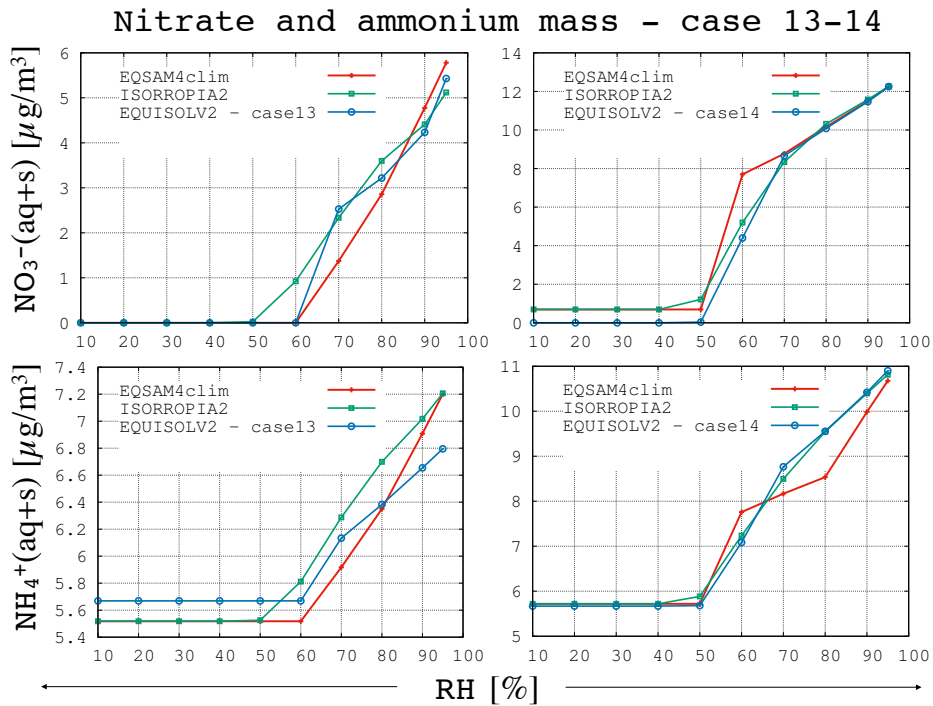


Figure S7.3: Case 13-14 of Figure S7 (Supplement).

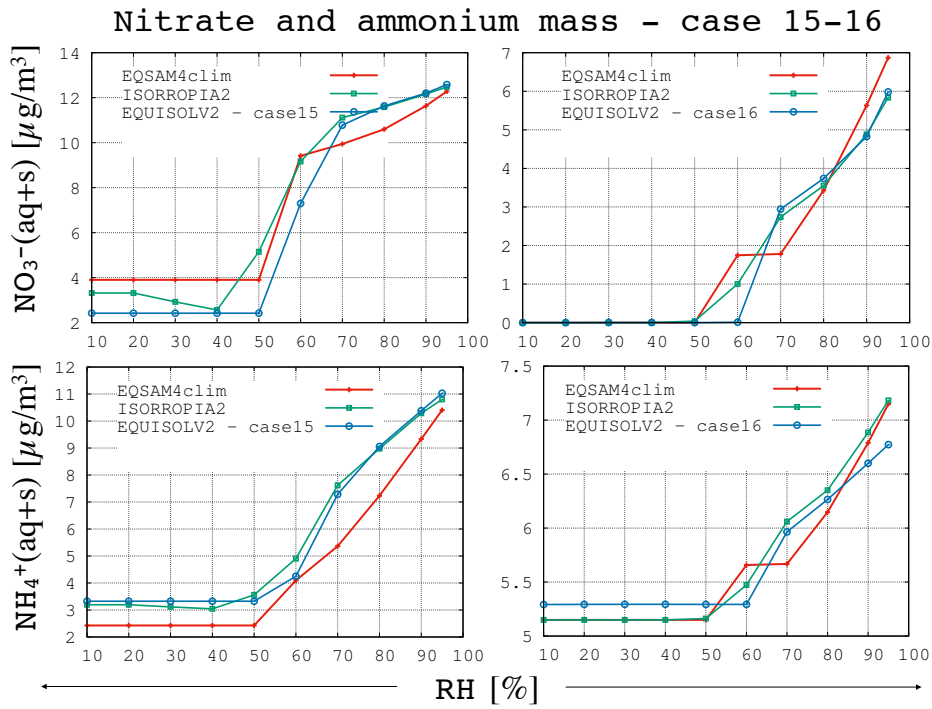


Figure S7.4: Case 15-16 of Figure S7 (Supplement).

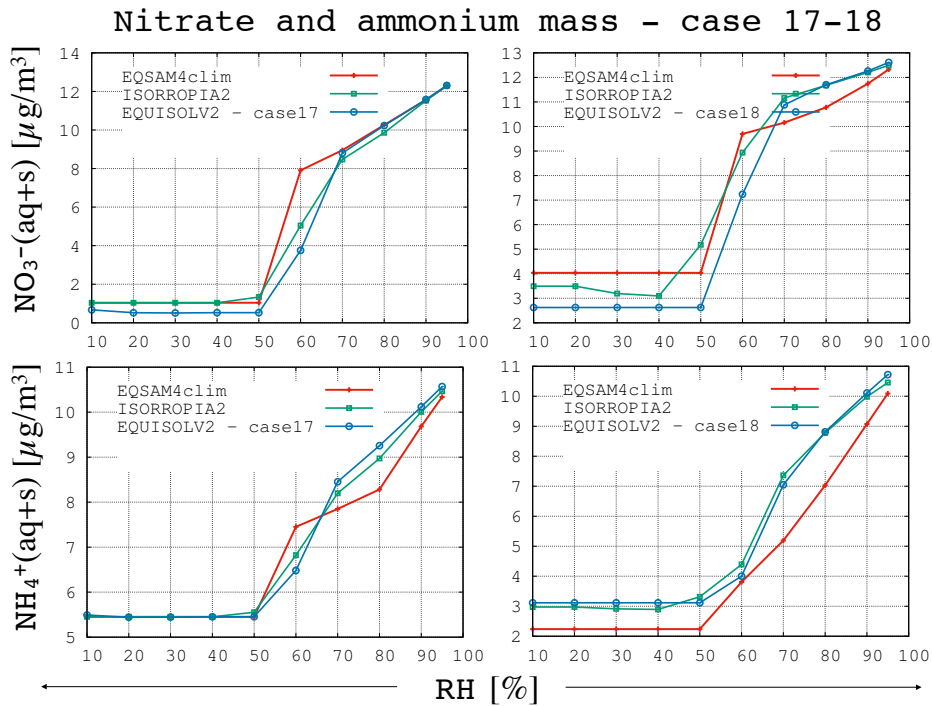


Figure S7.5: Case 17-18 of Figure S7 (Supplement).

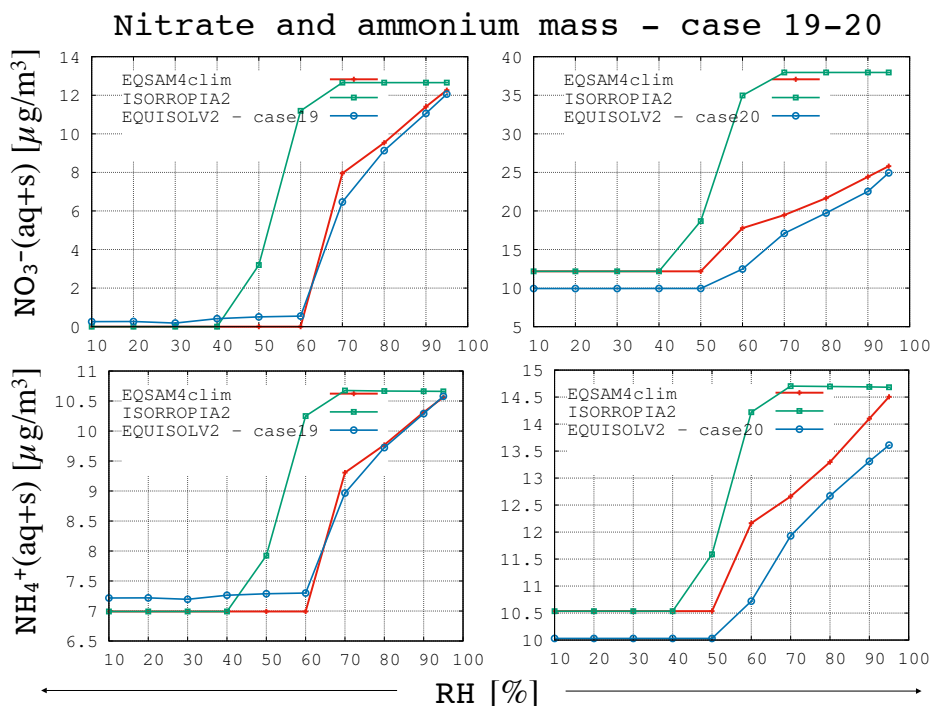


Figure S7.6: Case 19-20 of Figure S7 (Supplement).

### 338 S3.4 Field observations – MINOS campaign

339 Extension of Figure 8 and 9 of Sec. 3.4. Figures S8 and Figure S9 show the gas-liquid-solid  
 340 partitioning results of EQSAM4clim (red crosses) and ISORROPIA II (green squares).  
 341 The equilibrium computations are based on lumped cation and anion concentrations,  
 342 which were observed during MINOS in the aerosol fine and coarse mode, respectively.  
 343 Fig. S8, panels (1-20), show the model results for the aerosol fine mode (from left to  
 344 right, top to bottom): total aerosol water mass [ $\mu\text{g}/\text{m}^3(\text{air})$ ], total particulate (aque-  
 345 ous+solid) matter (PM) [ $\mu\text{g}/\text{m}^3(\text{air})$ ], total solid PM [ $\mu\text{g}/\text{m}^3(\text{air})$ ], total (aqueous+solid)  
 346 PM [ $\mu\text{mol}/\text{m}^3(\text{air})$ ], and in [ $\text{nmol}/\text{m}^3(\text{air})$ ] the (lumped) ion concentrations of: ammo-  
 347 nium ( $\text{NH}_4^+$ ), sodium ( $\text{Na}^+$ ), potassium ( $\text{K}^+$ ), calcium ( $\text{Ca}^{2+}$ ), magnesium ( $\text{Mg}^{2+}$ ), sulfate  
 348 ( $\text{SO}_4^{2-}$ ) – both as totals (aqueous+solid) and solids -, as well as total bi-sulfate ( $\text{HSO}_4^-$ )  
 349 and the residual gases, hydrochloric acid ( $\text{HCl}$ ), nitric acid ( $\text{HNO}_3$ ) and ammonia ( $\text{NH}_3$ ).

350 Fig. S9, panels (1-20), show the model results for the aerosol coarse mode (from left  
 351 to right, top to bottom): total aerosol water mass [ $\mu\text{g}/\text{m}^3(\text{air})$ ], total particulate (aque-  
 352 ous+solid) matter (PM) [ $\mu\text{g}/\text{m}^3(\text{air})$ ], total solid PM [ $\mu\text{g}/\text{m}^3(\text{air})$ ], total (aqueous+solid)  
 353 PM [ $\mu\text{mol}/\text{m}^3(\text{air})$ ], and in [ $\text{nmol}/\text{m}^3(\text{air})$ ] the (lumped) ion concentrations of: ammo-  
 354 nium ( $\text{NH}_4^+$ ), sodium ( $\text{Na}^+$ ), potassium ( $\text{K}^+$ ), calcium ( $\text{Ca}^{2+}$ ), magnesium ( $\text{Mg}^{2+}$ ),  
 355 sulfate ( $\text{SO}_4^{2-}$ ), bi-sulfate ( $\text{HSO}_4^-$ ), nitrate ( $\text{NO}_3^-$ ), chloride ( $\text{Cl}^-$ ), – all both as totals  
 356 (aqueous+solid) and solids, except ammonium and bi-sulfate, which are omitted because  
 357 of their very low (negligible) concentrations. Figures S8 and S9 are enlarged below, by  
 358 Fig. S8.1-S8.5 and Fig. S9.1-S9.5, respectively to show the details. Despite the differ-  
 359 ent approaches in the mixed solution treatment of EQSAM4clim and ISORROPIA II,  
 360 EQSAM4clim is relatively close to the results of ISORROPIA II, capturing many details  
 361 of the solid precipitation of individual compounds for both, the fine and coarse mode.

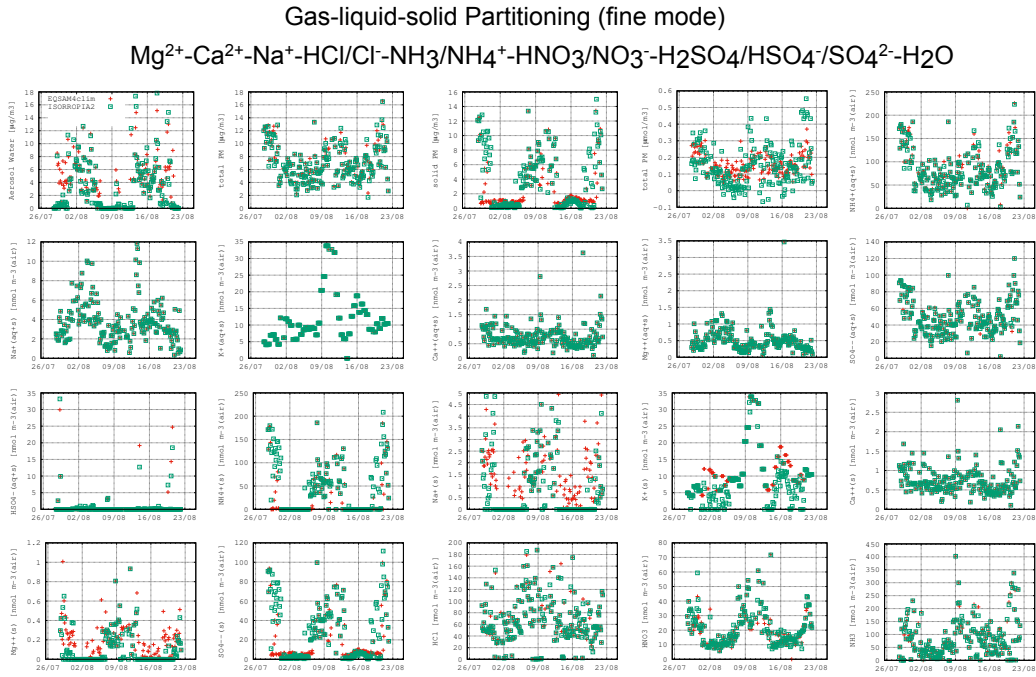


Figure S8: Extension of Figure 8 (main text): Aerosol water, total particulate matter and total solids [ $\mu g/m^3(air)$ ], the corresponding residual gases [ $\mu mol/m^3(air)$ ], and various ions for the fine mode. EQSAM4clim (red crosses), ISORROPIA II (green squares). A subset of four panels is shown in the following for better reading.

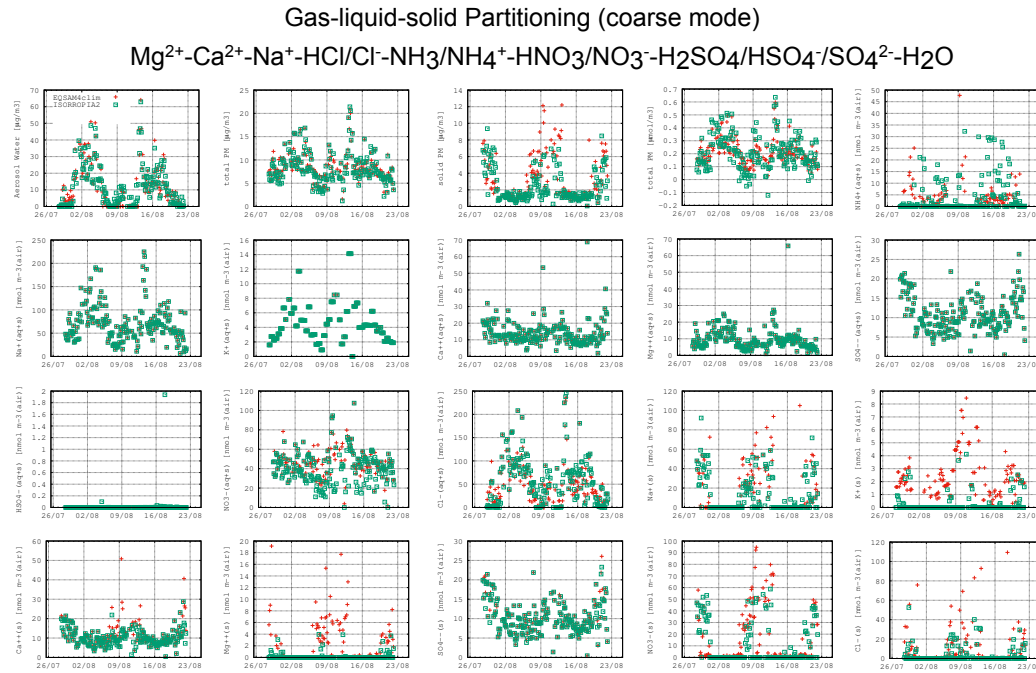


Figure S9: Extension of Figure S8 and Fig. 8 (main text) to the coarse mode.

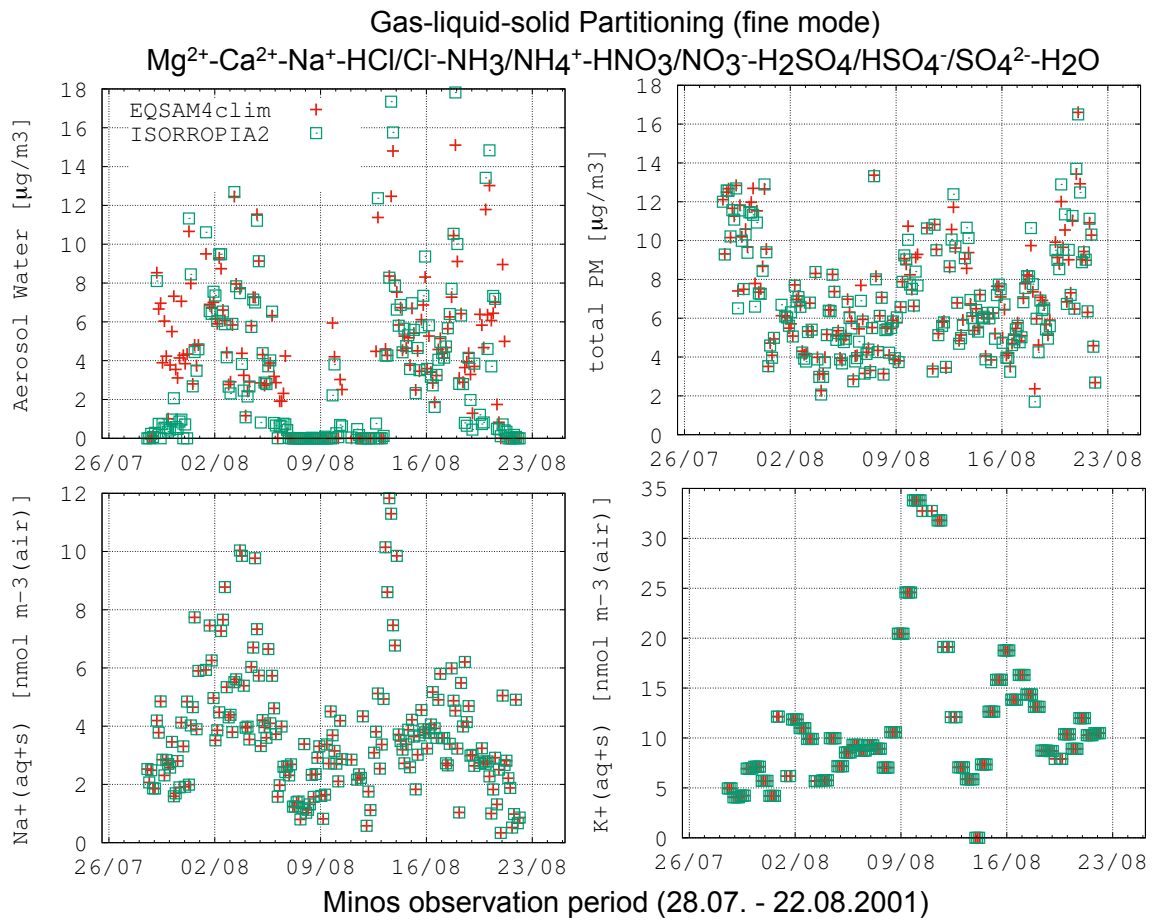


Figure S8.1: Details of Figure S8 (Supplement): Aerosol water(aq), total mass (aq+s), lumped  $Na^+$ (aq+s) and  $K^+$ (aq+s) (nano moles).

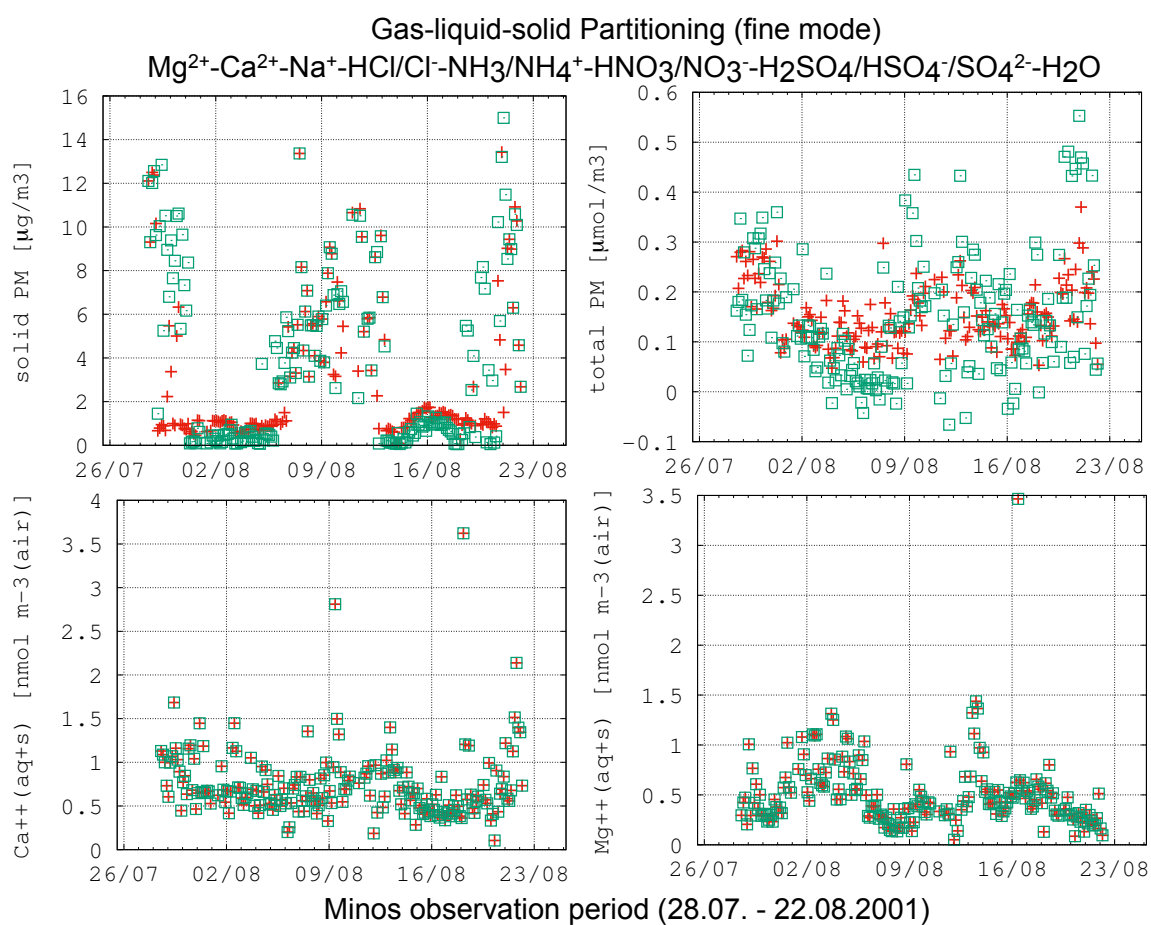


Figure S8.2: Details of Figure S8 (Supplement): solid mass(aq+s), total moles(aq+s), lumped  $Ca^{2+}$ (aq+s) and  $Mg^{2+}$ (aq+s) (nano moles).

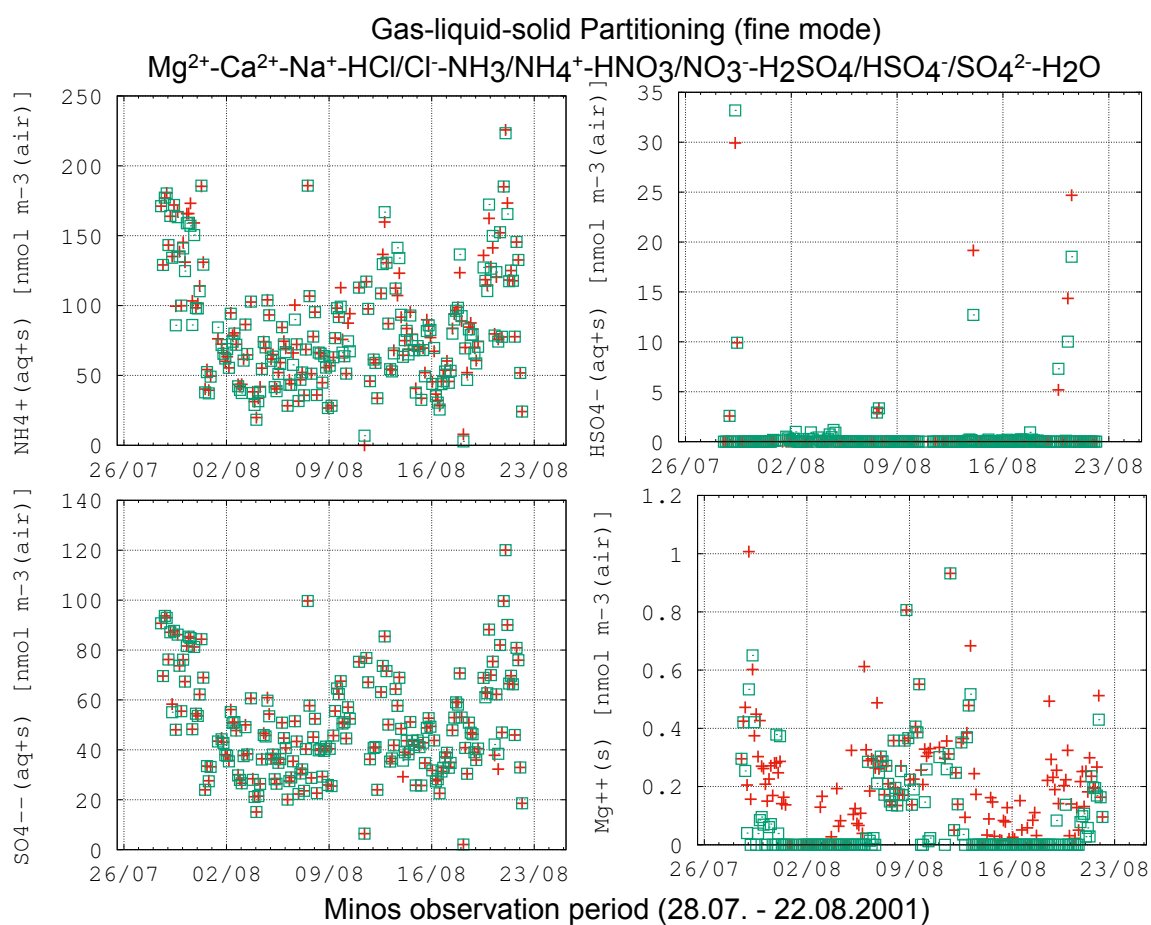


Figure S8.3: Details of Figure S8 (Supplement): Lumped  $NH_4^+(aq+s)$ ,  $HSO_4^-(aq+s)$ ,  $SO_4^{2-}(aq+s)$  and  $Mg^{2+}(s)$  (nano moles).

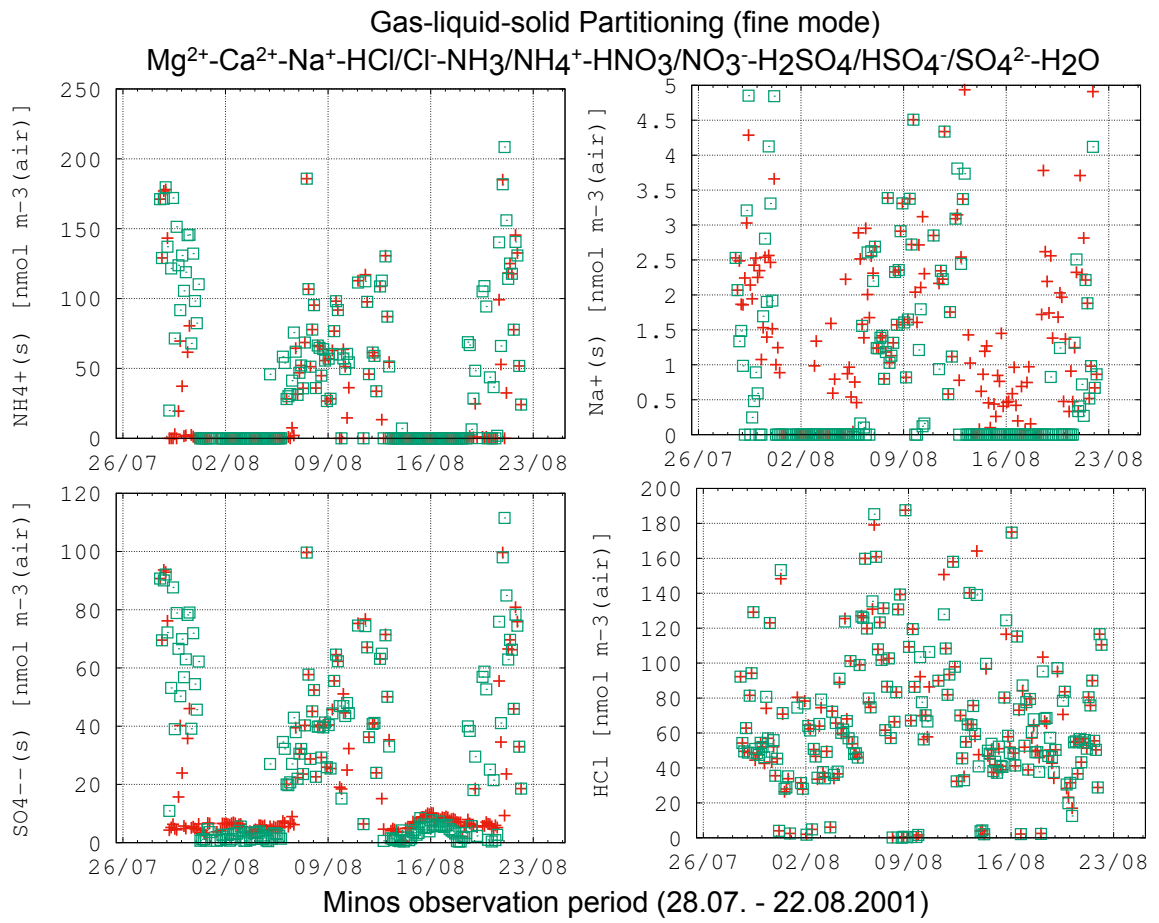


Figure S8.4: Details of Figure S8 (Supplement): Lumped  $NH_4^+(s)$ ,  $Na^+(s)$ ,  $SO_4^{2-}(s)$  and  $HCl(g)$  (nano moles).

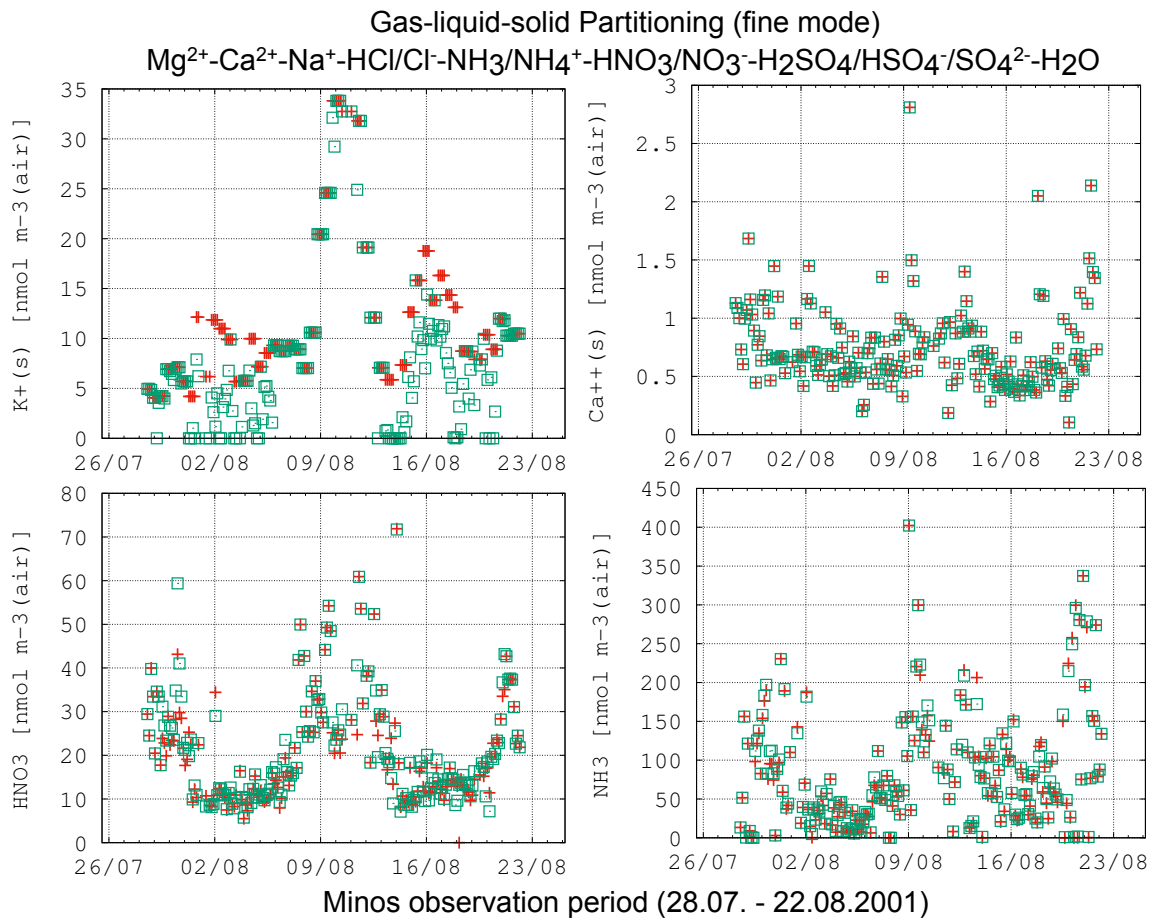


Figure S8.5: Details of Figure S8 (Supplement): Lumped  $K^+(s)$ ,  $Ca^{2+}(s)$ ,  $HNO_3(g)$  and  $NH_3(g)$  (nano moles).

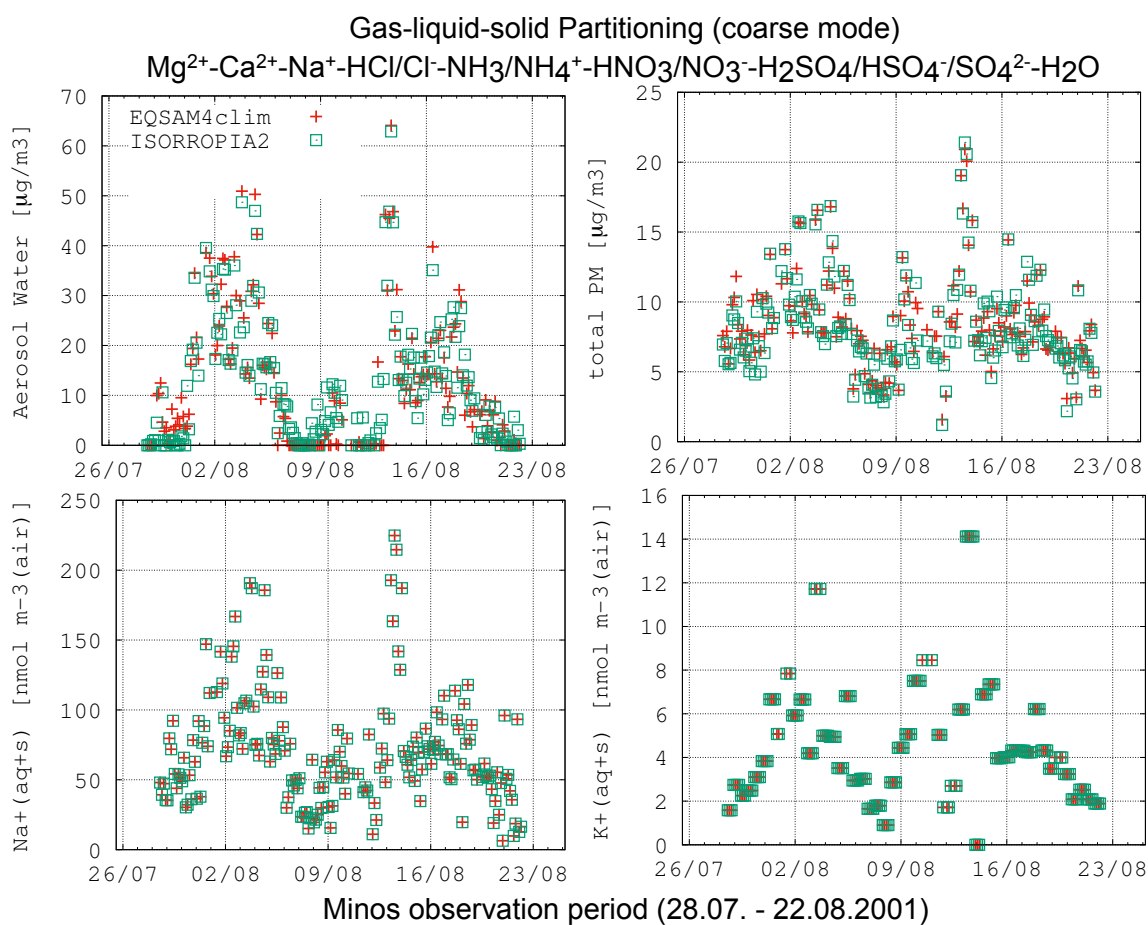


Figure S9.1: Details of Figure S9 (Supplement): Aerosol water(aq), total mass (aq+s), lumped  $Na^+$ (aq+s) and  $K^+$ (aq+s) (nano moles).

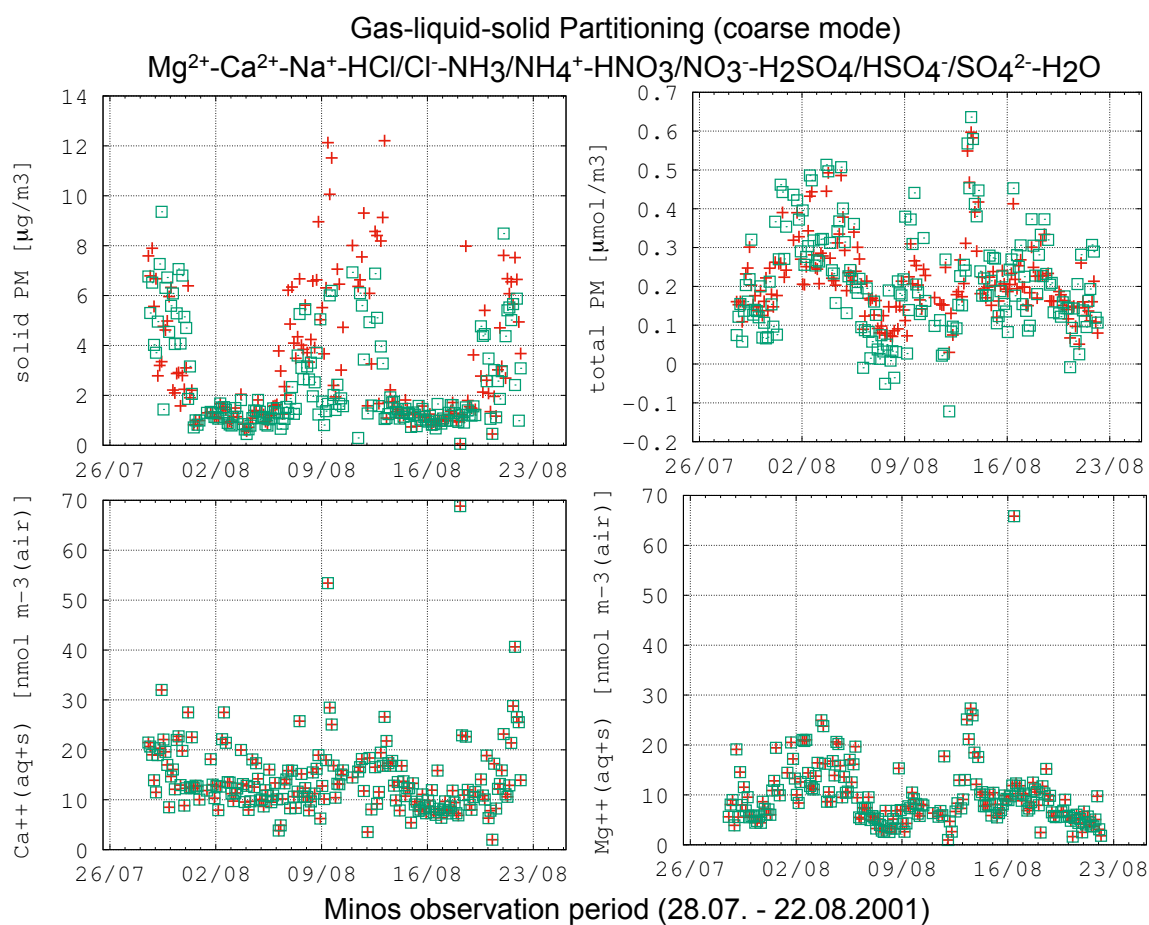


Figure S9.2: Details of Figure S9 (Supplement): solid mass(aq+s), total moles(aq+s), lumped  $Ca^{2+}(\text{aq+s})$  and  $Mg^{2+}(\text{aq+s})$  (nano moles).

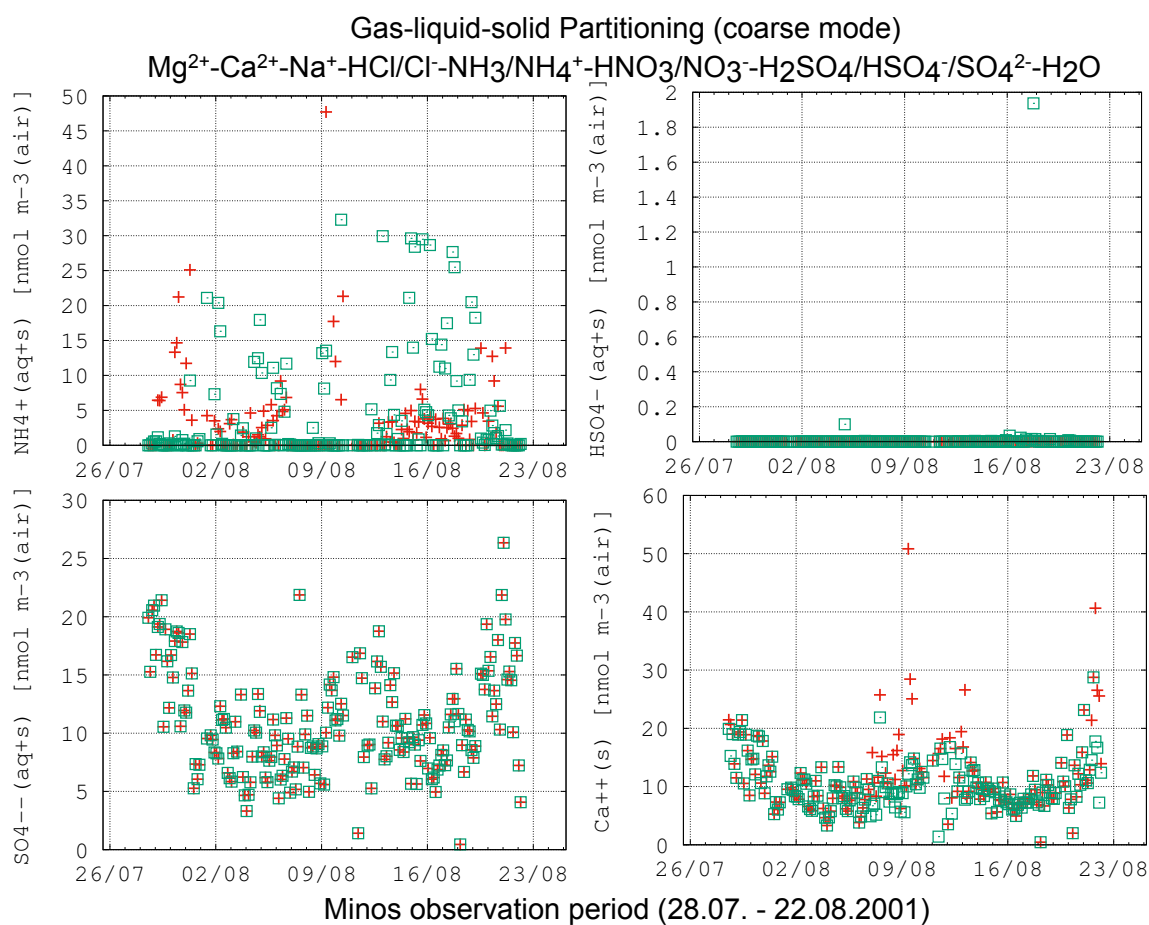


Figure S9.3: Details of Figure S9 (Supplement): Lumped NH<sub>4</sub><sup>+</sup>(aq+s), HSO<sub>4</sub><sup>-</sup>(aq+s), SO<sub>4</sub><sup>2-</sup>(aq+s) and Ca<sup>2+</sup>(s) (nano moles).

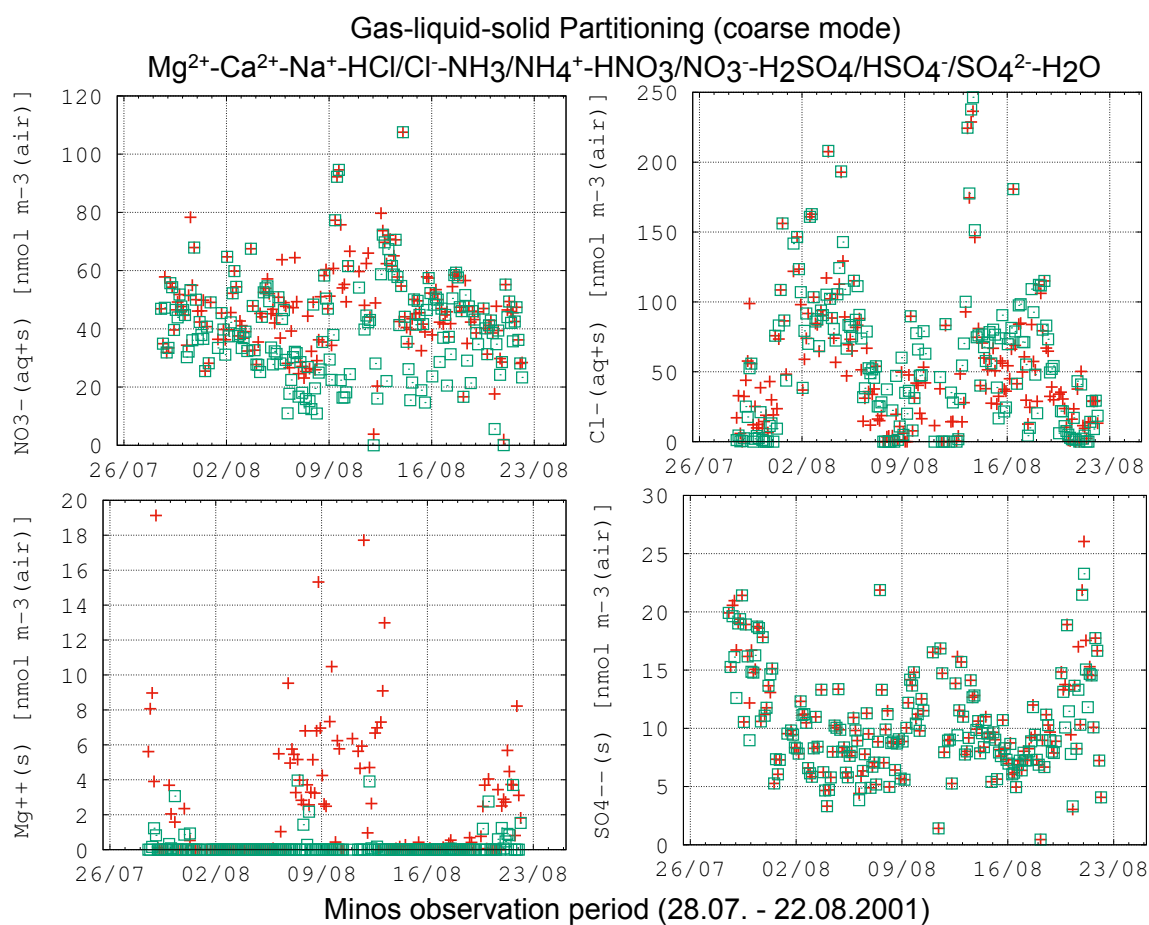


Figure S9.4: Details of Figure S9 (Supplement): Lumped  $\text{NO}_3^{-}(\text{aq+s})$ ,  $\text{Cl}^{-}(\text{aq+s})$ ,  $\text{Mg}^{2+}(\text{s})$  and  $\text{SO}_4^{2-}(\text{s})$  (nano moles).

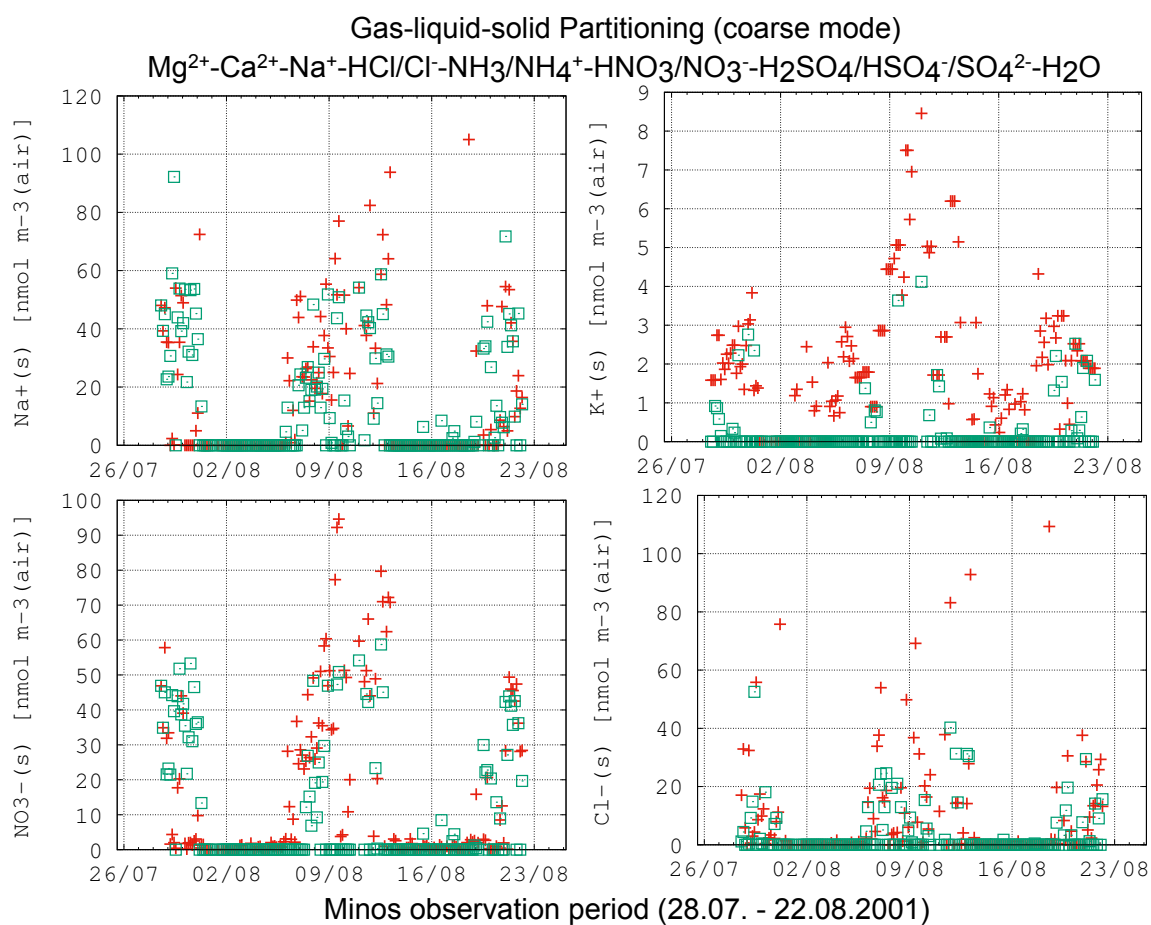


Figure S9.5: Details of Figure S9 (Supplement): Lumped  $Na^+$ (s),  $K^+$ (s),  $NO_3^-$ (s) and  $Cl^-$ (s) (nano moles).